University of Alberta

Tissue-specific gene expression of two class III *Arabidopsis* peroxidases under aluminum stress

by

Tianzhen Liu

A thesis submitted to the Faculty of Graduate Studies and Research
in partial fulfillment of the requirements for the degree of

Master of Science
in
Plant Biology

Department of Biological Sciences

Spring 2010
Edmonton, Alberta

Examining Committee

Dr. Gregory Taylor, Biological Sciences

Dr. Allen Good, Biological Sciences

Dr. Randall Weselake, Agricultural, Food and Nutritional Science

Abstract

Class III peroxidases have been identified as secreted proteins involved in plant defense, auxin metabolism, cell wall modification, and regulation of reactive oxygen species. Transcriptome analysis of *Arabidopsis* has identified many class III peroxidases that respond to aluminum stress. The large number and versatile function of peroxidases make functional characterization of individual peroxidases a challenging task. However, the use of promoter::*GUS* reporter fusions can help to elucidate the expression pattern of individual peroxidases. To investigate the expression of *PER22* and *PER73* under aluminum stress in *Arabidopsis*, single-copy, homozygous, transgenic plants harbouring promoter::*GUS* reporter fusions were generated through self-pollination and southern blot analyses. Histochemical *GUS* staining of transgenic lines revealed trichome-specific and vascular-specific expression patterns for *PER22* and *PER73*, respectively. The temporal and spatial expression of *PER22* and *PER73* suggest that they might be involved in pathogen defense and/or lignification. Further experiments will help define these peroxidase functions under aluminum stress.

Acknowledgements

Firstly I would like to thank my supervisor, Dr. Gregory Taylor, for his generous support and guidance throughout my graduate study. Dr. Taylor has been the most patient and supportive supervisor I can ever ask for. Without his help I would never have been able to complete my graduate study. I would also like to express my sincere gratitude to the members of my committee, Dr. Allen Good (Department of Biological Sciences) and Dr. Randall Weselake (Department of Agricultural, Food and Nutritional Science) for their guidance and help in my research.

I would like to thank Dr. Neil Harris for proofreading my thesis and Jennifer Francis for helping me with the lab techniques. They both have my deepest gratitude. I would also like to give my special thanks to Taylor lab crew; Dr. Glen Hawkins, Matt Bryman, Tara Narwani, Diana Lopez Santiago, Manjeet Kumari, and Dylan Silver for all their ideas and advice. I also want to thank everyone in the Department of Biological Sciences that I have worked with and sought help from as a graduate student and teaching assistant. It has been a great pleasure and great experience to get to know each and every one of you.

Finally, I would like to thank my parents for all their love and support, and for always trusting in me.

Table of Contents

List of Tables

List of Figures

List of Symbols, Nomenclature, or Abbreviations

Al, aluminum

$AlO_2^{\bullet 2+}$, aluminum superoxide

$Al(OH)_3$, gibbsite

AOX, alternative oxidase

APX, ascorbate peroxidases

BCB, blue copper binding protein

BLAST, basic local alignment and search tool

Ca, calcium

CaMV, cauliflower mosaic virus

CAT, catalase

CDS, coding region

CSPD, Disodium 3-(4-methoxyspiro {1,2-dioxetane-3,2´-(5'-chloro)tricyclo [3.3.1.1^{3,7}]decan}-4-yl) phenyl phosphate

CTPP, C-terminal propeptide

Cu, copper

dNTP, deoxyribonucleotides

DTZ, distal transition zone

EDTA, ethylenediamine tetraacetic acid

ETC, electron transport chain

Fe, iron

GFP, green fluorescent protein

GLR, glutaredoxin

GPX, glutathione peroxidase

GR, glutathione reductase

GST, glutathione S-transferase or glandular secreting trichome

GUS, β-glucuronidase

H_2O_2, hydrogen peroxide

HRP, horseradish peroxidase

IPTG, isopropyl-beta-D-thiogalactopyranoside

LB, left border

LC-MS/MS, liquid chromatography tandem mass spectrometry

MAPK, motigen-activated protein kinase

MDAR, monodehydroascorbate reductase

Mn, manganese

MnSOD, manganese superoxide dismutase

MS, Murashige-Skoog

Mud PIT, multidimensional protein identification technology

MW, molecular weight

NCBI, national centre for biotechnology information

Ni, nickel

$^{\cdot}OH$, hydroxyl radical

$O_2^{\cdot-}$, superoxite anion,

P, phosphorus

PAL, phenylalanine ammonia lyase

PCD, programmed cell death

PER or POX, peroxidase

pI, isoelectric point

PR, pathogenesis-related

PrxR, peroxiredoxin

qRT-PCR, quantitative reverse transcriptase-polymerase chain reaction

RB, right border

ROS, reactive oxygen species

RRGI, relative root growth increment

RT-PCR, reverse transcriptase-polymerase chain reaction

SOD, superoxide dismutase

ST, simple trichomes

TAIR, the *Arabidopsis* Information Resource

TE, tracheary element

TF, transcription factor

TIGR, the Institute of Genome Research

Trx, thioredoxins

UTR, untranslated region

WT, wild type

X-gluc, 5-bromo-4-chloro-3-indolyl-β-D-glucuronide

4-MUG, 4- methyl-lumbellyferyl-β-D-glucuronide

Chapter 1. Literature Review

1.1. Economic and agricultural impact of aluminum toxicity

Aluminum (Al) is the third most abundant element and the most abundant metal within the earth's crust, comprising 8.1 % of its total mass (Driscoll and Schecher, 1988). Soil acidification can solublize a phytotoxic form of aluminum, Al^{3+}, from the insoluble mineral gibbsite, $Al(OH)_3$ (Hartwell and Pember, 1918). As a result, Al^{3+} toxicity is one of the major factors limiting crop productivity on acidic soils (pH< 5.0) (Von Uexkull and Mutert, 1995).

Acidic soils have been estimated to cover thirty percent of the world's arable land. Of the 3,950 Mha of acid soils world-wide, 67% are covered by forests and woodlands, while approximately 18% support savanna, prairie or steppe ecosystems (Von Uexkull and Mutert, 1995). A smaller proportion (4.5%, 179 Mha) is cultivated for arable crops, while a further 33 Mha are used for tropical perennial crops (Von Uexkull and Mutert, 1995). Soil acidification is a slowly occurring, natural process, especially in high rainfall regions where base cations are leached from the soil and replaced on cation exchange sites by protons. Industrial and agricultural activities of modern society can accelerate this natural process (Porter, 1981). A number of factors contribute to soil acidification. Accumulation of organic matter in the soil can increase soil acidity through the release of organic acids during decomposition, not only in the surface soil but also in the subsoil as deep as 40 cm (Williams and Donald, 1954; 1957). Long-term use of ammonium-based nitrogen fertilizers (e.g., anhydrous ammonia and urea) is a major contributor to the acidification of agricultural soils (Andersson *et al.*, 2002). Nutrient absorption by plants can also lead to soil acidification due to

imbalance of cation/anion uptake (greater cation uptake). This would not lead to soil acidification in stable ecosystems where plant litter returns to the soil, but in agricultural soils, a net loss of cations resulting from crop harvesting contributes to soil acidification (Porter, 1981). In Canada, one of the contributors to soil acidification is acid rainfall, arising from sulphur dioxide and nitrous oxides released originally as industrial waste into the atmosphere (Environment Canada, 1997). Because the mechanisms of soil acidification are geologically specific and temporally variable, it is difficult to generalize about the relative contribution of one soil acidification process over another.

The most important consequence of soil acidification for crop growth is the release of toxic forms of Al from the soil. In neutral or weakly acidic soils, Al is present as insoluble, non-toxic $Al(OH)_3$ (gibbsite). When soil pH drops below 4.5, the most dominant form of Al becomes phytotoxic $Al(H_2O)_6^{3+}$ or Al^{3+}. Aluminum (Al) stress is one of the most important yield-limiting stresses on acidic soils. Inhibition of root growth is the most direct and earliest symptom of Al toxicity, which was first observed in barley and rye grown on acid soil (Hartwell and Pember, 1918). Despite several decades of intensive research, many questions remain to be answered about different aspects of the genetics and physiology of Al tolerance and toxicity. Recently, studies using *Arabidopsis*, wheat, and barley have provided important advances in our knowledge of the genetic basis of Al tolerance and toxicity (Kochian *et al.*, 2004).

1.2. Effects of aluminum toxicity at the whole-root and cellular level

The most immediate and distinctive symptom of Al toxicity is inhibition of root growth. Aluminum induced-stunting of root growth is a quick process that can be observed after minutes of exposure to Al in hydroponic solutions (Delhaize and Ryan, 1995). Suppression of root growth by Al can result in nutrient (Ca, P) deficiencies and limited water uptake (Foy 1983; Huang *et al.*, 1992; Gunse *et al.*, 1997; Kochian *et al.*, 2004).

The root apex (including root cap, root apical meristem, and elongation zone) is a major site of Al accumulation and plays an important role in perception of Al (Matsumoto, 2000). However, there is controversy around which component of the root apex is the major target for Al phytotoxicity. The root cap was initially proposed as the target site for Al injury based on the observation that resumption of root elongation of maize in an Al-free recovery solution was closely associated with the secretory activity and change of volume in peripheral root cap cells (Bennet and Breen, 1991). However, roots of maize with the root cap removed behaved the same as intact roots in terms of the onset and degree of inhibition of root growth under Al stress (Ryan *et al.*, 1993). In wheat, the root elongation zone was suggested as the primary target for injury as reduced viability of cells in this zone coincided with cells decreasing in length but increasing in diameter (Sasaki *et al.*, 1997). More recently, experiments using agar blocks infused with Al provided improved spatial resolution for identifying the site of Al injury (Sivaguru and Horst, 1998). Aluminum (Al) applied to individual 1-mm sections of the root apex showed that the distal transition zone (DTZ) (1-2 mm from root tip) was the most sensitive to Al (Sivaguru and Horst, 1998). The DTZ contains

cells that are in a preparatory phase for rapid elongation. Short-term application of Al to the DTZ resulted in the same level of inhibition as exposure of the entire root apex, whereas Al treatment applied to elongation zone had no effect on root growth (Sivaguru *et al.*, 1999; Kollmeier *et al.* 2000).

Even though the root cap may not participate directly in Al-induced inhibition of root growth, it is still likely that it contributes to Al tolerance by releasing mucilage that binds toxic Al (Archambault *et al.*, 1996) and by transducing the signals involved in maintaining basipetal polarity of auxin transport (Hasenstein and Evans, 1988). Based on the observed Al-induced inhibition of polar transport of auxin in roots of maize, a signaling pathway was proposed to exist between the region where Al is perceived (possibly the DTZ) and the region where cell elongation is inhibited (Kollmeier *et al.*, 2000). Aluminum-induced inhibition of basipetal auxin transport is also believed to be responsible for the Al-induced alteration of root cell patterning (Doncheva *et al.*, 2005). The exact mechanism for these effects is not understood. Furthermore, the mechanism of Al-induced inhibition of auxin transport could be complicated by the interaction of Al with calcium (Ca), since both cations change the polarity of the basipetal auxin transport in maize (Hasenstein and Evans, 1988). Aluminum appears to affect the cytoskeleton of outer cortical cells of the DTZ. Monoclonal antibodies revealed that Al caused disintegration of microtubules and altered the polymerization pattern of actin microfilaments (Sivaguru *et al.*, 1999). Further study of the DTZ revealed that disorganization of the cytoskeleton and inhibition of root elongation might be mediated by Al binding to the free carboxyl groups of the pectic matrix in the cell wall apoplasm (Horst *et al.*, 1999). Overall the meristem, distal transition, and apical elongation zones of the root apex are sensitive to Al toxicity.

Alteration of root morphology and reduced viability of cells in the elongation zone occurs as early as 0.5 to 2 h after exposure to Al (Barcelo and Poschenrieder, 2002; Ma, 2007). The effects of Al on root elongation rates are determined by the interaction between cell division and cell elongation in the root apex, which includes cells in various stages of mitotic activity, morphology and expansion rate. In a developing root, cell expansion takes place in the meristem, where cell elongation is accompanied by cell division. Further away from the meristematic region, the relative rate of elongation of cells increase. Although cell division *per se* does not contribute significantly to root length, both the rates of cell division and the number of cells remaining in cell division cycle affect the root elongation rate. Therefore, inhibition of cell division and cell elongation may occur together to result in immediate inhibition of root growth. A recent study demonstrated that disruption of cell division occurred within 5 min of exposure to Al in the proximal meristem (0.25-0.8 mm) of an Al-sensitive cultivar of maize, followed by immediate initiation of lateral root formation, indicating a fast rearrangement of root cell patterning (Doncheva *et al.*, 2005).

Increasing evidence suggest that the apoplast plays a major role in Al perception (Horst, 1995). Aluminum (Al) binds strongly to negatively charged pectins of the cell wall and specifically accumulates in root epidermal and cortical cells (Delhaize *et al.*, 1993; Horst *et al.*, 1999). In addition to the negatively charged binding sites in cell wall, organic acids in the root mucilage also bind Al in a dose dependent manner (Matsumoto, 2000; Ma, 2007). Although the majority of Al accumulated by roots is present in the apoplasm (30% to 90%); a small fraction of Al enters the symplasm of plant cells within minutes (Lazof *et al.*, 1994; Taylor *et al.*, 2000). In addition, cell wall bound Al can be actively transported into symplastic vacuoles as Al-P or Al-Si complexes as shown in roots of an Al

tolerant cultivar of maize (Vazquez *et al.*, 1999). Inhibition of cell division was found to be correlated with binding of Al to chromosomal DNA in the nuclei, which is possibly due to the abundant negatively charged phosphate groups of DNA (Naora *et al.*, 1961; Silva *et al.*, 2000). The mode of Al toxicity also depends on Al concentration and duration of Al exposure (Ma *et al.*, 2004).

Even though there are many theories about the specific Al lesion that causes inhibition of root growth, the exact mechanism is still elusive. Aluminum (Al) toxicity in the apoplastic space has been proposed to be caused by its binding to the negatively charged cell wall, disrupting the plasma membrane via lipid peroxidation, and interference with ion transport proteins in the plasma membrane (Matsumoto, 2000). Additionally, Al toxicity in the symplasm has been proposed to be caused by oxidative stress, inhibition of DNA synthesis and enzyme activity, disorganization of the cytoskeleton, disruption of signal transduction pathways, and disruption of general metabolism and mitochondrial function (Matsumoto, 2000; Ma, 2007).

In order to fully understand Al toxicity, it is necessary to identify where Al is localized and what molecules it interacts with. Due to the complex chemistry of Al, Al can exist in multiple hydration states and complexes (Matsumoto, 2000) and there are many potential target sites for toxicity (Kinraide and Parker, 1997). Perhaps unsurprisingly, there is more evidence for apoplastic Al lesions than there is for symplastic Al lesions. The apoplast is where Al initially contacts the root and is where the majority of Al is bound (Taylor *et al.*, 2000; Ma, 2007). Both the physical and chemical properties of the cell wall seem to be modified by Al, which supports the theory that Al-induced inhibition of root growth is initiated in the apoplast of the root apex (Horst, 1995). Supporting evidence has been

provided by experiments indicating that Al decreases cell wall extensibility, elasticity, and viscosity, which are essential for cell elongation (Tabuchi and Matsumoto, 2001; Ma *et al.*, 2004). Different densities of negatively charged binding sites in root cell walls has been proposed as the cause of differential Al resistance in two cultivars of maize (Schildknecht and Vidal, 2002). Interestingly, a large portion of these negative charges are carried by pectins in the cell wall (Horst, 1995), and plants with elevated pectin levels (by NaCl treatment) bind more Al in their root apices, display higher sensitivity to Al, and exhibit more severe root growth inhibition (Horst *et al.*, 1999). Aluminum interaction with pectins has been suggested to block the trafficking of water and nutrients through the apoplast by inducing callose deposition at the plasmodesmata (Blamey *et al.*, 1993; Blamey and Dowling, 1995; Schmohl *et al.*, 2000) and displacing Ca^{2+} from the calcium pectin matrix. These factors might also lead to stiffening of the cell wall and obstruct cell elongation (Gunse *et al.*, 1997). However, there is also evidence that Al can inhibit root growth without displacing Ca^{2+} from the apoplast (Ryan *et al.*, 1997; Schofield *et al.*, 1998). Cell elongation requires cell wall loosing and resynthesis. Aluminum might interfere with cell wall loosening by hindering the deposition of newly synthesized cell wall material and altering the cell wall structure (Ma *et al.*, 2004).

One of the important sites of Al toxicity at the cellular level is the plasma membrane. Aluminum (Al) has a strong affinity for the plasma membrane due to its strong electro-static interaction with negatively charged carboxyl and phosphate groups (Akeson *et al.*, 1989). The binding of Al to the plasma membrane can lead to a shift of the plasma membrane potential (Akeson *et al.*, 1989). Aluminum interaction with the plasma membrane can also reduce the uptake of many other cations such as Ca^{2+}, Mg^{2+}, K^{+}, and NH_4^{+} (Huang *et al.*,

1992; Nichol *et al.*, 1993; Ryan *et al.*, 1993) and enhance the uptake of NO_3^- and phosphate. This could be explained by direct interaction of Al with ion transport proteins (Pineros and Tester, 1995, 1997; Pineros and Kochian, 2001), changing concentrations of anions and cations at the plasma membrane surface (Zheng and Yang, 2005), and/or shifting of membrane potential, which could neutralize the voltage sensing mechanism for some ion channels (Very and Davies, 2000). These results contribute to the theory that Al binds to phospholipids in the plasma membrane to form a positively charged layer that restrains the movement of cations and increases the movement of anions to the plasma membrane (Nichol *et al.*, 1993). The fluidity of the plasma membrane was found to be weakened by displacement of Ca^{2+} (Matsumoto *et al.*, 1992) and binding of Al to phospholipids. Structural alteration of the plasma membrane increased membrane permeability to non-electrolytes and decreased the permeability of the membrane for water and lipid permeators (Zhao *et al.*, 1987). Aluminum has also been shown to trigger callose deposition, which in turn blocks symplastic transport through plasmodesmatal connections (Sivaguru *et al.*, 2000). Immediate synthesis of callose on the plasma membrane has often been used as an indicator of cellular Al toxicity (Horst *et al.*, 1997; Massot *et al.*, 1999; Bhuja *et al.*, 2004). There is still a lack of direct evidence for Al interaction with the plasma membrane *in vivo*. In general, it is accepted that Al toxicity is probably caused by the disturbance of multiple processes, including but not limited to altering the membrane surface potential, inducing lipid peroxidation of the plasma membrane, blocking ion transport channels, disrupting proton gradients, and altering ion homeostasis of root cells (Kochian *et al.*, 2005).

1.3. Aluminum triggers oxidative stress through increased reactive oxygen species

The phytotoxicity of several metals, such as copper (Cu), iron (Fe), manganese (Mn), and nickel (Ni), can often be attributed to their ability to promote damaging oxidative reactions (Becana *et al.*, 1998; Bueono and Piqueras, 2002). Redox-active metal ions such as Fe and Cu induce oxidative stress by generating reactive oxygen species (ROS) from oxygenated molecules through the Haber-Weiss and Fenton reactions. However, non-redox active metal ions, such as Al have been found to induce oxidative stress as well (Cakmak and Horst, 1991). Several studies on different plant species, such as wheat (Snowden *et al.*, 1995), tobacco (Ezaki *et al.*, 1996), maize (Boscolo *et al.*, 2003), rice (Meriga *et al.*, 2004; Sharma and Dubey, 2007), barley (Simonovicova *et al.*, 2004), and *Arabidopsis* (Richard *et al.*, 1998; Kumari *et al.*, 2008) have revealed that Al stress induced ROS including superoxide ($O_2^{\cdot-}$) and hydrogen peroxide (H_2O_2), as well as many genes involved in response to oxidative stress, including blue copper binding protein (BCB), peroxidase (POX), glutathione S-transferase (GST), phenalalanine ammonia lyase (PAL), superoxide dismutase (SOD), ascorbate peroxidase (APX), dehydroascorbate reductase, monodehydroascorbate reductase (MDHAR), glutathione reductase (GR), and many others.

The mechanisms of ROS production by Al are unclear, and a number of models have been proposed. For example, the relationship between Al and oxidative stress has been proposed to reflect an iron-induced lipid peroxidation resulting in increased rigidity of the plasma membrane (Gutteridge *et al.*, 1985). Aluminum has also been shown to promote biological oxidation through a non-iron-mediated formation of the hydroxyl radical ($HO^{\cdot}$) in animal cell systems (Mendez-Alvarez

et al., 2002). Recently it has been discovered that Al alone (without Fe supply) increases the production of ROS in tobacco cells and pea roots (Yamamoto *et al.*, 2002). Furthermore, it has been speculated that Al has pro-oxidant activity via the formation of the aluminum superoxide ($AlO_2^{\bullet 2+}$), a semi-reduced radical ion (Exley, 2004).

Aluminum-induced lipid peroxidation has been found in various plant species and tissues (Horst *et al.*, 1992; Oteiza, 1994). There is a complex interaction between lipid peroxidation and inhibition of root elongation induced by Al and/or Fe toxicity through the production of highly toxic ROS (Ono *et al.*, 1995; Simonovicova *et al.*, 2004). Aluminum-induced production of ROS and lipid peroxidation in root tips of soybean occurred only after a long duration (24 h or more) of Al treatment (Cakmak and Horst, 1991), however in pea roots they are immediate (4 h) symptoms (Yamamoto *et al.*, 2001). Further study revealed that the primary cause of Al-induced inhibition of root elongation in pea probably depends on Al-dependent production of ROS, depletion of ATP, inhibition of respiration, and induction of mitochondrial dysfunction, rather than lipid peroxidation (Yamamoto *et al.*, 2002). Application of a lipophilic antioxidant, butylated hydroxyanisole, reduced lipid peroxidation but not root inhibition (Yamamoto *et al.*, 2001). Therefore, lipid peroxidation might be a consequence of Al toxicity at the plasma membrane, but it is not the primary root growth-inhibiting factor.

Even though there is evidence linking Al toxicity and oxidative stress in plant roots (Yamamoto *et al.*, 2003), the exact mechanism by which Al stress alters ROS levels and activities of antioxidant enzymes remains unclear. Treatment with antioxidant compounds does provide protection from Al injury. Furthermore,

overexpression of a series of antioxidant enzymes, such as wheat mitochondrial manganese superoxide dismutase (MnSOD) in canola (Basu *et al.*, 2001) and tobacco glutathione S-transferase (parB) and peroxidase (NtPox) in *Arabidopsis* (Ezaki *et al.*, 2001) resulted in enhanced Al resistance. Aluminum also induces a class III peroxidase (*PER34*) in *Arabidopsis* (Richards *et al.*, 1998). However, overexpression of *PER34* in *Arabidopsis* alleviated oxidative stress, but failed to confer resistance to Al stress (Ezaki *et al.*, 2000). These findings suggest that Al-induced oxidative stress can be partially rescued by increased expression of antioxidant enzymes. Manipulation of oxidative defense genes, however, does not always confer resistance to Al stress. This is not surprising since oxidative stress accounts for only part of the Al toxicity syndrome and Al-induced genes involved in response of oxidative stress are just part of the plant oxidative defense system. Not all components of the oxidative defense system are well positioned within the plant or within plant cells to play a role in response to Al stress, which is primarily a root related phenomenon (Ryan *et al,*. 1993). The number of genes and proteins shown to be responsive to Al by transcriptomic profiling (Kumari *et al.*, 2008) and proteomic analyses (Zhou *et al.*, 2009) of different plant species have been increasing rapidly, but further work is necessary to clarify whether they are directly involved in Al tolerance.

Transcriptomic profiling of gene expression in roots of *Arabidopsis* grown under Al stress showed that expression patterns of a large portion of ROS response gene networks were altered following varying periods of Al exposure (Kumari *et al.*, 2008). Individual antioxidant genes and gene families, such as superoxide dismutase (SOD), glutathione reductase (GR), ascorbate peroxidase (APX), glutathione-s-transferase (GST) and class III peroxidases (PER) were induced after 48-hour exposure (Kumari *et al.*, 2008). In contrast, alternative oxidase

(AOX), glutaredoxin (GLR), peroxiredoxin (PrxR), monodehydroascorbate reductase (MDAR), and thioredoxins (Trx) were repressed in roots of *Arabidopsis* under Al stress (Kumari *et al.*, 2008). All of these genes are involved in detoxifying ROS generated by Al stress. Aluminum (Al) stress leads to the induction of both antioxidant enzymes and biosynthetic enzymes that regulate the levels of antioxidant metabolites. Interestingly, none of these ROS response network genes were consistently up-regulated or down-regulated between the time points of 6h and 48h (Kumari *et al.*, 2008). Despite the high homology of genes within the same gene family, their expression profiles were dissimilar. This is perhaps unsurprising given the complexity and redundancy of the regulatory network involved in production and removal of ROS (Mittler, 2002).

Although plants continuously produce low levels of ROS (Passardi *et al.*, 2005), elevated cytoplasmic Ca^{2+} induced by Al could perturb the endogenous ROS balance and subsequently cause oxidative stress (Jones *et al.*, 1997, 2006; Darko *et al.*, 2004). Most of the ROS in plants are generated continuously in subcellular compartments such as the chloroplasts, mitochondria, and peroxisomes (Apel and Hirt, 2004). Reactive oxygen species (ROS) are produced as side products of aerobic metabolism, specifically during oxidative phosphorylation, and the formation of disulfide bonds during protein folding (Mittler *et al.*, 2004). Plants also generate ROS spontaneously as signaling molecules to regulate a variety of cellular responses to pathogen attack, programmed cell death, and stomatal movement (Apel and Hirt, 2004). Due to their toxicity and chemically reactivity, ROS can cause oxidative damage to membrane lipids, proteins, and nucleic acids (Apel and Hirt, 2004). Therefore, plants have developed a variety of mechanisms to remove and limit the production of ROS. However, this regulation of ROS can be disrupted by a range of adverse biotic or abiotic conditions such as pathogen

attack, salinity, drought, low temperature, mechanical damage, and Al stress (Mittler *et al.*, 2004; Yamamoto *et al.*, 2001).

1.4. How does the antioxidant defense system respond to ROS triggered by aluminum?

Plants have two mechanisms to remove excessive ROS, enzymatic and non-enzymatic scavenging. Enzymatic scavenging exploits ROS-detoxifying enzymes including superoxide dismutase (SOD), catalase (CAT), ascorbate peroxidases (APX) and glutathione peroxidases (GPX) (Apel and Hirt, 2004). Superoxide dismutases form the initial step of detoxification by dismutating superoxide (O_2^-) to H_2O_2, which can be subsequently reduced to oxygen and H_2O by APX, GPX and CAT. Transgenic plants overexpressing some of these enzymes have shown increased tolerance to oxidative (Wang *et al.*, 1999; Alscher *et al.*, 2002; Murgia *et al.*, 2004), thermal (Roxas *et al.*, 1997), and Al stresses (Richard *et al.*, 1998; Basu *et al.*, 2001). Non-enzymatic scavenging of ROS uses cellular metabolites such as ascorbic acid, glutathione (GSH), tocopherol, flavonoids, alkaloids, and carotenoids (Mittler, 2002). Plants increase the expression of enzymes involved in the biosynthesis of these antioxidants in response to stresses (Apel and Hirt, 2004). Generation of ROS by metals and ROS detoxification pathways in plant mitochondria are illustrated in Figure 1.1.

The production of ROS *in planta* is an unavoidable consequence of respiration and photosynthesis, which are localized to organelles such as mitochondria, chloroplasts, and peroxisomes (Apel and Hirt, 2004). Among these three compartments, the majority of ROS is produced in chloroplasts and peroxisomes. The alternative oxidase (AOX) minimizes ROS levels in mitochondria by

preventing ROS production from the photosynthetic electron transport chain (ETC) or respiration pathway (Apel and Hirt, 2004). However, AOX expression in *Arabidopsis* roots was reduced during Al stress (Kumari *et al.*, 2008), which seems contradictory to the function of AOX. In fact, Al can induce ROS production in mitochondria, which causes ATP depletion and inhibition of respiration, resulting in mitochondrial dysfunction (Yamamoto *et al.*, 2002). The exact mechanism by which Al causes mitochondrial dysfunction remains unclear. The initial targeting sites of Al need to be determined. Does a small amount of Al cross the plasma membrane (Taylor *et al.*, 2000) and directly interact with mitochondria or does Al bind to the plasma membrane and disrupt an unknown signal transduction pathway between the plasma membrane and mitochondria?

Superoxide dismutases (SODs) are a family of enzymes that catalyze the dismutation of O_2^- to O_2 and H_2O_2 (Streller and Wingsle, 1994). Catalase converts H_2O_2 to O_2 and water. The protein activity of mitochondrial manganese superoxide dismutase (MnSOD) of wheat is increased under Al stress and has been reported to co-segregate with the Al-resistant phenotype in segregating population (Basu *et al.*, 1999). Overexpression of MnSOD in canola also conferred increased resistance to Al and oxidative stress (Basu *et al.*, 2001). Although expression of catalases were not affected in roots of *Arabidopsis* under Al stress (Kumari *et al.*, 2008), previous studies of catalase gene expression under Al stress indicate that catalase was either up-regulated or down-regulated, depending on the plant tissue and species tested. In root tips of soybean and *Arabidopsis*, catalase expression decreased (Cakmak and Horst, 1991; Richards *et al.*, 1998) while in hot pepper, catalase was increased under Al stress (Kwon and An, 2001).

Glutathione and ascorbate are involved in detoxification of ROS through two pathways: the ascorbate/glutathione cycle and the glutathione peroxidase system (Eshdat *et al.*, 1997; Noctor and Foyer, 1998). The ascorbate/glutathione cycle includes ascorbate, glutathione, and the enzymes ascorbate peroxidase (APX), dehydroascorbate reductase (DHAR), monodehydroascorbate reductase (MDAR), and glutathione reductase (GR). Metals like Cu and Zn have been reported to enhance enzymatic activities within this pathway (Cuypers *et al.*, 1999). Aluminum stress affected three of the four genes mentioned above (Kumari *et al.*, 2008). Glutathione is a non-protein tripeptide that is continuously cycled between its reduced (GSH) and oxidized (GSSG) forms through the action of glutathione peroxidase (GPX) and glutathione reductase (GR) (Edwards *et al.*, 1990). Genes encoding glutathione peroxidase (GPX) in yeast are induced by H_2O_2, and mutants of GPX are hypersensitive to H_2O_2 and Al (Basu *et al.*, 2004). Reduced glutathione (GSH) is also known to play a role in subcellular sequestration of toxic metals. Glutathione S-transferase (GST) catalyzes the formation of toxin-glutathione conjugate, which is transported to the vacuole via an ATP Binding Cassette (ABC)-type transporter (Edwards, 2000). While the chemistry of Al makes formation of a GSH-Al complex unlikely, spatial expression of GST in *Arabidopsis* indicates that they are induced under Al stress (Ezaki *et al.*, 2004) and overexpression of a tobacco GST gene in *Arabidopsis* conferred resistance to Al (Ezaki *et al.*, 2000). Glutathione S-transferases might also be involved in a signal transduction pathway between roots and shoots of *Arabidopsis* under various stresses including Al stress (Ezaki *et al.*, 2004).

Thioredoxin (TRX) is a small protein with two cysteines in its redox-active site that can form a disulfide in the oxidized form (TRX-S_2). It can function as a disulfide oxidoreductase (similar to GSH), or as an electron donor for TRX

peroxidase. The enzyme TRX reductase, which uses NADPH to reduce TRX-S_2 to TRX-$(SH)_2$, is involved in scavenging H_2O_2 and hydroperoxides (Meyer *et al.*, 1999) Thioredoxins and thioredoxin reductases identified in yeast have been found to protect against Al stress and oxidative stress (Pedrajas *et al.*, 1997; Cho *et al.*, 2001). Thioredoxins might also play a role in the activation of mitochondrial citrate synthase (Steven *et al.*, 1997) and the AOX (Vanlerberghe *et al.*, 1995), leading to increased exudation of citrate and therefore avoidance of Al stress and Al-induced ROS production. Exudation of organic anions and the subsequent formation of non-rhizotoxic Al-organic anion complexes is one of the major Al tolerance mechanisms (Kochian *et al.*, 2004). Manipulation of mitochondrial citrate synthase expression increased Al tolerance in yeast and canola (Anoop *et al.*, 2003).

Plants have evolved a complex array of defenses against ROS. These defenses appear to be coordinated by a complicated regulatory system (Apel and Hirt, 2004). Only a small of portion of this system has been characterized in the context of Al stress. Transcriptomic profiling of roots of *Arabidopsis* during Al stress revealed a large number of antioxidant defense genes are affected (Kumari *et al.*, 2008). Many questions about the link between Al toxicity and oxidative stress remained to be answered. For example how many components of the oxidative stress defense system are required to protect against Al injury and how are various components of this system regulated?

1.5. How do class III peroxidases control ROS triggered by aluminum in the apoplasm?

Plants have developed two different mechanisms to regulate ROS production and removal in response to biotic and abiotic stresses (Apel and Hirt, 2004). Upon biotic stresses (e.g., pathogen attack), plant cells increase ROS production in apoplast (oxidative burst) and suppress activity of intracellular ROS detoxification enzymes to induce programmed cell death (PCD) (Mittler *et al.*, 1999; Tiwari *et al.*, 2002). Plants utilize oxidative burst to kill invading pathogens and PCD to limit the spread of disease from the infection site (Bindschedler *et al.*, 2006). However, upon abiotic stresses, plant cells activate the intracellular antioxidant defense systems in various subcellular compartments to keep ROS level low, thus alleviating oxidative stress (Noctor and Foyer, 1998).

Plant cells achieve the oxidative burst through increased activities of NADPH-oxidases in the plasma membrane, and polyamine oxidases and class III peroxidases in cell walls (Grant and Loake, 2000). As enzymes involved in the regulation of ROS homeostasis, peroxidases have been shown to be involved in a wide range of physiological processes. There are three classes of plant heme peroxidases, the intracellular class I, the class II produced by fungi, and the secreted class III plant peroxidases (Valerio *et al*, 2004). Gene copy numbers of class III peroxidases have increased via extensive duplication. Consequently, gene structures of class III peroxidase are highly conserved (Passardi *et al.*, 2005). Higher plants possess a large set of class III peroxidases (Hiraga, 2001), which are present in soluble, ionically-bound, and covalently-bound forms in the cell wall. In *Arabidopsis*, 73 class III peroxidases have been identified (Valerio *et al*, 2004). The evolutionary relationship of these class III peroxidases is shown in Figure 1.2.

Class III peroxidases have been implicated in a wide array of physiological processes (Figure 1.3) such as detoxification of H_2O_2, auxin metabolism, polymerization of cell wall compounds, biosynthesis of lignin, defense against pathogens, cell elongation, and response to wounding (Yoshida *et al.*, 2003; Cosio and Dunand, 2009).

Class III peroxidases show diverse responses to Al stress at the transcriptional level. In roots of *Arabidopsis*, a total of fourteen peroxidase expression profiles were affected by Al treatment (Kumari *et al.*, 2008). Peroxidases are involved in two different catalytic cycles, peroxidative and hydroxylic (Passardi *et al.*, 2004). In the hydroxylic cycle, peroxidase is capable of producing H_2O_2, superoxide (O_2^-), and hydroxyl radicals (OH). This raises ROS levels, which can be used to defend against pathogens, modify the cell wall, and induce programmed cell death. In the peroxidative cycle, peroxidase is capable of reducing H_2O_2 by taking electrons from phenolic substrates, such as auxin, lignin precursors, and secondary metabolites, which can alleviate oxidative stress and catalyze the synthesis of lignin and suberin (Hiraga *et al.*, 2001). Although the function of peroxidases may seem paradoxical, their activity and expression are probably modulated precisely by internal substrate availability and external stimuli (Passardi *et al.*, 2005).

Many peroxidases are localized in the apoplast and are ionically or covalently attached to cell wall components. The apoplastic space and rhizosphere of roots have been suggested as major targeting sites of Al toxicity and one of the class III peroxidases (*PER22*) has been identified as an orthologue of root secreted extracytosolic protein in canola (Basu *et al.*, 2006). Root border cells (RBC) in root tips of barley have been demonstrated to secret peroxidase to the rhizosphere

under Al stress (Tamas *et al.*, 2005). This apoplastic peroxidase was responsible for the production of H_2O_2 in extracellular spaces, and was proposed to play an important role in Al-induced cell death of RBC in root tips of barley via oxidative burst (Pan *et al.*, 2001; Tamas *et al.*, 2005). Root tips of wheat and barley increase extracellular ROS levels through peroxidase and/or oxalate oxidase in response to Al stress. This may serve to trap Al in dead cells and prevent the further penetration of Al into the root tissue (Delisle *et al.*, 2001; Tamas *et al.*, 2005).

Aluminum (Al) toxicity has been reported to induce apoptotic like cell death in yeast, RBC of barley, and suspension cells of tomato (Zheng *et al.*, 2007; Tamas *et al.*, 2005; Yakimova *et al.*, 2007). Although evidence of Al-induced, apoptotic-like cell death is emerging, there is no systematic study of all the reported components involved in PCD in the context of Al toxicity. The extensive evidence for an interaction of Al toxicity and oxidative burst suggests that Al-induced apoptotic-like cell death might utilize a similar mechanism of pathogen-induced PCD. Upon pathogen attack, plant cells activate a coordinated production of ROS and suppression of ROS scavenging in order to increase ROS abundance to a sufficient level to trigger PCD (Mittler *et al.*, 1999). This is achieved by a simultaneous increase of extracellular ROS production by activating apoplast localized peroxidases, polyamine oxidases, and NADPH-oxidases (Grant and Loake, 2000) and a decrease of ROS scavenging capacity in the cytosol (Klessig *et al.*, 2000). It has shown that Al stress activates oxalate oxidase and apoplastic peroxidases (Tamas *et al.*, 2004; 2005), which are responsible for producing H_2O_2 in the extracellular space of barley roots (Simonovicova *et al.*, 2004). Aluminum stress has been reported to suppress catalase expression in root tips of *Arabidopsis* and soybean as well (Cakmak *et al.*, 1991; Richards *et al.*, 1998). This evidence seems to indicate that a pathogen defense-like PCD exist in Al injured root cells.

However, further experiments that simultaneously measure the activity of ROS regulating enzymes and ROS levels under Al stress are needed to confirm that Al-induced cell death of root border cells is indeed operated through PCD mechanism.

1.6. Modifications of cell walls by class III peroxidases under aluminum stress

Considerable experimental evidence from intact root cells (Jones *et al.*, 2006) or cell suspension cultures (Taylor *et al.*, 2000) indicates that the majority of Al accumulated by roots is bound to the cell walls. Aluminum toxicity has been shown to cause many alterations of the structure and function of cell walls through interaction with components of the cell wall matrix (xyloglucan, pectin, and cellulose) and induction of lignin and callose deposition (Sasaki *et al.*, 1996; Bhuja *et al.*, 2004). Aluminum is suggested to target specifically to the pectin matrix, which is primarily composed of negatively charged polygalacturonic acids (Ma *et al.*, 2007).

Aluminum (Al) has been reported to increase the synthesis of cell wall components (xyloglucan, pectin, and cellulose) in roots of squash (Le *et al.*, 1994). Cell wall composition was altered differently in roots of wheat by Al stress. Only xyloglucan and pectins were increased, but not cellulose (Hossain *et al.*, 2006). A recent study of maize suspension cells revealed that the degree of induction of pectin synthesis in the cell wall was closely associated with the extent of cell death caused by Al toxicity (Schmohl and Horst, 2000). A study of the interaction of Al with artificial Ca^{2+}-pectate membranes indicated that Al binding to pectin was affected by pH and Ca concentration (Blamey *et al.*, 1993). An Al-sensitive

cultivar of maize was found to bind more Al ions in pectin matrix of the cell wall (Schmohl and Horst, 2000), whereas an Al-resistant cultivar of maize could methylate pectin to reduce its negative charges and bind less Al in the root (Eticha *et al.,* 2005). Pectin was suggested to be the scaffold for class III peroxidases to mediate the polymerization of extensins (Dunand *et al.*, 2002).

Recently, Al stress has been reported to increase the accumulation of ferulic and diferulic acids in cell walls of an Al-sensitive cultivar of wheat by increasing the activity of phenylalanine ammonia lyase (PAL) (Hossain *et al.*, 2006). Increased accumulation of ferulic and diferulic acids in the cell wall are known to reduce cell elongation by providing more precursors for cell wall bound peroxidase to polymerize in the lignin biosynthesis pathway (Ralph *et al.*, 1995). Aluminum-induced lignin deposition is also related to peroxidase function via oxidative polymerization of lignin subunits (Sasaki *et al.*, 1996), which is associated with reduced cell wall extensibility (Lewis and Yamamoto, 1990). Therefore, it seems that Al-induced inhibition of cell elongation was caused by a decrease of cell wall extensibility and an increase of cell wall rigidification.

Class III peroxidases, due to their functions in peroxidative and hydroxylic cycles (Fig 1.4), play a paradoxical role in the regulation of cell wall extensibility and growth (Passardi *et al.*, 2004). Class III peroxidases inhibit cell elongation by reducing the extensibility of the cell wall (Fry, 1986, 1998; Biggs and Fry, 1987) by forming bonds between extensins, and by cross-linking lignin polymers and polysaccharide bound ferulates. This process is affected by the supply of phenol substrates and the concentrations of H_2O_2 and ascorbate (peroxidase inhibitor) (Schnabelrauch *et al.*, 1996). Class III peroxidases are also actively involved in lignin biosynthesis and lignification of cell walls. Histochemical staining and

fusion of promoters with reporter genes were employed to study peroxidase TP60 expression in tobacco (Blee *et al.*, 2003) and peroxidase A3a expression in hybrid aspen (Li *et al.*, 2003). Both studies revealed that these peroxidases were mainly expressed in lignifying tissues. Down-regulation of these peroxidases resulted in decreased levels of lignin and its precursors (Li *et al.*, 2003; Blee *et al.*, 2003). However, peroxidase activities were sometimes found to be negatively correlated with lignin levels in the elongation zone of onion root and in the hypocotyl of zucchini (Dunand *et al.*, 2003; Cordoba-Pedregosa *et al.*, 1996, 2003), which suggests that class III peroxidases were not the only candidate for cross-linking of lignin polymers.

Class III peroxidases can promote cell elongation by generating hydroxyl radical ($^{\bullet}OH$), which can cleave the cell wall polysaccharides, pectin and xyloglucan. This non-enzymatic cell wall loosening mechanism has been detected in the leaf expansion zone of maize (Rodriguez *et al.*, 2002) and root elongation zone of *Arabidopsis* (Foreman *et al.*, 2003). Recently, a study of two homologous class III peroxidises (*PER33* and *PER34*) from *Arabidopsis* using knockout and overexpression mutants indicated these peroxidases function in promoting cell elongation of roots of *Arabidopsis* (Passardi *et al.*, 2006). However, these mutants were not tested for Al tolerance. Overall, class III peroxidases can regulate cell elongation by generating reactive hydroxyl radicals ($^{\bullet}OH$) via the hydroxylic cycle to promote cell wall loosening, or by cross-linking cell wall polymers to promote cell wall stiffening (Mittler *et al.*, 2004).

1.7. Conclusions and objectives

Aluminum (Al) stress presents an increasing threat to agriculture as soil acidification intensifies, especially in developing countries. Improving Al tolerance is of paramount importance for fully maximizing the productivity of crops. In the past few decades, plant biologists have made enormous progress in elucidating the mechanisms of Al toxicity and tolerance as well as developing various genetically engineered, Al tolerant plants.

Aluminum (Al) toxicity triggers the expression of a number of genes that are related to oxidative stress, so characterizing one of the ROS regulating enzymes, class III peroxidases, draws great interest in my research. Class III peroxidases include a large number of apoplastic, cell wall bound, and vacuolar proteins that function in hydroxylic and peroxidative cycles. While it appears that some peroxidases are associated with control of growth, some peroxidises regulate ROS levels, and some might be responsible for PCD in plant cells (Passardi *et al.*, 2005). It is challenging to pinpoint the role of specific peroxidases in each pathway or the process in which they are involved.

In roots of *Arabidopsis*, fourteen class III peroxidases were up- and down-regulated following Al stress (Kumari *et al.*, 2008), which highlights the diverse functions of class III peroxidases and the multiple targets of Al toxicity in plant roots. Among the 73 class III peroxidases in *Arabidopsis thaliana*, several functions have been characterized using transcriptomic or proteomic analyses, and generation of transgenic plants harbouring specific peroxidase promoter::reporter gene fusion. However, the function of the majority of the class III peroxidase remains elusive.

Arabidopsis class III peroxidase (*PER53*) cloned from lignifying cell suspension cultures of *Arabidopsis*, was homologous to horseradish peroxidase (HPR) A2 (Ostergaard *et al.*, 2000). A promoter::*GUS* fusion study revealed that this peroxidase was mainly expressed in lignifying vascular tissues (Ostergaard *et al.*, 2000). A well characterized peroxidase gene of zinnia, *ZPO-C*, was found to be involved in vessel lignification and expressed specifically in differentiating tracheary elements (Sato *et al.*, 2006). Fusion of the promoter of *ZPO-C*'s homolog, *PER66*, in *Arabidopsis* with yellow fluorescent protein (YFP) revealed that its expression was restricted to root vessels, suggesting its function in lignifications as well (Sato *et al.*, 2006). The *Arabidopsis PER3* was isolated as a cold inducible gene. Its promoter::*GUS* fusion showed that expression was restricted to the endodermis in roots (Llorente *et al.*, 2002). Reverse genetics studies indicated that *PER3* was also regulated by ABA, salt stress, and dehydration (Llorente *et al.*, 2002). Overexpression and knock-out mutants showed salt and dehydration tolerant or salt and dehydration sensitive phenotypes, respectively (Llorente *et al.*, 2002). The most interesting peroxidases characterized so far are *Arabidopsis PER33* and *PER34*, which are suggested to be involved in developmental process (Passardi *et al.*, 2006) and defense mechanisms via the oxidative burst (Bindschedler *et al.*, 2006). Transgenic *Arabidopsis* expressing an anti-sense french bean peroxidase type 1 (FBP1) cDNA silenced its two orthologues *PER33* and *PER34*, which resulted in an impaired oxidative burst in response to pathogen attack (Bindschedler *et al.*, 2006). After detecting *PER33* and *PER34* expression in cell walls of roots, T-DNA insertion mutants of *PER33* and double mutant of *PER33* and *PER34* exhibited shorter root lengths than WT (Passardi *et al.*, 2006). Overexpression of

PER34 resulted in longer root length than WT, which was achieved by modifying cell walls to promote cell elongation (Passardi *et al.*, 2006).

Transcriptomic analysis of root tissue from Al-treated *Arabidopsis* seedlings and untreated controls identified *PER73* as the most differentially expressed class III peroxdiase under Al stress (Kumari *et al.*, 2008). Proteomic analysis of extracytosolic proteins secreted by root tissues of *Arabidopsis* and canola identified *PER22* as a homologue of one of the most abundant root protein exuded from canola (Basu *et al.*, 2006). These preliminary transcriptome and proteome analyses present *PER22* and *PER73* as interesting candidate genes to elucidate the link between class III peroxidases and Al stress. The objective of my research was to test the hypothesis that these genes play a role in mediating the response of *Arabidopsis* to Al. To test this hypothesis, I studied the spatial and temporal expression of *PER22* (At2g38380) and *PER73* (At5g67400) under conditions of Al stress in *Arabidopsis*. My approach was to utilize reporter constructs with the promoter from each gene of interest fused to the *GUS* reporter gene. These constructs were introduced into *Arabidopsis* and homozygous, single-copy insertion lines were analyzed for patterns of gene expression. Histochemical staining revealed the spatial expression of these two peroxidases, which helps shed light on their possible function(s), helps us understand the biological processes in which they are involved (e.g. cell wall modification, ROS regulation, or the oxidative burst), and how these processes might contribute to plant response to Al .

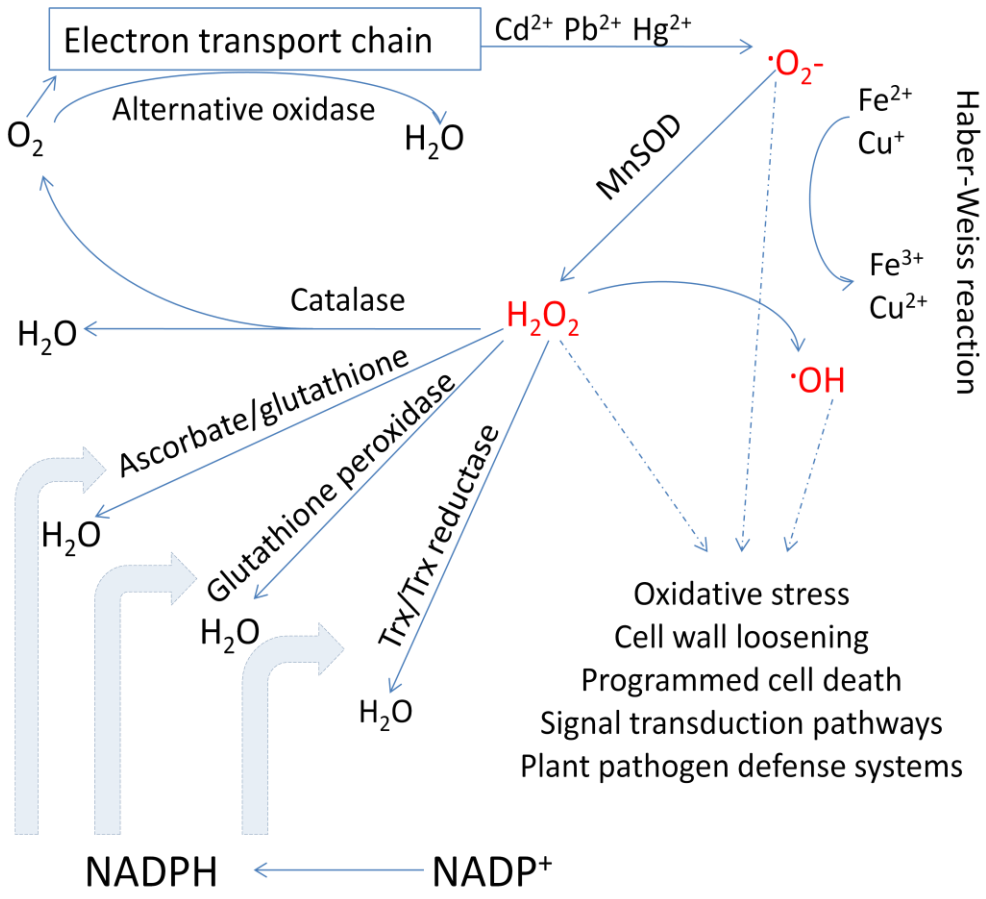

Figure 1.1. Generation of reactive oxygen species (ROS) by metals and ROS detoxification pathways in plant mitochondria. Reactive oxygen species (Red color) have been known to contribute positive and negative effects in plant systems. Positive effects include cell signaling, cell wall loosening, and plant pathogen defense via the oxidative burst. Negative effects include triggering of oxidative stress and programmed cell death (PCD) (adapted from Moller, 2001).

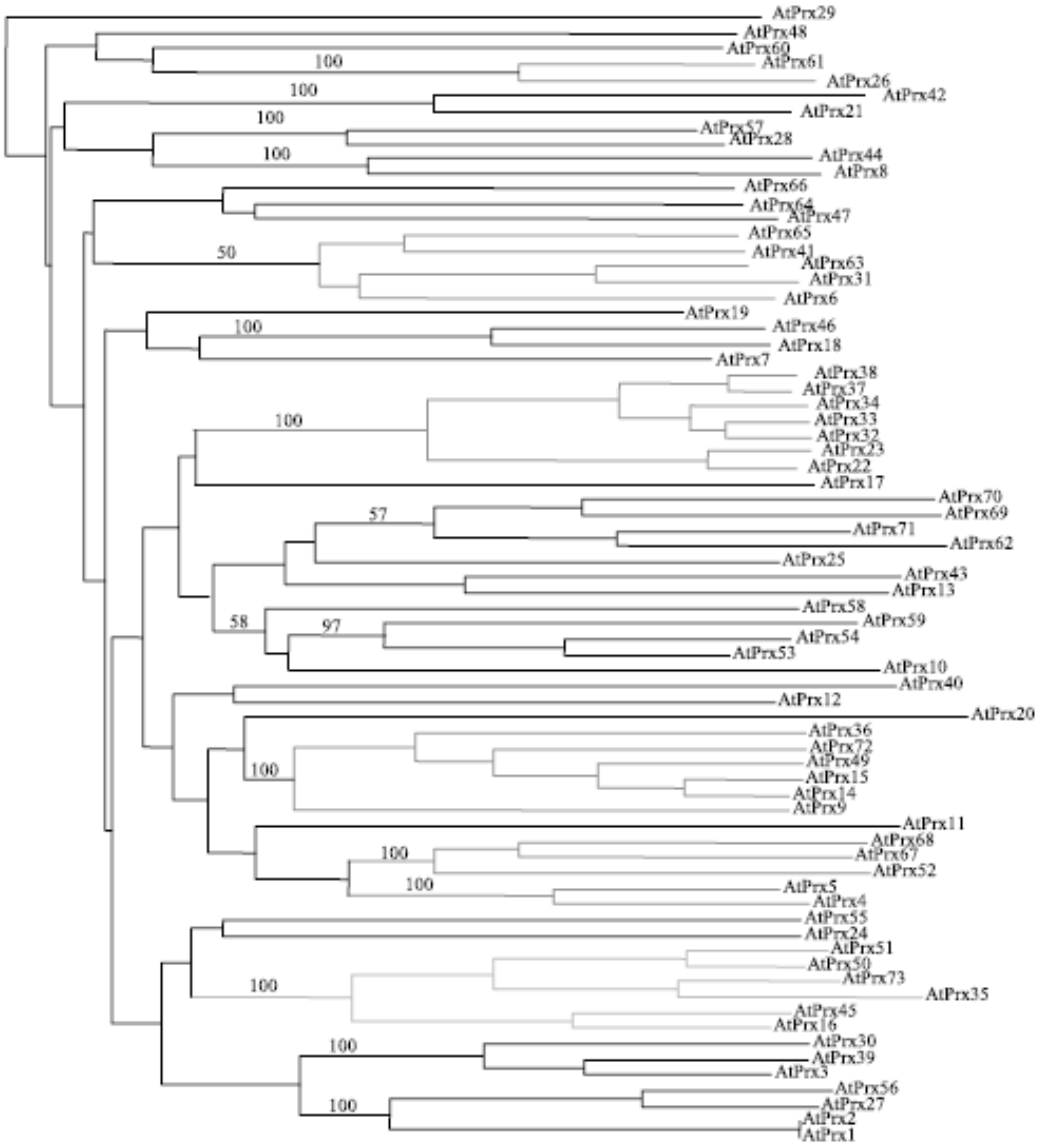

Figure 1.2. Phylogenetic tree of *Arabidopsis* class III peroxidases based on the sequence alignments of coding regions (from Valerio *et al.*, 2004).

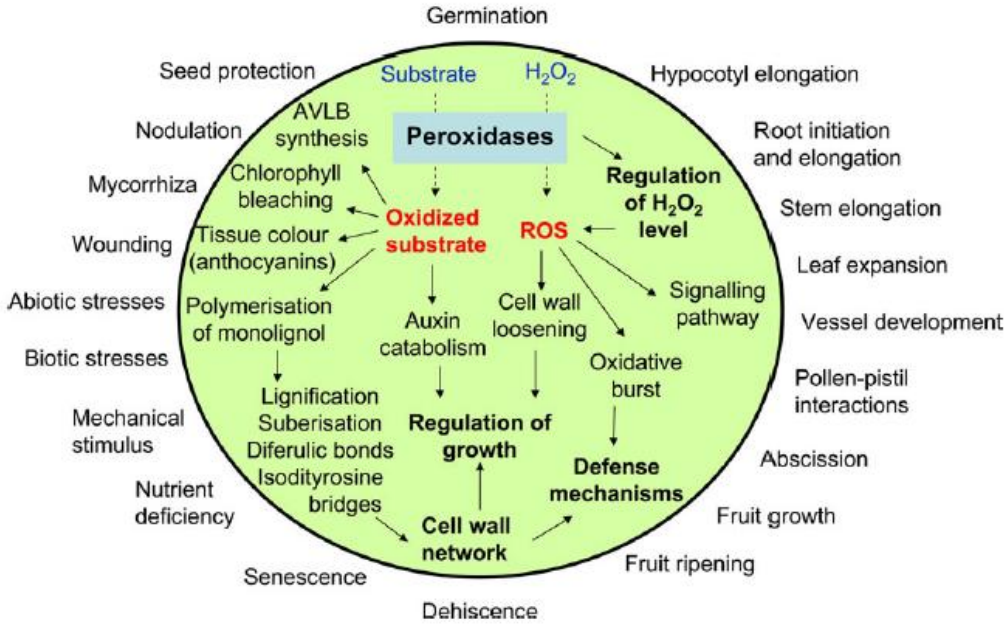

Figure 1.3. The versatile functions and roles of class III peroxidases in plant systems. Functions can be classified into four major catagories: plant defense mechanism, lignification, ROS regulation, and cell wall modifications (from Cosio and Dunand, 2009).

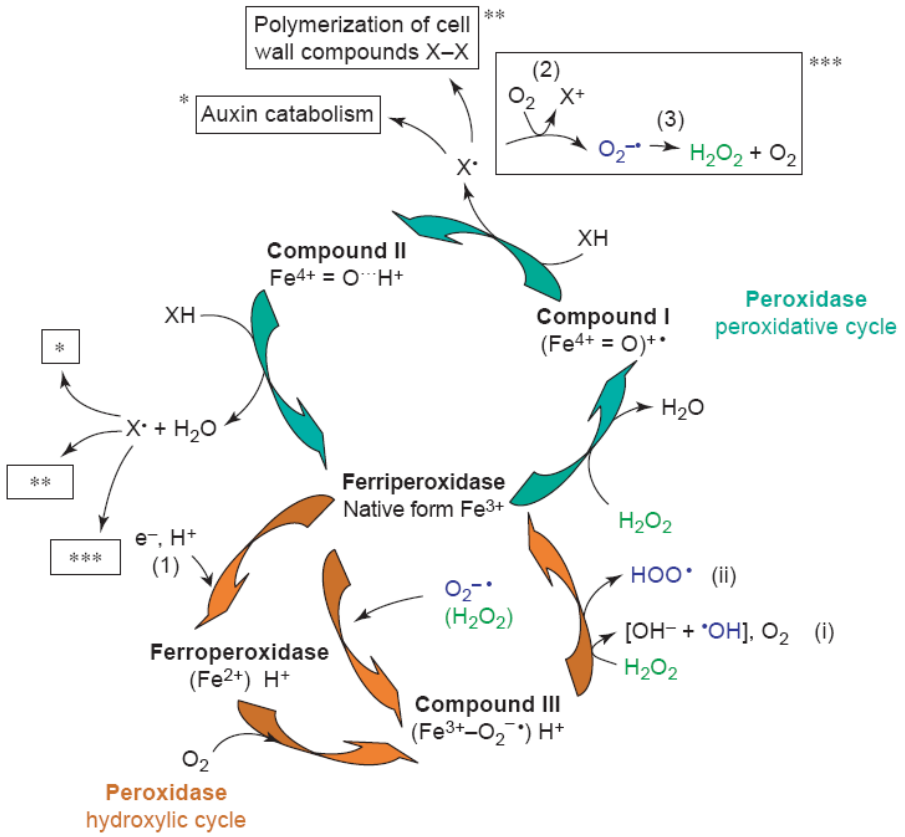

Figure 1.4. The hydroxylic and peroxidative cycles of class III peroxidases. The hydroxylic and peroxidative cycles are represented in orange and green colors, respectively. The hydroxylic cycle produces reactive oxygen species (ROS) such as ȮH (Liszkay *et al.*, 2003; Kawano *et al.*, 2003). Both hydroxylic and peroxidative cycles can regulate H_2O_2 and $ȮO_2^-$ levels (from Passardi *et al.*, 2004).

1.8. References

Akeson MA, Munns DN. 1989. Lipid bilayer permeation by neutral aluminum citrate and by three -hydroxy carboxylic acid. Biochim Biophys Acta 984: 200-206.

Akeson MA, Munns DN, Burau RG. 1989. Adsorption of Al^{3+} to phosphatidylcholine vesicles. Biochim Biophys Acta 986: 33-40.

Alscher RG, Erturk N, Heath LS. 2002. Role of superoxide dismutases (SODs) in controlling oxidative stress in plants. J Exp Bot 53: 1331-1341.

Andersson P, Berggren D, Nilsson SI. 2002. Experimental studies of nitrogen mineralization and nitrification and model simulation of nitrogen saturation. Forest Ecol Manag. 157: 39-53.

Anoop VM, Basu U, McCammon MT, McAlister-Henn L, Taylor GJ. 2003. Modulation of citrate metabolism alters aluminum tolerance in yeast and transgenic canola overexpressing a mitochondrial citrate synthase. Plant Physiol 132: 2205-2217.

Apell K, Hirt H. 2004. Reactive oxygen species: metabolism, oxidative stress, and signal transduction. Annu Rev Plant Biol 55: 373-399.

Archambault DJ, Zhang G, Taylor GJ. 1996. Accumulation of Al in root mucilage of an Al-resistant and an Al-sensitive cultivar of wheat. Plant Physiol 112: 1471-1478.

Barcelo J, Poschenrieder C. 2002. Fast root growth responses, root exudates, and internal detoxification as clues to the mechanisms of aluminium toxicity and resistance. Environ Exp Bot 48: 75-92.

Basu A, Basu U, Taylor GJ. 1994. Induction of microsomal membrane proteins in roots of an aluminum-resistant cultivar of *Triticum aestivum* L. under conditions of aluminum stress. Plant Physiol 104: 1007-1013.

Basu U, McDonald-Stephens JL, Archambault DJ, Good AG, Briggs KG, Taing-Aung, Taylor GJ. 1997. Genetic and physiological analysis of doubled-haploid, aluminum resistant lines of wheat provide evidence for the

involvement of a 23 kD, root exudate polypeptide in mediating resistance. Plant Soil 196: 283-288.

Basu U, Good AG, Aung T, Slaski JJ, Basu A, Briggs KG, Taylor GJ. 1999. A 23 kD, aluminum-binding, root exudates polypeptide co-segregates with the aluminum-resistant phenotype in *Triticum aestivum*. Physiol Plant 106: 53-61.

Basu U, Good A, Taylor GJ. 2001. Transgenic *Brassica napus* plants overexpressing aluminum-induced mitochondrial manganese superoxide dismutase cDNA are resistant to aluminum. Plant Cell Environ 24: 1269-1278.

Basu U, Southern JL, Stephens JL, Taylor GJ. 2004. Reverse genetic analysis of the glutathione metabolic pathway suggests a novel role of PHGPX and URE2 genes in aluminum resistance in *Saccharomyces cerevisiae*. Mol Gen Genetics 271: 627-637.

Basu U, Francis JL, Whittal RM, Stephens JL, Wang Y, Zaiane OR, Goebel R, Muench DG, Good AG, Taylor GJ. 2006. Extracellular proteomes of *Arabidopsis thaliana* and *Brassica napus* roots: Analysis and comparison by MudPIT and LC-MS/MS. Plant Soil 286: 357-376.

Becana M, Moran JF, Iturbe-Ormaetxe I. 1998. Iron-dependent oxygen free radical generation in plants subjected to environmental stress: toxicity and antioxidant protection. Plant Soil 201:137-147.

Bennet RJ, Breen CM. 1991. The recovery of the roots of Zea mays L. from various Aluminum treatments: Towards elucidating the regulatory processes that underlie root growth control. Envir Exp Bot 31:153-163.

Bhuja P, McLachlan K, Stephens J, Taylor GJ. 2004. Accumulation of 1,3-beta-D-glucans, in response to aluminum and cytosolic calcium in *Triticum aestivum*. Plant Cell Physiol 45: 543-549.

Biggs KJ, Fry SC. 1987. Phenolic cross-linking in the cell wall. In DJ Cosgrove, DP Knievel, eds, Physiology of Cell Expansion during Plant Growth. American Society of Plant Physiologists, Rockville, MD, pp 46-57.

Bindschedler LV, Dewdney J, Blee KA, Stone JM, Asai T, Plotnikov J, Denoux C, Hayes T, Gerrish C, Davies DR, Ausubel FM, Bolwell GP. 2006.

Peroxidase dependent apoplastic oxidative burst in *Arabidopsis* required for pathogen resistance. Plant J 47: 851-863.

Blamey FPC, Asher CJ, Kerven GL, Edwards DG. 1993. Factors affecting aluminium sorption by calcium pectate. Plant Soil 149: 87-94.

Blamey FPC, Dowling AJ. 1995. Antagonism between aluminium and calcium for sorption by calcium pectate. Plant Soil 171: 137-140.

Blee KA, Choi JW, O'Connell AP, Schuch W, Lewis NG, Bolwell GP. 2003. A lignin-specific peroxidase in tobacco whose antisense suppression leads to vascular tissue modification. Phytochemistry-US 64: 163-176.

Boscolo PR, Menossi M, Jorge RA. 2003. Aluminum-induced oxidative stress in maize. Phytochemistry-US 62: 181-189.

Bueono P, Piqueras A. 2002. Effect of transition metals on stress, lipid peroxidation and antioxidant enzyme activities in tobacco cell cultures. Plant Growth Regul 36: 161-167.

Cakmak I, Horst WJ. 1991. Effect of aluminum on lipid peroxidation, superoxide dismutase, catalase, and peroxides activities in root tips of soybean (*Glycine max*). Physiol Plant 83: 463-468.

Cho Y, Shin YH, Kim Y, Kim H, Lee Y, Park E, Fuchs JA, Lim C. 2001. Characterization and regulation of Schizosaccharomyces pombe gene encoding thioredoxin. Biochim Biophys Acta 1518: 194-199.

Cordoba-Pedregosa M, González-Reyes JA, Cañadillas M, Navas P, Córdoba F. 1996. Role of apoplastic and cell-wall peroxidases on the stimulation of root elongation by ascorbate. Plant Physiol 112: 1119-1125.

Cordoba-Pedregosa M, Cordoba F, Villalba JM, Gonzalez-Reyes JA. 2003. Zonal changes in ascorbate and hydrogen peroxide contents, peroxidase, and ascorbate-related enzyme activities in onion roots. Plant Physiol 131: 697-706.

Cosio C, Dunand C. 2009. Specific functions of individual class III peroxidase genes. J Exp Bot 60: 391-408.

Cuypers A, Vangronsveld J, Clijsters H. 1999. The chemical behaviour of heavy metals plays a prominent role in the induction of oxidative stress. Free Rad Res 31: 39-43.

Darko E, Ambrus H, Stefanovits-Banyai E, Fodor J, Bakos F, Barnaba B. 2004. Aluminium toxicity, Al tolerance and oxidative stress in an Al-sensitive wheat genotype and in Al-tolerant lines developed by in vitro microspore selection. Plant Sci 166: 583-591.

Delhaize E, Craig S, Beaton CD, Bennet RJ, Jagadish VC, Randall PJ. 1993. Aluminum tolerance in wheat (*Triticum aestivum* L.).I. Uptake and distribution of aluminum in root apices. Plant Physiol 103: 685-693.

Delhaize E, Ryan PR. 1995. Aluminum toxicity and tolerance in plants. Plant Physiol. 107: 315-321.

Delisle G, Champoux M, Houde M. 2001. Characterization of Oxalate Oxidase and Cell Death in Al-Sensitive and Tolerant Wheat Roots. Plant Cell Physiol 42: 324-333.

Doncheva S, Amenos M, Poschenrieder C, Barcelo J. 2005. Root cell patterning: A primary target for aluminium toxicity in maize. J Exp Bot 56: 1213-1220.

Driscoll CT, Schecher WD. 1988. Aluminum in the environment. In ‘‘Metal Ions in Biological Systems: Aluminum and Its Role in Biology’’ (H. Sigel and A. Sigel, Eds.), Vol. 24, pp. 59-122. Marcel Dekker, New York.

Dunand C, Tognolli M, Overney S, Tobel L, Meyer M, Simon P, Penel C. 2002. Identification and characterisation of Ca^{2+}-pectate binding peroxidases in *Arabidopsis thaliana*. J Plant Physiol 159: 1165-1171.

Dunand C, Meyer MD, Crèvecoeur M, Penel C. 2003. Expression of a peroxidase gene in zucchini in relation with hypocotyl growth. Plant Physiol Biochem 41: 805-811.

Edwards EA, Rawsthorne S, Mullineaux P. 1990. Subcellular distribution of multiple forms of glutathione reductase in leaves of pea (*Pisum sativum* L.). Planta 180: 278-284.

Edwards, R, Dixon, DP, Walbot, V. 2000. Plant glutathione S-transferases: enzymes with multiple functions in sickness and in health. Trends Plant Sci 5: 193-198.

Eshdat Y, Holland D, Faltin Z, Ben-Hayyim G. 1997. Plant glutathione peroxidases. Physiol Plant 100: 234-240.

Eticha D, Stass A, Horst WJ. 2005. Cell-wall pectin and its degree of methylation in the maize root-apex: Significance for genotypic differences in aluminium resistance. Plant Cell Environ 28: 1410-1420.

Ezaki B, Yamamoto Y, Matsumoto H. 1995. Cloning and sequencing of the cDNAs induced by aluminum treatment and Pi starvation in cultured tobacco cells. Physiol Plant 93: 11-18.

Ezaki B, Tsugita S, Matsumoto H. 1996. Expression of a moderately anionic peroxidases is induced by aluminum treatment in tobacco cells: possible involvement of peroxidase isozymes in aluminum ion stress. Physiol Plant 96: 21-28.

Ezaki B, Sivaguru M, Ezaki Y, Matsumoto H, Gardner RC. 1999. Acquisition of aluminum tolerance in Saccharomyces cerevisiae by expression of the BCB or NtGDI1 gene derived from plants. FEMS Microbiol Lett 171: 81-87.

Ezaki B, Gardner RC, Ezaki Y, Matsumoto H. 2000. Expression of aluminum-induced genes in transgenic *Arabidopsis* plants can ameliorate aluminum stress and/or oxidative stress. Plant Physiol 122: 657–665.

Ezaki B, Katsuhara M, Kawamura M, Matsumoto H. 2001. Different mechanisms of four aluminum (Al)-resistant transgenes for Al toxicity in *Arabidopsis*. Plant Physiol 127: 918–927.

Ezaki B, Suzuki M, Motoda H, Kawamura M, Nakashima S, Matsumoto H. 2004. Mechanism of gene expression of *Arabidopsis* glutathione S-transferase, AtGST1, and AtGST11 in response to aluminum stress. Plant Physiol 134: 1672-1682.

Exley C. 2004. The pro-oxidant activity of aluminum. Free Radic Biol Med 36: 380-387.

Foreman J, Demidchik V, Bothwell JH, Mylona P, Miedema H, Torres MA, Linstead P, Costa S, Brownlee C, Jones JD, Davies JM, Dolan L. 2003. Reactive oxygen species produced by NADPH oxidase regulate plant cell growth. Nature 422: 442-446.

Foy CD. 1983. The physiology of plant adaptation to metal stress. Iowa State J Res 57: 355-391.

Fry SC.1986. Cross-linking of matrix polymers in the growing cell wall of angiosperms. Annu Rev Plant Physiol 37: 165-186.

Fry SC. 1998. Oxidative scission of plant cell wall polysaccharides by ascorbate-induced hydroxyl radicals. Biochem J 332: 507-515.

Fryer MJ, Oxborough K, Mullineaux PM, Baker NR. 2002. Imaging of photooxidative stress responses in leaves. J Ex Bot 53: 1249-1254.

Grant JJ, Loake GJ. 2000. Role of reactive oxygen intermediates and cognate redox signaling in disease resistance. Plant Physiol 124: 21-29.

Gunse B, Poschenrieder C, Barcelo J. 1997. Water transport property of roots and root cortical cells in proton- and Al-stressed Maize varieties. Plant Physiol 113: 595-602.

Gutteridge JMC, Qiunlan, GJ, Clark I, Halliwell B. 1985. Aluminum salts accelerate peroxidation of membrane lipids stimulated by iron salts. Biochim Biophys Acta 835: 441-447.

Hartwell BL, Pember FR. 1918. The presence of Aluminum as a reason for the difference in the effect of so-called acid soil on barley and rye Soil Sci 6: 259-279.

Hasenstein KH, Evans ML. 1988. Effects of cations on hormone transport in primary roots of *Zea mays*. Plant Physiol 86: 890-894.

Hiraga S, Sasaki K, Ito H, Ohashi Y, Matsui H. 2001. A large family of class III plant peroxidases. Plant Cell Physiol 42: 462-468.

Horst WJ, Asher CJ, Cakmak I, Szulkiewica P,Wissemeier AH. 1992. Short-term responses of soybean roots to Al. J Plant Physiol 140: 174-178.

Horst WJ. 1995. The role of the apoplast in aluminium toxicity and resistance of higher plants: a review. Z Pflanzenernahr Bodenk 158: 419-428.

Horst WJ, Püschel AK, Schmohl N. 1997. Induction of callose formation is a sensitive marker for genotypic aluminium sensitivity in maize. Plant Soil 192: 23-30.

Horst WJ, Schmohl N, Kollmeier M, Baluska F, Sivaguru M. 1999. Does aluminium affect root growth of maize through interaction with the cell wall-plasma membrane-cytoskeleton continuum? Plant Soil 215: 163-174.

Hossain A, Koyama H, Hara T. 2006. Growth and cell wall properties of two wheat cultivars differing in their sensitivity to aluminum stress. J Plant Physiol 163: 39-47.

Huang JW, Grunes DL, Kochian LV. 1992. Aluminum effects on the kinetics of calcium uptake into cells of the wheat root apex. Planta 188: 414-421.

Huang JW. Shaff JE, Grunes DL, and Kochian LV. 1992. Aluminium effects on calcium fluxes at the root apex of aluminum-tolerant and aluminum-sensitive wheat cultivars. Plant Physiol 98: 230-237.

Inoue Y, Matsuda T, Sugiyama K, Izawa S, Kimura A. 1999. Genetic analysis of glutathione peroxidase in oxidative stress response of *Saccharomyces cerevisiae*. J Biol Chem 274: 27002-27009.

Jonak C, Ökresz L, Bögre L, Hirt H. 2002. Complexity, cross talk and integration of plant MAP kinase signaling. Curr Opin Plant Biol 5: 415-424.

Jones DL, Kochian LV. 1997. Aluminum interaction with plasma membrane lipids and enzyme metal binding sites and its potential role in Al cytotoxicity. FEBS Lett 400: 51-57.

Jones DL, Gilroy S, Larsen PB, Howell SH, Kochian LV. 1998. Effect of aluminum on cytoplasmic Ca^{2+} homeostasis in root hairs of *Arabidopsis thaliana*. Planta 206: 378-387.

Jones DL, Blancaflor EB, Kochian LV, Gilroy S. 2006. Spatial coordination of aluminium uptake, production of reactive oxygen species, callose

production and wall rigidification in maize roots. Plant Cell Environ 29: 1309-1318.

Kawano T. 2003. Roles of the reactive oxygen species-generating peroxidase reactions in plant defense and growth induction. Plant Cell Rep. 21: 829-837.

Klessig DF, Durner J, Noad R, Navarre DA, Wendehenne D, Kumar D, Zhou JM, Shah J, Zhang S, Kachroo P, Trifa Y, Pontier D, Lam E, Silva H. 2000. Nitric oxide and salicylic acid signaling in plant defense. Proc Natl Acad Sci USA 97: 8849-8855.

Kochian LV, Hoekenga OA, Pineros MA. 2004. How do crop plants tolerate acid soils? Mechanisms of aluminum tolerance and phosphorous efficiency. Annu Rev Plant Biol 55: 459-493.

Kollmeier M, Felle HH, Horst WJ. 2000. Genotypical differences in aluminum resistance of maize are expressed in the distal part of the transition zone. Is reduced basipetal auxin flow involved in inhibition of root elongation by aluminum? Plant Physiol 122: 945-956.

Kumari M, Taylor GJ, Deyholos MK. 2008. Transcriptomic responses to aluminum stress in roots of *Arabidopsis thaliana*. Mol Genet Genomics 279: 339-357.

Kwon SI, An CS. 2001. Molecular cloning, characterization and expression analysis of a catalase cDNA from hot pepper (*Capsicum annuum* L.). Plant Sci 160: 961-969.

Lazof DB, Goldsmith JG, Rufty TW, Linton RW. 1994. Rapid uptake of Aluminum into cells of intact soybean root tips: A microanalytical study using secondary ion mass spectrometry. Plant Physiol 106:1107-1114.

Le Van H, Kuraishi S, Sakurai N. 1994. Aluminum-induced rapid root inhibition and changes in cell-wall components of squash seedings. Plant Physiol 106: 971-976.

Lewis NG, Yamamoto E. 1990. Lignin: occurrence, biogenesis and biodegradation. Annu Rev Plant Physiol Plant Mol Biol 41: 455-496.

Li Y, Kajita S, Kawai S, Katayama Y, Morohoshi N. 2003. Down-regulation of an anionic peroxidase in transgenic aspen and its effect on lignin characteristics. J Plant Res 116: 175-182.

Liszkay A, Kenk B, Schopfer P. 2003. Evidence for the involvement of cell wall peroxidase in the generation of hydroxyl radicals mediating extension growth. Planta 217:658-667.

Llorente F, Lopez-Cobollo RM, Catala R, Martinez-Zapater JM, Salinas J. 2002. A novel cold-inducible gene from *Arabidopsis*, RCI3, encodes a peroxidase that constitutes a component for stress tolerance Plant J 32: 13-24.

Ma JF, Ryan PR, Delhaize E. 2001. Aluminium tolerance in plants and the complexing role of organic acids. Trends Plant Sci 6: 273-278.

Ma JF, Shen RF, Nagao S, Tanimoto E. 2004. Aluminum targets elongating cells by reducing cell wall extensibility in wheat roots. Plant Cell Physiol 45: 583-589.

Ma JF. 2007. Syndrome of aluminum toxicity and diversity of aluminum resistance in higher plants. Int Rev Cytol 264: 225-252.

Massot N, Llugany M, Poschenrieder C, Barcel ó J. 1999. Callose production as indicator of aluminum toxicity in bean cultivars. J Plant Nutr 22: 1-10.

Matsumoto H, Yamamoto Y, Kasai M. 1992. Changes of some properties of the plasma membrane-enriched fraction of barley roots related to aluminum stress: Membrane associated ATPase, aluminum and calcium. Soil Sci Plant Nutr 38: 411-419.

Matsumoto H. 2000. Cell biology of aluminum toxicity and tolerance in higher plants. Int Rev Cytol 200: 1-46.

Mendez-Alvarez E, Soto-Otero R., Hermida-Ameijeiras A, Lopez-Real AM, Labandeira-Garcia JL. 2002. Effects of aluminum and zinc on the oxidative stress caused by 6-hydroxydopamine autoxidation: relevance for the pathogenesis of Parkinson's disease. Biochim Biophys Acta 1586: 155-168.

Meriga B, Reddy BK, Rao KR, Reddy LA, Kishor PB. 2004. Aluminium-induced production of oxygen radicals, lipid peroxidation and DNA damage in seedlings of rice (*Oryza sativa*). J Plant Physiol 161: 63-68.

Mittler R, Herr EH, Orvar BL, Van Camp W, Willekens H, Inzé D, Ellis BE. 1999. Transgenic tobacco plants with reduced capability to detoxify reactive oxygen intermediates are hyperresponsive to pathogen infection. Proc Natl Acad Sci USA 96: 14165-14170.

Mittler R. 2002. Oxidative stress, antioxidants and stress tolerance. Trends in Plant Sci 7: 405-410.

Mittler R, Vanderauwera S, Gollery M, Van Breusegem F. 2004. Reactive oxygen gene network of plants. Trends Plant Sci 9: 490-498.

Murgia I, Tarantino D, Vannini C, Bracale M, Carravieri S, Soave C. 2004. *Arabidopsis thaliana* plants overexpressing thylakoidal ascorbate peroxidase show increased resistance to Paraquat-induced photooxidative stress and to nitric oxide-induced cell death. Plant J 38: 940-953.

Meyer Y, Vervoucz L, Vignols F. 1999. Plant thioredoxins and glutaredoxins: identity and putative roles. Trends Plant Sci 4: 388-394.

Naora H, Naora H, Mirsky AE, Allfrey VG. 1961. Magnesium and Calcium in isolated cell nuclei. J Gen Physiol 44: 731-741.

Nichol B, Oliveira LA, Glass ADM, Siddiqi MY. 1993. The effects of aluminum on the influx of calcium, potassium, ammonium, nitrate, and phosphate in an aluminum sensitive cultivar of barley (*Hardeum vulgare* L.). Plant Physiol 101: 1263-1266.

Noctor G, Foyer C. 1998. Ascorbate and Glutathione: Keeping active oxygen under control. Annu Rev Plant Physiol Plant Mol Biol 49: 249-279.

Ono K, Yamamoto Y, Hachiya A, Matsumoto H. 1995. Synergistic inhibition of growth by aluminum and iron of tobacco (*Nicotiana tabacum* L.) cells in suspension culture. Plant Cell Physiol 36: 115-125.

Ostergaard L, Teilum K, Mirza O, Mattsson O, Petersen M, Welinder KG, Mundy J, Gajhede M, Henriksen A. 2000. *Arabidopsis* ATP A2 peroxidase.

Expression and high-resolution structure of a plant peroxidase with implications for lignification. Plant Mol Biol 44: 231-243.

Oteiza PL. A mechanism for the stimulatory effect of aluminum on iron-induced lipid peroxidation. 1994. Arch Biochem Biophys 308: 374-379.

Pan J, Zhu M, Chen H. 2001. Aluminum-induced cell death in root-tip cells of barley. Environ Exp Bot 46: 71-79.

Passardi F, Penel C, Dunand C. 2004. Performing the paradoxical: how plant peroxidases modify the cell wall. Trends Plant Sci 9: 534-540.

Passardi F, Cosio C, Penel C, Dunand C. 2005. Peroxidases have more functions than a Swiss army knife. Plant Cell Rep. 24: 255-65.

Passardi F, Tognolli M, De Meyer M, Penel C, Dunand C. 2006. Two cell wall associated peroxidases from *Arabidopsis* influence root elongation. Planta 223: 965-974.

Pedrajas JR, Kosmidou E, Miranda-Vizuete A, Gustafsson JA, Wright AP, Spyrou G. 1999. Identification and functional characterization of a novel mitochondrial thioredoxin system in *Saccharomyces cerevisiae*. J Biol Chem 274: 6366-6373.

Pineros MA, Tester M. 1995. Characterization of a voltage-dependent Ca^{2+} selective channel from wheat roots. Planta 195: 478-488.

Pineros MA, Tester M. 1997. Calcium channels in higher plant cells: sensitivity, regulation and pharmacology. J Exp Bot 46: 551-577.

Pineros MA, Kochian LV. 2001. A patch-clamp study on the physiology of aluminum toxicity and aluminum tolerance in maize. Identification and characterization of Al^{3+}-induced anion channels. Plant Physiol 125: 292-305.

Porter WM. 1981. Soil acidification-the cause. Proceedings Riverina Outlook Conference: 3l-46.

Ralph J, Grabber JH, Hartfield RD. 1995. Lignin-ferulate crosslinking in grasses: active incorporation of ferulate polysaccharides esters into ryegrass lignins. Carbohydrate Res 1275: 167-178.

Richards KD, Schott EJ, Sharma YK, Davis KR, Gardner RC. 1998. Aluminum induces oxidative stress genes in *Arabidopsis thaliana*. Plant Physiol 116: 409-418.

Rodriguez AA, Grunberg KA, Taleisnik EL. 2002. Reactive oxygen species in the elongation zone of maize leaves are necessary for leaf extension. Plant Physiol 129: 1627-1632.

Roxas VP, Smith RK Jr, Allen ER, Allen RD. 1997. Overexpression of glutathione S-transferase/glutathione peroxidase enhances the growth of transgenic tobacco seedlings during stress. Nat Biotechnol 15: 988-991.

Ryan PR, Ditomaso JM, Kochian LV. 1993. Aluminum toxicity in roots: An investigation of spatial sensitivity and the role of the root cap. J Exp Bot 44: 437-446.

Ryan PR, Reid RJ, Smith FA. 1997. Direct evaluation of the Ca^{2+} displacement hypothesis for Al toxicity. Plant Physiol 113: 1351-1357.

Sasaki M, Yamamoto Y, Matsumoto H. 1996. Lignin deposition induced by aluminum in wheat (*Triticum aestivum*) roots. Physiol Plant 96: 193-198.

Sasaki M, Yamamoto Y, Ma JF, Matsumoto H. 1997. Early events induced by aluminum stress in elongating cells of wheat root. Soil Sci Plant Nutr 43:1009-1014.

Sato Y, Demura T, Yamawaki K, Inoue Y, Sato S, Sugiyama M, Fukuda H. 2006. Isolation and characterization of a novel peroxidase gene ZPO-C whose expression and function are closely associated with lignification during tracheary element differentiation. Plant and Cell Physiol 47: 493-503.

Schildknecht P, Vidal B. 2002. A role for the cell wall in Al^{3+} resistance and toxicity: crystallinity and availability of negative charges. Int Arch Biosci 2002: 1087-1095.

Schmohl N, Horst WJ. 2000. Cell wall pectin content modulates aluminium sensitivity of *Zea mays* (L.) cells grown in suspension culture. Plant Cell Environ 23: 735-742.

Schnabelrauch LS, Kieliszewski M, Upham BL, Alizedeh H, Lamport DT. 1996. Isolation of pl 4.6 extensin peroxidase from tomato cell suspension

cultures and identification of Val-Tyr-Lys as putative intermolecular cross-link site. Plant J 9: 477-489.

Schofield RMS, Pallon J, Fiskesjö G, Karlsson G, Malmqvist KG. 1998. Aluminum and calcium distribution patterns in aluminum-intoxicated roots of *Allium cepa* do not support the calcium-displacement hypothesis and indicated signal-mediated inhibition of root growth. Planta 205: 175-180.

Sharma P, Dubey RS. 2007. Involvement of oxidative stress and role of antioxidative defense system in growing rice seedlings exposed to toxic concentrations of aluminum. Plant Cell Rep 26:2027-2038.

Simonovicova M, Huttova J, Mistrık I, Siroka B, Tamas L. 2004. Root growth inhibition by aluminum is probably caused by cell death due to peroxidase-mediated hydrogen peroxide production. Protoplasma 224: 91-98.

Simonovicova M, Tamás L, Huttová J, Mistrík I. 2004. Effect of aluminium on oxidative stress related enzyme activities. Biol Plant 48: 261-266.

Sivaguru M, Horst WJ. 1998. The distal part of the transition zone is the most aluminum-sensitive apical root zone of maize. Plant Physiol 116: 155-163.

Sivaguru M, Baluska F, Volkmann D, Felle HH, Horst WJ. 1999. Impacts of aluminum on the cytoskeleton of the maize root apex. short-term effects on the distal part of the transition zone. Plant Physiol 119:1073-1082.

Sivaguru M, Fujiwara T, Samaj J, Baluska F, Yang Z, Osawa H, Maeda T, Mori T, Volkmann D, Matsumoto H. 2000. Aluminum-induced 1-->3-beta-D-glucan inhibits cell-to-cell trafficking of molecules through plasmodesmata. A new mechanism of aluminum toxicity in plants. Plant Physiol 124:991-1006.

Silva IR, Smyth TJ, Moxley DF, Carter TE, Allen NS, Rufty TW. 2000. Aluminum accumulation at nuclei of cells in the root tip. Fluorescence detection using lumogallion and confocal laser scanning microscopy. Plant Physiol 123: 543-552.

Snowden KC, Richards KD, Gardner RC. 1995. Aluminum-induced genes. Induction of toxic metals, low calcium, and wounding and pattern of expression in root tips. Plant Physiol 107: 341-348.

Stevens FJ, Li AD, Lateef SS, Anderson LE. 1997. Identification of potential interdomain disulfides in three higher plant mitochondrial citrate synthases: Paradoxical differences in redox-sensitivity as compared to the animal enzyme. Photosynth Res 54:185-197.

Streller S, Wingsle G. 1994. *Pinus sylvestris* L. needles contain extracellular CuZn superoxide dismutase. Planta 192: 195-201.

Tabuchi A, Matsumoto H. 2001. Changes in cell-wall properties of wheat (*Triticum aestivum*) roots during aluminum-induced growth inhibition. Physiol Plant 112: 353-358.

Tamas L, Simonovicová M, Huttová J, Mistrík I. 2004. Elevated oxalate oxidase activity is correlated with Al-induced plasma membrane injury and root growth inhibition in young barley roots. Acta Physiol Plant 26: 85-93.

Tamas L, Budíková S, Huttová J, Mistrík I, Simonovicová M, Siroká B. 2005. Aluminum-induced cell death of barley-root border cells is correlated with peroxidase- and oxalate oxidase-mediated hydrogen peroxide production. Plant Cell Rep 24: 189-194.

Taylor GJ. 1991. Current views of the stress response: physiological basis of tolerance. Curr Topics Plant Biochem Physiol 10: 57-93.

Taylor GJ, McDonald-Stephens JL, Hunter DB, Bertsch PM, Elmore D, Rengel Z, Reid RJ. 2000. Direct measurement of aluminum uptake and distribution in single cells of *Chara corallina*. Plant Physiol 123: 987-996.

Tiwari BS, Belenghi B, Levine A. 2002. Oxidative stress increased respiration and generation of reactive oxygen species, resulting in ATP depletion, opening of mitochondrial permeability transition, and programmed cell death. Plant Physiol 128: 1271-1281.

Valerio L, De Meyer M, Penel C, Dunand C. 2004. Expression analysis of the *Arabidopsis* peroxidase multigenic family. Phytochemistry 65: 1331-1342.

Vanlerberghe GC, Day DA, Wiskich JT, Vanlerberghe AE, McIntosh L. 1995. Alternative oxidase activity in tobacco leaf mitochondria. Dependence on tricarboxylic acid cycle-mediated redox regulation and pyruvate activation. Plant Physiol 109: 353-361.

Vazquez MD, Poschenrieder C, Corrales I, Barcelo J. 1999. Change in apoplastic aluminum during the initial growth response to aluminum by roots of a tolerant maize variety. Plant Physiol 119: 435-444.

Very AA, Davies J. 2000. Hyperpolarization-activated calcium channels at the tip of *Arabidopsis* root hairs. Proc Natl Acad Sci U S A 97: 9801-9806.

Von Uexkull HR, Mutert,E. 1995. Global extent, development and economic impact of acid soils. Plant Soil 171: 1-15.

Wang J, Zhang H, Allen RD. 1990. Overexpression of an *Arabidopsis* peroxisomal ascorbate peroxidase gene in tobacco increases protection against oxidative stress. Plant Cell Physiol 40: 725-732.

Williams CH, Donald CM. 1954. Fertility and productivity of a podzolic soil as influenced by subterranean clover (*Trifolium Subterranean* L.) and superphosphate. Aust J of Agr Res 5: 674-687.

Williams CH, Donald CM. 1957. Changes in organic matter and pH in a podzolic soil as influenced by subterranean clover and superphosphate. Aust J of Agr Res 8: 179-189.

Yakimova ET, Kapchina-Toteva VM, Woltering EJ. 2006. Signal transduction events in aluminum-induced cell death in tomato suspension cells. J Plant Physiol 164: 702-708.

Yamamoto Y, Kobayashi Y, Matsumoto H. 2001. Lipid peroxidation is an early symptom triggered by aluminum, but not the primary cause of elongation inhibition in pea roots. Plant Physiol 125:199-208.

Yamamoto Y, Kobayashi Y, Devi SR, Rikiishi S, Matsumoto H. 2002. Aluminum toxicity is associated with mitochondrial dysfunction and the production of reactive oxygen species in plant cells. Plant Physiol 128: 63-72.

Yamamoto Y, Kobayashi Y, Devi SR, Rikiishi S, Matsumoto H. 2003. Oxidative stress triggered by aluminum in plant roots. Plant Soil 255: 239-243.

Yoshida K, Kaothien P, Matsui T, Kawaoka A, Shinmyo A. 2003. Molecular biology and application of plant peroxidase genes. Appl Microbiol Biotechnol 60: 665-670.

Zhao XJ, Sucoff E, Stadelmann EJ. 1987. Al^{3+} and Ca^{2+} alteration of membrane permeability of *Quercus rubra* root cortex cells. Plant Physiol 83: 159-162.

Zheng K, Pan JW, Ye L, Fu Y, Peng HZ, Wan BY, Gu Q, Bian HW, Han N, Wang JH, Kang B, Pan JH, Shao HH, Wang WZ, Zhu MY. 2007. Programmed cell death-involved aluminum toxicity in yeast alleviated by antiapoptotic members with decreased calcium signals. Plant Physiol 143: 38-49.

Zheng SJ. Yang JL. 2005. Target sites of aluminum phytotoxicity. Biol Plantarum 49: 321-331.

Zhou S, Sauvé R, Thannhauser TW. 2009. Proteome changes induced by aluminium stress in tomato roots. J Exp Bot 60: 1849-1857.

Chapter 2. Generation of single-copy, homozygous, transgenic lines of *Arabidopsis* harbouring peroxidase promoter::*GUS* reporter fusions

2.1. Introduction

Plant class III peroxidases are defined as enzymes that contain the signature peroxidase motif PEROXIDASE _4 (prosite PS50873) (Nunn *et al.*, 2002) and catalyze the reduction of hydrogen peroxide through the oxidation of various substrates (Bakalovic *et al.*, 2006; Passardi *et al.*, 2007). The class III peroxidases also bind calcium ions, form disulfide bonds, and contain predicted N- and/or C-terminal signal peptide that target the protein to the apoplasm or vacuole (Passardi *et al.*, 2004). Recently, new functions of class III peroxidases have been reported for catalyzing a second hydroxylic cycle that produces hydroxyl radicals ($^{\cdot}$OH) (Passardi *et al.*, 2005). The class III peroxidase family of *Arabidopsis* is composed of 73 proteins that are involved in a broad range of physiological and developmental processes (Passardi *et al.*, 2004). Due to their diverse potential catalytic functions and the large number of isoforms, the catalytic specificity and individual functional roles of most *Arabidopsis* peroxidases remain elusive.

The gene expression profiles of *Arabidopsis* class III peroxidases have been studied under Al stress by both oligonucleotide microarray and quantitative reverse transcriptase-polymerase chain reaction (qRT-PCR) techniques (Kumari *et al.*, 2008). Of the 71 Class III peroxidase genes represented on the *Arabidopsis* microarray described by Kumari *et al.* (2008), hybridization was observed for 36 and 41 of these peroxidases at 6 and 48h, respectively. Ten peroxidase genes were

induced and four were repressed after 6 h of Al exposure. After 48 h of Al treatment, the RNA levels for only a single peroxidase gene were increased and those of three peroxidase genes were decreased (Kumari *et al.*, 2008). Quantitative RT-PCR (qRT-PCR) studies showed similar up- and down-regulation profiles for the class III peroxidase genes as microarray analysis. However, the magnitude of changes in expression levels differed, perhaps reflecting the greater sensitivity of the qRT-PCR technique (Kumari *et al.*, 2008). Overall, class III peroxidases seem to be involved in the early responses to Al stress, rather than at a later stage.

Among the ten Al-induced class III peroxidases identified in the oligonucleotide microarray experiment, *PER73*, which is highly homologous to *PER35* at the mRNA level (76.5%), was the most increased (Kumari *et al.*, 2008). Comparison of the 70-mer oligo sequences printed on the *Arabidopsis* array suggested the observed up-regulation of *PER73* transcripts by Al stress (Kumari *et al.*, 2008) could have reflected combined transcript abundance of *PER35* and *PER73* genes.

Secretion of organic anions from roots has been identified as one of the main mechanisms that plants use to cope with Al stress. Several extracelluar proteins have also been observed to increase in abundance in wheat under Al stress (Basu *et al.*, 1994). A large suite of proteins exuded by wheat and canola have been observed in the apoplasm/rhizosphere (Basu *et al.*, 1996, 1997, 2006). Rhizosecretion has been shown to affect a number of plant processes, including protection from pathogen attack, nutrient acquisition (Shepherd and Davies, 1994), and resistance to toxic metals (Costa *et al.*, 2006). Recent efforts to characterize extracellular proteins using two-dimensional gel electrophoresis combined with liquid chromatography tandem mass spectrometry (LC-MS/MS) or

multidimensional protein identification technology (Mud PIT) provide further reason to explore the role of peroxidases in Al stress. Despite sequence information that suggests PER35 and PER73 are targeted to the apoplasm or vacuole, (both are predicted to be secreted; TargetP 1.1 server; Emanuelsson *et al.*, 2000, 2007), neither PER35 nor PER73 were detected as proteins exuded by roots of *Arabidopsis* or canola. This could reflect the low abundance of these proteins. Another possibility is that PER35 and PER73 are not exuded by the cells that contribute to root exudates.

Another interesting paradox is apparent in the abundance of PER22, not PER23, in root exudates. Both PER22 and PER23 have a C-terminal extension and are predicted to be targeted to the vacuole or secreted (TargetP 1.1 server; Emanuelsson *et al.*, 2000, 2007). PER22 has been identified as an orthologue of an extracytosolic protein secreted by roots of canola (Basu *et al.*, 2006). In spite of high conservation of *PER22* and *PER23* at the DNA level (89.5% identity), the predicted isoelectric points of PER22 and PER23 differ significantly; PER22 is anionic (pI = 5.67), while PER23 is cationic (pI = 8.45). Thus, these proteins can be differentiated through isoelectric focusing electrophoresis with peptide sequencing. Basu *et al.* (2006), however, did not identify PER23 as an extracytosolic protein.

A phylogenetic study of class III peroxidase promoter sequences revealed a low level of conservation between highly homologous peroxidase genes (Cosio and Dunand, 2009), which could explain the weak correlation between the identity of gene-coding sequences and temporal expression patterns (Cosio and Dunand, 2009). For example, two highly homologous peroxidases (90.3% sequence similarity in the coding region), *PER33* and *PER34*, which evolved from tandem

duplication, were both found to be associated with the cell wall and promoted root elongation in *Arabidopsis*. Nevertheless, a low level of homology (35% sequence similarity) between their promoters coincided with different spatial expression patterns (Passardi *et al.*, 2006). In contrast, two peroxidases with low sequence identity, *PER17* and *PER30*, exhibited similar temporal expression patterns in stems of *Arabidopsis* (Ehlting *et al.*, 2005) and were both involved in lignin biosynthesis, cell wall modification in the stamen abscission zone (Cai and Lashbrook, 2008) and pod shattering through lignification of siliques (Cosio *et al.*, 2008). These results indicate that expression of peroxidase genes and their specific functional activities have to be well coordinated in response to tissue locations and environmental stimuli.

Efforts to determine the specific function(s) of individual class III peroxidases have been hindered by their low substrate specificity *in vitro*. Therefore, a more plausible approach to unravel this complex functional network is to study specific functions by analyzing individual members of the class III peroxidase gene family under specific environments. Studies utilizing reporter genes fused with peroxidase promoters can help to reveal the spatial expression profiles of these peroxidases and determine their functions. I have chosen to focus on *PER22* and *PER73* in my research based on previous reports that suggest *PER22* is an orthologue of a root exudate protein encoding gene in canola (Basu *et al.*, 2006) and *PER73* showed the highest increase in mRNA level in roots of *Arabidopsis* after Al exposure (Kumari *et al.*, 2008). In order to undertake a peroxidase promoter::*GUS* reporter analysis, homozygous transgenic lines of *Arabidopsis* with single-copy T-DNA insertions need to be generated.

2.2. Materials and methods

2.2.1. Plant material and growth conditions

Seeds of *Arabidopsis thaliana* (Columbia Col-0, Lehle Seeds, catalog number WT-2) were surface sterilized in 30% bleach and 0.08% Tween 20 in sterile Milli-Q water (18 MΩ·cm) for 10 min and rinsed five times in sterile Milli-Q water. Seeds were then suspended in 0.1% sterilized agar solution and stratified for 3 days at 4 ℃, before pipetting into 5-inch square pots containing a commercially available soil (Metromix 350, Scotts Company, Marysville OH). Eighteen pots were placed in one supporting tray and transferred to a growth chamber at 22 ℃, 70% relative humidity, and 16 h/8 h light to dark cycle (150 μmoles m^{-2} sec^{-1} light intensity). Trays were subirrigated every other day to keep the soil damp, but not saturated. Five nutrient stock solutions were made according to Lehle Seeds instruction manual, and 1 L of irrigation solution (containing 5.0 ml 1 M KNO_3, 2.5 ml 1 M KH_2PO_4 (pH 5.6), 2.0 ml 1 M $MgSO_4$, 2.0 ml 1 M $Ca(NO_3)_2$, 2.5 ml Fe-EDTA stock solution) was applied to each tray once a week. The Fe-EDTA stock solution was prepared by dissolving 2.5 g $FeSO_4.7H_2O$ and 3.36 g of NaEDTA in a final volume of 450 ml solution.

2.2.2. PCR cloning of *PER22* and *PER73* promoters

Peroxidase promoters were amplified by PfuUltra DNA polymerase

Genomic DNA was extracted from leaves of 14-day-old *Arabidopsis* seedlings using the QIAGEN DNeasy Plant Mini Kit (catalog number 69104) following the manufacturer's instructions. Extracted DNA was quantified using a NanoDrop

ND-1000 Spectrophotometer (NanoDrop Technologies, Wilmington DE) and stored at -20 ℃.

Polymerase chain reaction (PCR) primers were designed using the online primer design software WebPrimer (www.yeastgenome.org) and features of the primers were double checked using DNAMAN 4.0 bioinformatics software (Lynnon Corporation, Quebec, Canada). The designed primers met all the requirements for standard PCR primers described in the QIAGEN Taq DNA Polymerase Kit (catalog number 201203) and were synthesized by Integrated DNA Technologies (1710 Commerical Park, Coraville, IA 52241). Primers were suspended in nuclease free water as 100 pmol μl^{-1} stocks and working stocks were prepared with a concentration of 12.5 pmol μl^{-1} by further dilution with nuclease free water. Table 2.1 provides the summary of all the primers used in this chapter.

To design primers for the amplification of the promoter regions of the *PER22* and *PER73*, nucleotide sequences were obtained from the Arabidopsis information resource (TAIR) website (www.*Arabidopsis*.org). An *Nco*I restriction enzyme recognition site was added to the 5' end of the reverse primers to facilitate fusion of the peroxidase promoters with *GUS/GFP* reporter genes.

PfuUltra High-Fidelity DNA Polymerase (Stratagene, catalog number 600380) was used to amplify *PER22* and *PER73* promoters and facilitate the selection of promoter sequences free from PCR errors. According to the manufacturer's manual, PfuUltra high-fidelity DNA polymerase has an 18-fold lower error rate than Taq DNA polymerase (an error rate of 4.3×10^{-7}, in comparison to Taq DNA polymerase's 8.0×10^{-6}). A stock solution of dNTP mix (10 mM each) was made from the Amersham Pharmacia Biotech (GE Healthcare) Ultrapure dNTP Set

(Catalog number 27-2035-01, discontinued). Each master mix was setup with a 10-15% excess to prevent shortages when dividing into aliquots for individual reactions.

Standard polymerase chain reactions (PCRs) were setup according to QIAGEN Taq DNA Polymerase Kit (Catalog number 201203) as master mixes that contained all the PCR components (0.5 µM of each primer, 1x PCR buffer, 0.4 x Q-solution, 0.4 mM of each dNTP, 2.5 mM $MgCl_2$, and 0.5 unit Taq DNA polymerase) except the template. A GeneAmp PCR System 9600/9700 was used for all PCR runs. The annealing temperature (Ta) was set 5 ℃ below the average Tm of the primers based on the formula Tm = 4(G + C) + 2(A + T) ℃. Other parameters were used as standard PCR setup according to QIAGEN instruction manual (5 min initial denaturation at 94 ℃; 35 cycles of 1 min denaturation at 94 ℃, 1 min annealing at Ta, time of extension was applied by 1 min per 1 kb at 72 ℃; and a 10 min final extension at 72 ℃). The final volume of all the PCRs was 25 µl. The promoter region including 5'-untranslated region of *PER22* (1022 bp) and *PER73* (1055 bp) were verified using agarose gel electrophoresis. A negative control with no template was included in every run of the PCR reaction.

All the DNA fragments were resolved on 0.5 to 2.0% 1X TAE agarose gel using the Sub-Cell GT Agarose Gel Electrophoresis Systems (Bio-Rad Laboratories (Canada) Ltd., Ontario). In order to optimize separation, the percentage of agarose used for the gel was chosen according to the calculated molecular weight of the expected DNA product. For example, 2% w/v agarose gels were used to separate DNA bands ranging from 50-200 bp, and 1% w/v agarose gels were used to separate DNA from 500-10,000 bp.

Peroxidase promoters were introduced into pBluescriptSK- vector via the TA cloning method

The TA cloning strategy was selected to utilize the adenine (A) overhang created on PCR products amplified by Taq DNA polymerase to subsequently ligate PCR products into a T-vector. However, PfuUltra high-fidelity DNA polymerase does not add an adenine (A) residue to the 3' ends of amplified PCR products. Consequently an adenine (A) residue was added to the 3' end of PfuUltra high-fidelity DNA polymerase-generated PCR products by incubation in the presence of 1X Taq DNA Polymerase PCR buffer with $MgCl_2$, 0.5 mM dATP, and 5 units of QIAGEN Taq DNA polymerase in a 10 µl final reaction volume at 70 ℃ for 1 hour.

A T-vector was created by first cutting the pBluescriptSK- vector (Stratagene, discontinued, Fig 2.1) with *Eco*RV (4 µg pBluescriptSK- vector DNA and 36 units *Eco*RV in final volume of 20 µl at 37 ℃ for 1 hour) to produce a linearized vector with blunt ends. Thymine (T) overhangs were then added to the 3' ends of this vector using Taq DNA polymerase in a reaction mix containing 1X Taq DNA Polymerase PCR buffer with $MgCl_2$, 2mM of dTTP, 5 units of QIAGEN Taq DNA polymerase mixed with 4 µg of the linearized pBluescriptSK- vector (100 µl final reaction volume) in a 0.2 ml tube incubated at 70 ℃ for 2 hours. The DNA products from the A-tailing reactions and T-vector reactions were purified using QIAquick PCR Purification Kit (catalog number 28104) according to the manufacturer's manual. All the DNA components for TA cloning of *PER22* and *PER73* promoters were analyzed by gel electrophoresis.

Ligation of the TA cloning components was carried out using T4 DNA Ligase (Gibco BRL-Division of Invitrogen, catalog number 15224-017). The ligation

reactions were carried out according to the manufacturer's cohesive ends ligation protocol, with 30 fmol ends T-vector and 90 fmol ends A-tailed promoter insert DNAs in a 20 µl reaction volume. The ligation time was extended to 1 hour instead of 5 minutes to maximize the number of ligated products. A negative control was included whenever possible by adding sterile Milli-Q water instead of the ligase.

Subcloning Efficiency^{TM} DH5α^{TM} Chemically Competent *E. coli* (Invitrogen catalog number 18265-017) were transformed with 5 µl of diluted (5X) TA cloning ligation mixture. The transformation procedure was performed according to the manufacturer's manual. Both 100 µl of the transformation culture and cells from the remaining 900 µl culture (spun down and resuspended in 100 µl LB medium) were plated on LB plates with 100 µg ml^{-1} ampicillin. A positive control containing 500 pg pUC19 vector was also carried out in parallel. Blue and white screening was used to select for transformants with inserts; 50 µl of 50 µg ml^{-1} X-gal dissolved in dimethylformamide solution was spread on the surface of the LB plates one hour prior to applying the transformation culture. Ten to fifteen isolated white colonies were restreaked using a sterile toothpick or a 10 µl pipette tip onto the LB+Amp+X-gal agar plates and incubated at 37 ℃ overnight. Cells from the same toothpick or pipette tip were transferred to a PCR tube containing 10 µl of sterile Milli-Q water. This mixture was used as a template in the subsequent colony PCR reaction (section 2.2.2).

Identification of the correct insert in pBluescriptSK- vector by colony PCR, restriction enzyme digestion analysis, and sequencing

Fifteen to twenty colony PCRs were setup for each ligation/transformation. The PCR tubes containing the transferred cells suspended in 10 µl of sterile Milli-Q water were heated at 95 ℃ for 5 minutes in order to disrupt the cell membranes and release the DNA templates. Aliquots of a master mix containing the rest of the PCR components were added to these tubes (25 µl final volume) and a standard PCR program was run. Additional colony PCR reactions were set up using the vector-specific SK primer in combination with each forward and reverse promoter cloning primers of *PER22* and *PER73* to determine the orientation of promoter inserts.

Colony PCRs yielding a single positive band on the gel were used to select original colonies containing vectors harbouring the *PER22* and *PER73* promoters and an isolated white colony from the corresponding restreaked LB+Amp+X-gal agar plates was used to inoculate 5 ml sterile LB+Amp liquid medium. Plasmid DNA was extracted from 2-4 independently inoculated liquid LB cultures using QIAprep Spin Miniprep Kit (Catalog number 27104) for subsequent diagnostic restriction enzyme digestion analysis and sequencing.

A *Bam*HI/*Nco*I double restriction enzyme digest was performed on the extracted plasmid DNA corresponding to colonies yielding a single positive band in the colony PCR reaction. *Bam*HI was first used to digest the plasmid DNA in 2X One-Phor-All Buffer PLUS at 30 ℃ for one hour, the reaction mix was then heated at 60 ℃ for 15 minutes to inactivate the enzyme. Next, *Nco*I was added to the reaction and incubated at 37 ℃ for one hour. Results of the double digest

were checked on a 1.0% agarose gel. For each of the two promoter DNA fragments cloned into pBluescriptSK- vector, one of the vectors identified via colony PCR and restriction enzyme digestion analysis as having the promoter insert in the right orientation was sequenced.

All the sequencing reactions were run using the BigDye Terminator v3.1 Cycle Sequencing Kit (Applied Biosystems, catalog number 4337454) and the protocol from the molecular biology service unit (MBSU, University of Alberta, Edmonton, Alberta). The pBluescriptSK- vector specific T_3 and T_7 primers, located on the opposite sides of the multiple cloning site, were used for sequencing. The sequencing reactions yield 400-800 bp of unambiguous sequence for each primer. The *PER22* and *PER73* promoter insert sequences were run through the BLAST search on NCBI database and compared with the matching sequences. Both *PER22* and *PER73* promoter insert sequences were also aligned with the corresponding promoter sequences available from the TAIR website (www.*Arabidopsis*.org) using DNAMAN 4.0 bioinformatics software (Lynnon Corporation, Quebec, Canada). These vectors will be referred to as pBluescriptSK-*PER22*PR and pBluescriptSK-*PER73*PR respectively.

2.2.3. Construction of plant transformation binary vectors and transformation of *Agrobacterium tumefaciens*

Constructs created in the pCAMBIA1303 binary vector (CAMBIA, Canberra, Australia; Fig 2.2) were used for transformation of *Agrobacterium* and *Arabidopsis*. pCAMBIA1303 contains two reporter genes, β-glucuronidase (*GUS*) and green fluorescent protein (*GFP*) in the T-DNA region. *Bam*HI and *Nco*I restriction enzymes were used to subclone the *PER22* promoter from

pBluescriptSK- vector into pCAMBIA1303. Restriction digest conditions were the same as described in section 2.2.2. While *Eco*RI and *Nco*I restriction enzymes were used for subcloning the *PER73* promoter, restriction digest was set up in the 2X One-Phor-All Buffer PLUS at 37 ℃ for one hour. The above subcloning resulted in replacement of the CaMV35S promoter that drives constitutive expression of the reporter genes in the original pCAMBIA1303 vector (Fig 2.2).

Initially, DNA fragments produced by the restriction enzyme digests described above were separated by gel electrophoresis and the DNA fragments of interest were isolated using the QIAquick Gel Extraction kit (Catalog number 28704) according to manufacturer's protocol (optional Buffer QG wash step was always incorporated). Numerous cloning attempts were made using high transformation efficiency competent cells (*E. coli* strain HB101 and JM 109 with transformation efficiency > $1X10^8$ cfu μg^{-1} obtained from Dr. Andrew Simmonds' lab (Department of Cell Biology, University of Alberta). Despite optimization of the ligation and transformation protocols, there were no transformants on the kanamycin selective plates. Optimizations included verification that the isolated DNA fragments were of sufficient concentration (50-100 ng μl^{-1}) and ligation reactions setup in parallel with modified ratios of insert to vector Fmol ends of 1:1, 3:1, 10:1, 100:1, 1:3, 1:10, and 1:100.

A different approach was used to circumvent the low biological activity of DNA recovered from agarose gels. Restriction enzyme digested products were purified using QIAquick PCR Purification Kit (catalog number 28104), then mixed together in one ligation reaction to transform Subcloning Efficiency™ DH5α™ Chemically Competent *E. coli* (Invitrogen catalog number 18265-017). This yielded a high number of transformants. The different selectable markers of

pBluescriptSK- (Ampicillin 100 μg ml^{-1}) and pCAMBIA1303 (Kanamycin 50 μg ml^{-1}) allowed transformants containing pCAMBIA1303 (Kanamycin + / Ampicillin -) to be selected. The presence of LacZ α fragement in pCAMBIA1303 vector enabled selection of vectors with inserts via blue and white screening method. The pCAMBIA1303 vectors containing sequenced *PER22*, *PER73*, or CaMV35S promoter were verified through restriction enzyme(s) digestion analysis. These vectors will be referred to as pCAMBIA-*PER22*PR, pCAMBIA-*PER73*PR, and pCAMBIA-*35S* respectively.

The *Agrobacterium* strain GV3101 (pMP90) was used in this experiment for its antibiotic compatibility with pCAMBIA binary vector and its strong virulency to allow transformation of *Arabidopsis* via the floral dip method and (Koncz and Schell, 1986). The *Agrobacterium* strain GV3101 (pMP90) contains antibiotic resistant markers on its chromosome (rifampicin resistant gene) and the trans-acting Ti plasmid (gentamycin resistant gene). Rifampicin (25 μg ml^{-1}) and gentamycin (50 μg ml^{-1}) were added to all plates and liquid media to ensure that only *Agrobactierum* GV3101 (pMP90) with Ti plasmid were carried forward during the transformation process.

The freeze-thaw method was used to transform *Agrobacterium* GV3101 (pMP90) competent cells (Hofgen and Willmitzer, 1988). The *Agrobacterium* cells were grown to log phase (OD_{550} 0.62). Approximately 2.5 μg of pCAMBIA1303 plasmid DNA containing CaMV35S promoter, *PER22* promoter, or *PER73* promoter were independently transformed into competent *Agrobacterium* cells. Transformants were selected on LB agar plates containing gentamycin, rifampcin, and the antibiotic hygromycin B (50 μg ml^{-1}), which is used to select plants with the pCAMBIA1303 vector following transformation. Successful transformants

containing pCAMBIA-*PER22*PR and pCAMBIA-*PER73*PR were identified using colony PCR with PfuUltra promoter cloning primers.

Glycerol stocks of *E. coli* strains containing pBluescriptSK-*PER22*PR, pBluescriptSK-*PER73*PR, pBluescriptSK-SouthernProbe, pCAMBIA-*PER22*PR, pCAMBIA-*PER73*PR, pCAMBIA-*35S* and *Agrobacterium* strains containing pCAMBIA-*PER22*PR, pCAMBIA-*PER73*PR, pCAMBIA-*35S* vectors were generated. All glycerol stocks were created by adding 2 volumes of an overnight cell culture to a mixture solution with equal volume of sterile glycerol and LB liquid medium. This mixture was then aliquoted into 1.5 ml sterile microcentrifuge tubes, flash frozen with liquid nitrogen, and stored in a -80 ℃ freezer.

2.2.4. *Agrobacterium*-mediated transformation of *Arabidopsis*

The *Arabidopsis thaliana* (Col-0) plants to be transformed (T_0 plants; Fig 2.3) were grown in 4 inch square pots under the same conditions described in section 2.2.1. A plastic mesh was placed on top of the Metromix 350 to prevent soil from falling out of the pots when the *Arabidopsis* inflorescences were dipped into the *Agrobacterium* transformation solution. Seedlings growing in each pot were thinned, leaving approximately 15-20 healthy plants to grow to four weeks old. The entire first inflorescence on these plants was removed in order to boost the growth of secondary inflorescences.

The floral dip method (Clough and Bent, 1998) was used to transform these T_0 plants with *Agrobacterium* GV3101 (pMP90) harboring the appropriate vector. Optional YEP medium was used instead of LB medium in order to increase the

density of *Agrobacterium* cells in the liquid culture. The *Agrobacterium* cells were pelleted at the log phase (OD_{550} values of 0.75, 0.78, and 0.74 for pCAMBIA-*35S*, pCAMBIA-*PER22PR*, and pCAMBIA-*PER73PR*, respectively). The pellets were resuspended in 250 ml 5% sucrose solution with 0.05% v/v surfactant Silwet L-77 (Lehle Seeds, catalog number VIS-01). After dipping the inflorescences of plants in *Agrobacterium* solution for approximately 5 seconds with gentle agitation, the shoot tissue of all the plants was covered with a plastic bag for 24 hours at room temperature. A week later, the floral dip transformation was repeated on the same plants. All the transgenic plants were generated from the same batch and lot number of WT *Arabidopsis* seed source.

2.2.5. Screening of transgenic, homozygous lines by genomic PCR and antibiotic resistance selection

A flowchart of the strategy used to develop "homozygous, single-copy", transgenic lines containing the pCAMBIA-promoter T-DNA constructs is illustrated in Figure 2.3. The T_1 seeds for each T-DNA construct (Fig 2.2 B, C, and D) were screened on 1/2 x Murashige & Skoog (MS) medium plates containing hygromycin B (25 μg ml^{-1}). The genotype of these T_1 plants is either Aa or aa, where "A" indicates a T-DNA insertion and "a" indicates no insertion. Only the Aa plants can continue to grow in the presence of hygromycin B. The hygromycin B phosphotransferase gene exists only in the T-DNA insert and is not endogenous to *Arabidopsis* genome. Fifteen T_1 lines (Aa) were selected for each T-DNA construct and the presence of the T-DNA insert of interest was confirmed by genomic PCR using the Extract-N-Amp Plant PCR kit (Sigma-Aldrich, catalog number XNAP2) and construct-specific forward primers (Fig 2.2 C and D). The pCAMBIA1303-*35S* forward (GenomicPCR_*35S*_F) and *GUS* reverse

(GenomicPCR_*GUS*_R) primers (Fig 2.2 B, Table 2.1) were designed for use in genomic PCR to identify transgenic plants containing pCAMBIA-*35S* T-DNA construct. The GenomicPCR_*35S*_F primer was located in the LacZ alpha promoter region and the GenomicPCR_*GUS*_R primer was located in the middle of the *GUS* reporter gene coding region (Fig 2.2 B). The *GUS* reverse primer was designed to be compatible with the both *PER22* and *PER73* PfuUltra promoter cloning forward primers (Fig 2.2 C and D, Table 2.1) resulting in primer pairs to be used in genomic PCRs to identify transgenic plants containing T-DNA constructs of pCAMBIA-*PER22PR* and pCAMBIA-*PER73PR*. Genomic DNA extraction and PCR amplification conditions were performed according to the manufacturer's instruction manual (Sigma-Aldrich, catalog number XNAP2). Leaf tissue of each tested plant was collected by using a microcentrifuge tube cap to cut a leaf disk from 2-3 weeks old seedlings, which were subsequently submerged in the extraction buffer.

Fifteen T_1 plants ($T_{1\text{-}1,1\text{-}2,1\text{-}3\ldots1\text{-}15}$) identified by genomic PCR (Fig 2.3) for each construct were grown in the ARASYSTEM Starter Kit 360 (Lehle Seeds, catalog number AS-01) and allowed to self-fertilized to produce T_2 seeds. Sixteen T_2 seeds from each T_1 plant were then planted in the ARASYSTEM. In order to maintain negative siblings, these T_2 seeds were not subjected to hygromycin B screening prior to planting. Genomic PCR was consequently used to determine whether these T_2 plants contained an insert (Aa or AA) or not (aa) (Fig 2.3). Two lines of negative siblings were carried forward in parallel with the process used to development homozygous transgenic lines. In order to determine the putative copy number of T-DNA insert(s) for each T_1 plant, eighty to one hundred T_2 seeds harvested from these T_1 plants were independently plated on 1/2 x MS basal medium (Sigma-Aldrich, catalog number M5519) agar plates with and without

hygromycin B (50 μg ml^{-1}). The hygromycin B plates were scored for resistant seedlings and non-resistant/ungerminated seeds, while the number of seedlings and ungerminated seeds on the plates without hygromycin B was recorded (Table 2.2). Seventy to one hundred and thirty T_3 seeds separately collected from the sixteen T_2 plants (except the genomic PCR confirmed negative sibling lines) were then tested on plates with and without hygromycin B to identify lines homozygous for the T-DNA of interest. All the above T_2 and T_3 seeds were sterilized under the same protocol as described in section 2.2.1.

2.2.6. Identification of single-copy T-DNA insertion lines using southern blot analysis

The QIAGEN DNeasy Plant Maxi Kit (catalog number 68163) was used to extract genomic DNA from each of the T_3 homozygous transgenic lines. Genomic DNA was eluted from the DNeasy Maxi spin column using 2,000 μl buffer AE that had been diluted 1/20 with sterile Milli-Q water. This allows the reconcentration of the genomic DNA to ~100-150 μl using SpeedVac SC100 (Savant, Holbrooke NY) without resulting in a high salt concentration. The *Bam*HI and *Eco*RI restriction enzymes were chosen to digest the transgenic genomic DNA. The restriction digest reaction was carried out according to the Southern Blotting: Capillary Transfer of DNA to Membranes protocol described in Molecular Cloning-A Laboratory Manual (Third Edition, Cold Spring Harbor Laboratory Press, Woodbury NY). Digested genomic DNA was ethanol precipitated, and resuspended in 35 μl TE by incubation overnight at 37 ℃. The digested DNA, at least 10 μg per lane, was separated using a 0.7% w/v agarose gel run at 45 volts for ~14-15 hours.

The probe for the southern analysis was designed to hybridize with the *GUS* and *GFP* gene coding region, which is common to all of the T-DNA inserts (Fig 2.15 C) and could be used to detect the copy number of T-DNA inserts for all three types of transgenic plants. The DNA fragment to be used as the southern probe was amplified by the QIAGEN Taq DNA Polymerase Kit (catalog number 201203) under a standard PCR reaction (3 min initial denaturation at 94 ℃; 35 cycles of 1 min denaturation at 94 ℃, 1 min annealing at 66.5 ℃, 1.5 min extension at 72 ℃; and a 10 min final extension at 72 ℃) with the forward primer SouthernProbe_F and reverse primer SouthernProbe_R using pCAMBIA1303 vector as the template (Table 2.1). This PCR product was cloned into pBluescriptSK- vector via TA cloning method (see section 2.2.2) to construct pBlusecriptSK-SouthernProbe vector. Desired transformants were identified by colony PCR and isolated vectors were sequenced using T_3/T_7 primers (see section 2.2.2). The southern probe was generated by cutting pBlusecriptSK-SouthernProbe vector DNA with *Pst*I and *Sal*I in buffer H at 37 ℃ for one hour. The restriction digestion products were separated by gel electrophoresis. Southern probe was gel purified (see section 2.2.3) and subsequently labeled.

Initial labeling and detection was attempted with the digoxigenin-dUTP by DIG-High random primed DNA labeling method according to the manufacturer's manual included for the DIG High Prime DNA Labeling and Detection Starter Kit II (Roche Applied Science, catalog number 11585614910). The efficiency of the DIG-High random labeling was determined by comparing the serial diluted probe of interest with labeled control 5 μg ml^{-1} pBR328 DNA, and 35 ng μl^{-1} probe of interest was successfully labeled. DIG Wash and Block Buffer Set (Roche Applied Science, catalog number 11585762001) was used for the chemiluminescent detection with disodium 3-(4-methoxyspiro {1,2-dioxetane-

3,2 ´-(5'-chloro)tricyclo [3.3.1.1^{3,7}]decan}-4-yl) phenyl phosphate (CSPD). Despite the very detailed instruction manual provided by the manufacturer, the result of this non-radioactive southern blot analysis was too weak to be detected due to the low hybridization efficiency with plant genome. The Southern probe was therefore labeled with radioactive [α^{32}P] dCTP using the Ready·To·Go^{TM} DNA Labeling Beads (Amersham Biosciences-GE Healthcare, catalog number XY-061-00-13). Approximately 150-200 ng of denatured DNA was added to the labeling reaction with 5 µl of [α^{32}P] dCTP in a total volume of 50 µl, and incubated at 37 ℃ for 30 min. Radioactive-labeled probes were separated from the unincorporated α^{32}P labeled nucleotides using the Sephadex G-50^{TM} DNA grade NICK column (Amersham Biosciences-GE Healthcare, catalog number 17-0855-01). Approximately 380 µl of the 400 µl of the labeled probe was used each time.

Digested genomic DNA was transferred to a positive-charged nylon membrane GeneScreen Plus® (catalog number NEF988, PerkinEllmer Inc.) using alkaline transfer buffer. Hybridization was performed in hybridization bottles in a hybridization oven. Prehybridization, hybridization, and washing procedures were carried out as described in Southern Hybridization of Radiolabeled Probes to Nucleic Acids Immobilized on Membranes protocol in Molecular Cloning-A Laboratory Manual (Third Edition, Cold Spring Harbor Laboratory Press, Woodbury NY). Approximately 190 µl of the labeled probe was added to each hybridization bottle. Following washing, the hybridized membranes were covered with Saran Wrap, and exposed to KODAK BioMax MR autoradiography films (Marketlink Scientific, Burlington, Ontario) for 6h and 24 h. All the x-ray films were developed by the Kodak X-OMAT 2000 processor in the dark room (Department of Biological Scicences, University of Alberta).

2.3. Results and discussion

2.3.1. Cloning of peroxidase promoters

The promoter regions of the Class III *Arabidopsis PER22* and *PER73* were PCR amplified from *Arabidopsis* genomic DNA using the high fidelity PfuUltra DNA polymerase. Single products of the expected size, 1022 bp for the *PER22* promoter and 1055 bp for the *PER73* promoter, were amplified in both PCR reactions (Fig 2.4). These PCR products were gel purified, A-tailed (Fig 2.5), and ligated with a T-vector created by digesting pBluescriptSK- with the blunt-end restriction enzyme *Eco*RV (Fig 2.5). After successful transformation of competent *E. coli* cells, the pBluescriptSK- vectors harbouring the desired promoters were identified and characterized using colony PCR (Fig 2.6), restriction digestion analysis (Fig 2.7), and DNA sequencing (Fig 2.8 and 2.10), before being subcloned into the plant transformation vector pCAMBIA1303 (Fig 2.2 A).

Colony PCR was applied to select the desired *E. coli* transformants containing the pBluescriptSK-*PER22*PR and pBluescriptSK-*PER73*PR vectors. As shown in Fig 2.6 A and B, colony PCRs with the forward and reverse primers for PfuUltra DNA polymerase amplification of *PER22* and *PER73* promoters identified two positive *E. coli* transformants containing pBluescriptSK- vectors with an *PER22* promoter insert as *PER22*-4PR (Fig 2.6 A, lane 4), and *PER22*-5PR (Fig 2.6 A, lane 5), and four positive *E. coli* transformants containing pBluescriptSK- vectors with an *PER73* promoter insert as *PER73*-2PR, *PER73*-3PR, *PER73*-4PR, and *PER73*-5PR (Fig 2.6 B, lane 2-5).

The *Nco*I cutting site present in the reverse primers of PCR cloning of *PER22* and *PER73* promoters (section 2.2.2) was designed to fuse the peroxidase promoters with the start codon of the *GUS* reporter gene upstream, which requires *PER22* and *PER73* promoters inserted in the same 5' to 3' direction as the multiple cloning site (MCS) in pBluescriptSK- vector. However, the TA cloning method is known to ligate DNA at either direction (Fig 2.6 A, lane 9 and 15). Colony PCRs using pBluescriptSK- vector specific SK primer in combination with *PER22* and *PER73* forward or reverse primer helped determine the direction of the promoter inserts (Fig 2.6 A and B). Amplicons produced by colony PCRs with SK and reverse primers of *PER22* and *PER73* (*PER_22* _PR_R or *PER_73* _PR_R, Table 2.1) indentified that *PER22*-4PR (Fig 2.6 A, lane 9), *PER73*-3PR (Fig 2.6 B, lane 8), and *PER73*-5PR (Fig 2.6 B, lane 10) were the desired pBluescriptSK-*PER22*PR and pBluescript SK-*PER73*PR vectors. Colony PCR with SK primer and forward primers (*PER_22* _PR_F or *PER_73* _PR_F, Table 2.1) determined that *PER22*-5PR (Fig 2.6 A, lane 15) contained the *PER22* promoter in an undesired direction, and no DNA products were observed for *PER73*-2PR (Fig 2.6 B, lane 12) and *PER73*-4PR (Fig 2.6 B, lane 14). As the desired pBluescriptSK-*PER22*PR and pBluescript SK-*PER73*PR vectors were acquired, no troubleshooting experiments for colony PCRs to amplify *PER73*-2PR and *PER73*-4PR vectors were conducted.

PER22 and *PER73* promoter sequences were analyzed for *Bam*HI and *Nco*I restriction digestion pattern with DNAMAN 4.0 bioinformatics software (Lynnon Corporation, Quebec, Canada). Only one *Bam*HI restriction site was predicted to be within the *PER73* promoter region (423 bp from the start codon). As a restriction site for *Bam*HI was present in MCS (1 copy) of the pBluescriptSK- vector and promoter region of *PER73* (1 copy), and a restriction site of *Nco*I was

in the reverse primers of *PER22* and *PER73*, *Bam*HI and *Nco*I restriction digestion of pBluescriptSK-*PER*22PR (*PER22*-4PR) and pBluescriptSK-*PER*73PR (*PER73*-3PR and *PER73*-5PR) vectors would produce two (2929 bp and 1042 bp) and three DNA fragments (2938 bp, 653 bp, and 423 bp) of different sizes (Fig 2.7). Restriction enzyme *Bam*HI and *Nco*I digestion further confirmed that *PER22*-4PR, *PER73*-3PR, and *PER73*-5PR were the desired vectors containing *PER22* and *PER73* promoter inserts in the correct direction (Fig 2.7).

The pBluescriptSK-*PER22*PR (*PER22*-4PR) and pBluescriptSK-*PER73*PR (*PER73*-3PR) vectors containing the *PER22* and *PER73* promoter inserts were sequenced (Fig 2.8 and Fig 2.10), respectively, using both T_3 and T_7 primers located at the 5' and 3' ends of the promoter insert. A sequence alignment search in the NCBI database was done using the Basic Local Alignment Search Tool (BLAST) (Zhang *et al.*, 2000) for highly similar sequences within the *Arabidopsis thaliana* genome. The matching sequence for the *PER22* promoter found in the NCBI database was submitted by Dr. Rockville's lab (the Institute for Genomic Research, 9712 Medical Center, MD) using the same cultivar (Columbia) as this study. However, the *PER22* promoter sequence obtained using the T_7 primer produced a cluster of 20 adenines approximately 150 bp upstream of the start codon, which is one more adenine than the submitted sequence in the NCBI database (Fig 2.9). A partial sequence of *PER22* promoter reported in a salinity study also showed a cluster of 20 adenines in the same location (Wanapu and Shimyo, 1996). The chromatographic sequencing result containing the cluster of 20 adenines was of high quality with sharp peaks (Fig 2.8). In contrast, the *PER73* promoter showed 100% alignment with the entry sequences in the NCBI database (Fig 2.11). Apparent discrepancies of two base pair mismatch in both *PER22* and *PER73* promoter sequences (within the red circles) were due to the added *Nco*I

restriction site engineered for promoter::*GUS* fusion immediately upstream of the start codon (Fig. 2.9 and Fig. 2.11).

2.3.2. Construction of plant transformation vectors

Sequenced promoters of *PER22* and *PER73* were introduced into pCAMBIA1303 (Fig. 2.2 A) via double restriction digest with *Bam*HI or *Eco*RI in combination with *Nco*I, respectively. The restriction digest products were confirmed using gel eletrophoresis (Fig. 2.12). Each promoter region was fused with the *GUS* reporter gene at the insertion site utilizing the *Nco*I restriction site, which cuts one base upstream of the start codon site (Fig 2.9 and Fig 2.11). All three promoter::*GUS* fusion vectors, pCAMBIA-*35S*, pCAMBIA-*PER22*PR, and pCAMBIA-*PER73*PR (Fig 2.2 B, C, and D) were constructed and used to transform *Agrobacterium*, and subsequently wild type *Arabidopsis* plants.

Even though it seems to be a routine and standard cloning procedure to construct plant transformation vectors, the cloning experiments I attempted with protocols available in the Molecular Cloning – A Laboratory Manual (Third Edition, Cold Spring Harbor Laboratory Press, Woodbury NY) did not yield positive results. Troubleshooting of these cloning experiments were conducted on ligation and transformation procedures.

The size of the reconstructed pCAMBIA1303 transformation vector is greater than 13 kb, which makes it difficult to be introduced into competent cells. Thus, high transformation efficiency strains of *E. coli* competent cells such as HB 101 and JM 109 (transformation efficiency > $1X10^8$ cfu μg^{-1}) were utilized. This did not produce any colonies on LB+Kanamycin plates. However, the negative

control using intact pCAMBIA1303 vector (12,361 bp) yielded positive blue colonies. So the ligation reaction was suspected to be the bottleneck of generating positive clones.

A two-component (insert and vector) ligation reaction was set up using *PER22* and *PER73* promoter inserts and pCAMBIA1303 vectors cut with the same corresponding double restriction enzymes, producing the same compatible sticky ends. Both inserts and linearized vectors were recovered from agarose gel after electrophoresis, which prevented the possibility of the incompletely digested DNA products, restriction enzymes, and/or EDTA salts interfering with the ligation reaction. The standard ligation reaction using T4 DNA ligase was initially attempted at the optimal temperature (25 ^{o}C) (Gibco BRL-Division of Invitrogen). Due to the large size of the linearized vector, ligation reactions were also set up at low temperatures (4 ^{o}C and 16 ^{o}C), and incubated for a prolonged period of time. I hoped this would facilitate recircularization of large linearized pCAMBIA1303 vectors and lower the kinetic energy of the promoter inserts to promote homologous pairing of the sticky ends through hydrogen bonding (Stanley, 2001). Fresh batches of T4 DNA ligase and buffers were ordered and always thawed on ice to prevent the breakdown of ATP, which could reduce the ligation efficiency (Gibco BRL-Division of Invitrogen). Unfortunately all these optimizations did not result in any positive clones.

A ‘shot-gun’ cloning method was designed to increase the ligation efficiency by mixing all the DNA products in one ligation reaction. The pBluescriptSK-*PER22*PR and pBluescriptSK-*PER73*PR, and pCAMBIA1303 vectors were not gel separated after the restriction enzyme digestion. All the DNA products generated from cutting pBluescriptSK-*PER22*PR and pCAMBIA1303 vectors by

*Bam*HI and *Nco*I were purified and added into one ligation reaction mixture. The same procedure was applied to pBluescriptSK-*PER73*PR and pCAMBIA1303 vectors. This approach avoided the UV exposure of the DNA products before ligation and transformation of competent cells. The approach yielded a large number of transformants. All undesired transformants produced from the random ligation of any DNA products with compatible sticky ends were eliminated through selection with different antibiotic resistance genes and incompatible origins of replication (Yamaguchi *et al.,* 1982) for pBluescriptSK- (ampicillin resistance, pUC ori) and pCAMBIA1303 (kanamycin resistance, pBR322 ori).

Colony PCRs identified 9 positive transformants (Fig 2.13 A) containing the pCAMIBA-*PER22*PR vector and 7 positive transformants (Fig 2.13 B) containing the pCAMBIA-*PER73*PR vector using the 'shot-gun' cloning method. Four independent plasmids of pCAMBIA-*PER22*PR (pCAM-*PER22-1*PR and pCAM-*PER22-2*PR) and pCAMBIA-*PER73*PR (pCAM-*PER73-1*PR and pCAM-*PER73-2*PR) were extracted from positive *E. coli* transformants. Further restriction digests analysis using multiple restriction enzymes on these plasmids confirmed that the desired plant transformation vectors, pCAMIBA-*PER22*PR and pCAMBIA-*PER73*PR, were successfully constructed (Fig 2.14). The same colony PCRs were also used to identify the positive *Agrobacterium* transformants containing pCAMBIA-*PER22*PR and pCAMBIA-*PER73*PR vectors (Fig 2.15).

2.3.3. Generation of single-copy, homozygous lines harbouring promoter::*GUS* fusion T-DNA constructs

Homozygous, transgenic *Arabidopsis* lines harbouring each T-DNA construct were generated by selfing transgenic lines for two generations after floral dip

transformation. Genomic PCR and antibiotic hygromycin B selection methods, either alone or together, were applied to select the homozygous transgenic seedlings. The genotypes of all the fifteen transgenic T_1 seedlings of each T-DNA construct were identified using genomic PCR. Sixteen T_2 seedlings of each of the identified fifteen T_1 lines were tested by genomic PCR to prevent losing T-DNA insert(s) in segregating progenies during the selfing process. An example of genomic PCR testing of sixteen T_2 seedlings of one T_1 line for each construct is shown in Figure 2.16. Hygromycin B was not used to screen for T-DNA insert(s) in order to preserve negative siblings for *GUS* staining assays. The phenotypic contrast of seed germination and sustainable growth of resistant versus non-resistant lines was screened on hygromycin B plates (Fig 2.17). Hygromycin B selection proved to be an effective way of screening for transgenic lines.

Segregation of the hygromycin B resistant phenotype in T_2 and T_3 progenies of the same transgenic line was analyzed to determine the possible copy number of T-DNA inserts in the genome. T_2 and T_3 seeds from the same transgenic line were tested on plates with hygromycin B. Control plates without antibiotics were included in parallel to calculate the germination efficiency of the transgenic seeds. After correction for germination efficiency, transgenic lines showing a 3:1 (resistant : non-resistant) segregation ratio of T_2 seeds and 100% resistance of T_3 seeds were identified as putative "single-copy" homozygous lines (Fig 2.17). Transgenic plants with T_2 seeds showing greater than 90% resistance were identified as "multiple copy" lines. Progeny segregation results of all the putative "single-copy" transgenic lines can be found in Table 2.2. Eleven and twelve putative "single-copy" homozygous lines were obtained for transgenic plants harbouring pCAMBIA-*PER22*PR or pCAMBIA-*PER73*PR T-DNA construct,

respectively. Ten putative "single-copy" homozygous lines harbouring the pCAMBIA-*35S* T-DNA construct were obtained as well.

All of the putative, "single-copy", homozygous lines were tested for cross contamination by genomic PCR using DNA pools of transgenic lines of pCAMBIA-*35S*, pCAMBIA-P*ER22*PR, and pCAMBIA-*PER73*PR (Fig 2.18). The genomic DNA pools for this analysis were generated by collecting leaf tissue from each putative line containing the same T-DNA construct, and subsequently pooled together for genomic DNA extraction. All the putative, "single-copy", homozygous transgenic lines of pCAMBIA-*35S*, pCAMBIA-P*ER22*PR, and pCAMBIA-*PER73*PR were subjected to southern blot analysis. Five single-copy, homozygous, transgenic lines of each peroxidase promoter::*GUS* fusion construct were acquired, and four single-copy homozygous lines of the control vector pCAMBIA-*35S* were acquired (Fig 2.19).

A number of reasons can account for a false number of putative "single-copy" homozygous transgenic lines. If T-DNA inserts were not genetically linked, transgenic lines with two T-DNA inserts would generate a 93.75% (15/16) hygromycin B resistant, T_2 seed pool and transgenic lines with three T-DNA inserts would generate a 98.44% (63/64) resistant T_2 seed pool. Progeny segregation analysis on independently harvested T_2 seeds can only rule out the transgenic lines with multiple-copy, genetically-unlinked T-DNA inserts, which includes non-syntenic T-DNA inserts (T-DNA inserts located on different chromosomes), and syntenic T-DNA inserts allowing free crossing-overs (recombination frequency (RF) greater or equal to 50%). If the two T-DNA inserts are genetically-linked, segregation ratio of these transgenic lines would

resemble that of single-copy transgenic lines as the two T-DNA inserts tend to assort together to the next generation.

In the *Arabidopsis* genome, 1 mapping unit (1 cM) corresponds on average to 200 kb in physical distance, with numbers varying from 100 to 400 kb cM^{-1} (The *Arabidopsis* Genome Initiative, 2000). Recombination rates vary among different species (Chen *et al.*, 2002), different regions of the same chromosome, and even between gene coding and intergenic regions, actively expressed genes and silent genes (Lin *et al.*, 1999), the lowest being found at centromeric regions (Copenhaver *et al.*, 1998).

When the southern blot probe was designed, sequences of the probe were checked to make sure neither *Bam*HI nor *Eco*RI restriction site was present within this region. Sequences of T-DNA constructs of pCAMBIA-*35S*, pCAMBIA-*PER22*PR, and pCAMBIA-*PER73*PR were checked for *Bam*HI and *Eco*RI restriction sites as well, *Bam*HI and *Eco*RI were expected to digest all three T-DNA constructs to two DNA fragments of different sizes (~ 2,500 bp and ~ 4,000 bp). Since restriction enzymes *Bam*HI and *Eco*RI are predicted to cut the *Arabidopsis* genome on average every 6,000 bp and 2,600 bp (Dale and Schantz, 2003), respectively, the resolution of this southern blot analysis can identify any multiple copy, genetically-linked transgenic lines. Southern blot analysis of all the putative "single-copy" transgenic lines of pCAMBIA-*35S*, pCAMBIA-P*ER22*PR, and pCAMBIA-*PER73*PR revealed that more than half of the transgenic lines contained genetically-linked, multiple T-DNA inserts, which can only be separated by the cutting of restriction enzymes. Therefore, southern blot analysis proved to be a reliable approach to identify the single-copy transgenic lines.

In summary, in order to examine the gene expression patterns of *PER22* and *PER73* in *Arabidopsis*, the putative promoter regions of *PER22* and *PER73* (1022 bp and 1055 bp upstream of the start codon, respectively) were cloned into a sequencing vector (pBluescriptSK-). After successful sequencing of *PER22* and *PER73* promoters, each of them was fused to the β-glucuronidase (*GUS*) reporter gene in the T-DNA region of pCAMBIA1303 plant transformation vector. Three different T-DNA constructs containing promoter::*GUS* reporter gene fusion were created, and subsequently used to transform WT *Arabidopsis* via the floral dip method. Transgenic *Arabidopsis* were identified through genomic PCR and hygromycin B antibiotic selection. Homozygous, transgenic lines were generated by selfing T_1 lines for two generations. The copy numbers of the T-DNA insert(s) in these transgenic lines were determined through southern blot analysis. In the end, a total of fourteen single-copy, homozygous, transgenic *Arabidopsis* plants harbouring promoter::*GUS* fusion T-DNA constructs including a control CaMV*35S*::*GUS* fusion were created for subsequent histochemical *GUS* staining assays.

Table 2.1. Sequences and functions of oligonucleotide primers used for generation of single-copy, homozygous, transgenic lines.

Primer Name	Sequence (5'→ 3')	Function
*PER*_22 _PR_F	TGCGTTATTTACGGGAAATGG	Forward primer for i) *PER22* promoter cloning and ii) genomic PCR amplification of pCAMBIA-*PER*22PR
*PER*_22 _PR_R	C**C↓CATGG**TTGTAGGAGGAAGAC	Reverse primer for *PER 22* promoter cloning with *NcoI* cutting site (in bold)
*PER*_73 _PR_F	GGGCATATTTTGCACATCAG	Forward primer for i) *PER73* promoter cloning and ii) genomic PCR amplification of pCAMBIA-*PER*73PR
*PER*_73 _PR_R	**C↓CATGG**CGTTGGAAATTACAAG	Reverse primer for *PER73* promoter cloning with *NcoI* cutting site (in bold)
pBluescriptSK-SK	CGCTCTAGAACTAGTGGATC	Primer used in colony PCR to determine the orientation of promoter insert
pBluescriptSK-T_3	AATTAACCCTCACTAAAGGG	Sequencing primer for the promoter insert of interest
pBluescriptSK-T_7	GTAATACGACTCACTATAGGGC	Same as above
GenomicPCR_*35S*_F	AGGCATGCAAGCTTGGCAC	Forward primer for genomic PCR amplification of pCAMBIA-*35S*
GenomicPCR_*GUS* _R	TACGAATATCTGCATCGGCG	Reverse primer for genomic PCR amplification of pCAMBIA-*35S*, pCAMBIA-*PER*22/73PR
SouthernProbe_F	ATACGTTAGCCGGGCTGCACTC	Forward primer for southern probe amplification
SouthernProbe_R	TGAAGAAGATGGTCCTCTCCTGCA	Reverse primer for southern probe amplification

Table 2.2. Segregation analysis of putative single-copy, homozygous, transgenic lines (T_2 progeny).

Transgenic line	Seed germination efficiency	Control plate (dead/total)	Test plate (dead/total)	T_2 seed segregation ratio	Chi-square value	single-copy confirmed by southern
35ST_3-1-8	0.95	4/85	37/110	0.698	1.501	
35ST_3-2-5	0.90	8/81	32/104	0.763	0.086	
35ST_3-3-3	0.92	7/82	25/95	0.802	1.252	√
35ST_3-4-1	0.94	5/85	21/80	0.781	0.384	√
35ST_3-5-4	0.98	2/88	23/116	0.820	2.976	
35ST_3-6-3	0.97	3/87	25/101	0.777	0.373	√
35ST_3-7-3	0.75	17/68	62/130	0.693	1.696	
35ST_3-8-1	0.89	9/80	38/101	0.704	0.988	√
35ST_3-9-5	0.93	6/84	25/103	0.812	1.991	
35ST_3-11-4	0.95	4/85	29/82	0.682	1.902	
*PER22*T_3-1-7	0.87	10/78	29/106	0.832	3.325	
*PER22*T_3-2-5	0.97	3/86	27/92	0.732	0.152	√
*PER22*T_3-3-1	0.93	6/84	31/98	0.733	0.149	√
*PER22*T_3-4-4	0.95	4/85	29/82	0.679	2.068	
*PER22*T_3-5-3	0.89	9/80	32/101	0.765	0.105	
*PER22*T_3-6-5	0.96	4/85	37/110	0.695	1.703	
*PER22*T_3-8-7	0.97	2/87	25/101	0.774	0.301	√
*PER22*T_3-9-2	0.96	4/86	21/80	0.771	0.180	
*PER22*T_3-11-4	0.93	6/84	31/98	0.733	0.139	√
*PER22*T_3-12-8	0.97	3/87	27/92	0.729	0.203	
*PER22*T_3-14-11	0.92	7/82	32/104	0.756	0.018	√
*PER73*T_3-1-5	0.91	8/82	35/94	0.691	1.573	
*PER73*T_3-2-5	0.88	9/79	26/89	0.804	1.198	
*PER73*T_3-3-3	0.87	10/79	32/105	0.796	1.029	
*PER73*T_3-5-3	0.91	8/82	35/108	0.746	0.009	
*PER73*T_3-6-4	0.96	3/87	25/101	0.781	0.512	
*PER73*T_3-8-4	0.89	9/80	34/116	0.790	0.905	√
*PER73*T_3-9-1	0.86	11/77	24/86	0.839	3.141	√
*PER73*T_3-10-9	0.90	8/81	34/101	0.738	0.064	√
*PER73*T_3-11-7	0.91	7/82	26/101	0.815	2.065	
*PER73*T_3-12-12	0.88	10/79	34/112	0.791	0.915	√
*PER73*T_3-13-3	0.93	6/84	28/101	0.778	0.403	
*PER73*T_3-14-11	0.83	13/75	45/104	0.681	2.215	√

The Chi-square (χ^2) statistical test (χ^2 = Sum of $(O-E)^2/E$) was used with degree of freedom 1 ($\chi^2_{0.95} = 3.841$).

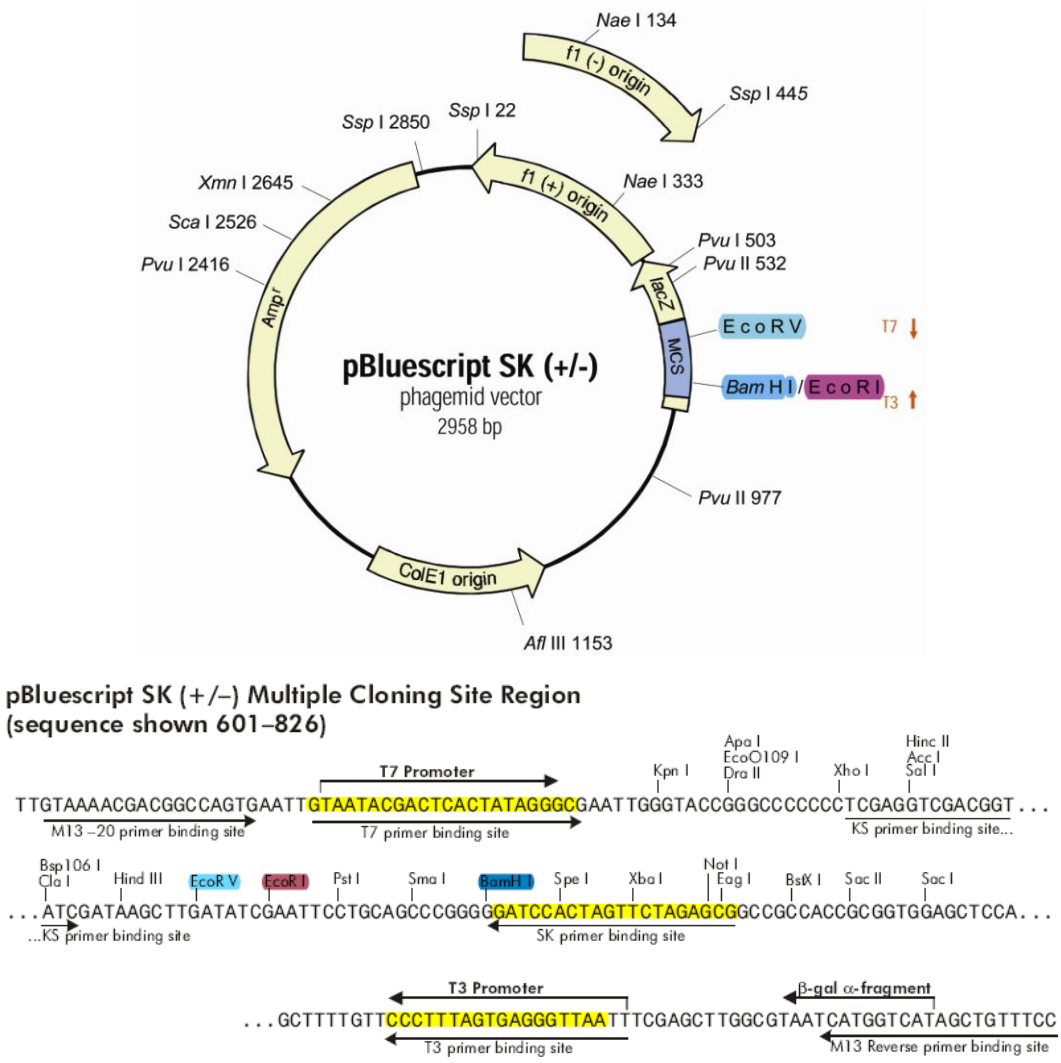

Figure 2.1. Map of pBluescriptSK- cloning vector with the restriction enzymes used in the TA cloning and promoter sub-cloning process. Primers used in the colony PCR and sequencing reactions are highlighted. *PER22* and *PER73* promoters were cloned into the *Eco*RV restriction site within MCS via the TA cloning method. Colony PCRs using *PER22* and *PER73* PfuUltra forward, reverse, and SK primers were applied to confirm the orientation and size of each promoter insert. Each of the *PER22* and *PER73* promoters was sequenced using both T_3 and T_7 primers.

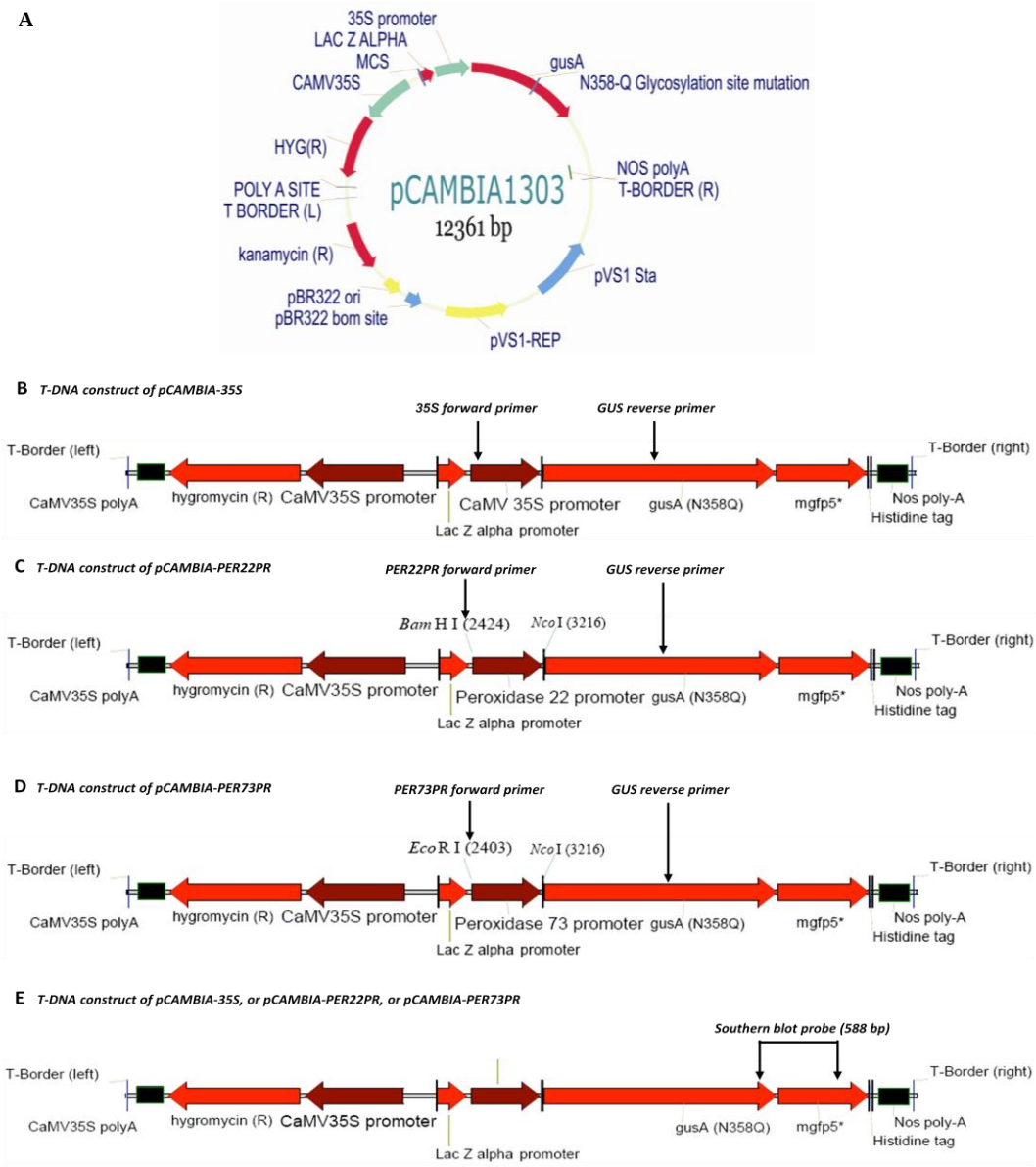

Figure 2.2. Map of the plant transformation vector, pCAMBIA1303, and the T-DNA inserts of pCAMBIA-*35S*, pCAMBIA-*PER22*PR, and pCAMBIA-*PER73*PR vectors. (A) pCAMBIA1303 vector map. (B) T-DNA construct of pCAMBIA-*35S* vector with primer locations for genomic PCR. (C). T-DNA construct of pCAMBIA-*PER22*PR vector with primer locations for genomic PCR. (D) T-DNA construct of pCAMBIA-*PER73*PR vector with primer locations for genomic PCR. (E) The probe location on the T-DNA construct for southern blot analysis.

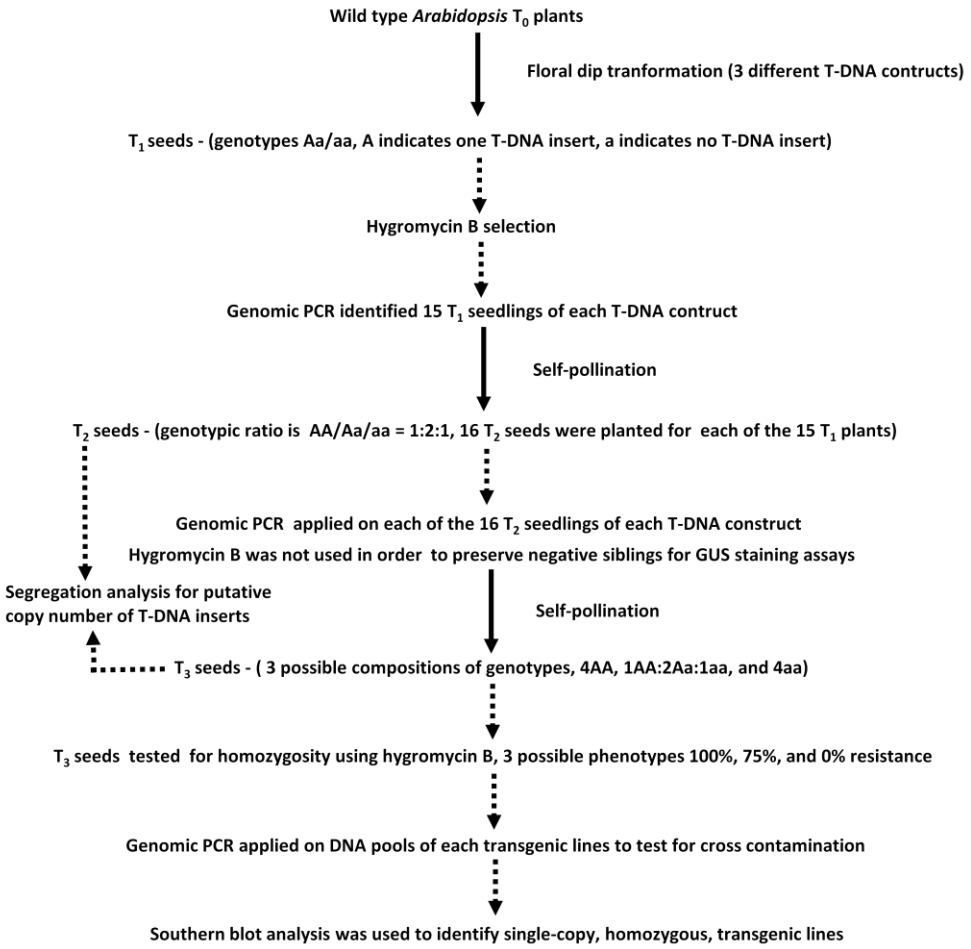

Figure 2.3. Flowchart of the development of single-copy, homozygous, transgenic *Arabidopsis* lines. Solid arrows indicate the selfing of *Arabidopsis* plants to produce the next generation. Dotted arrows indicate the application of a method (genomic PCR, Hygromycin B screening, segregation and southern blot analyses) to identify the desired transgenic lines. To simplify the flowchart, only a single-copy transgenic line scenario is illustrated.

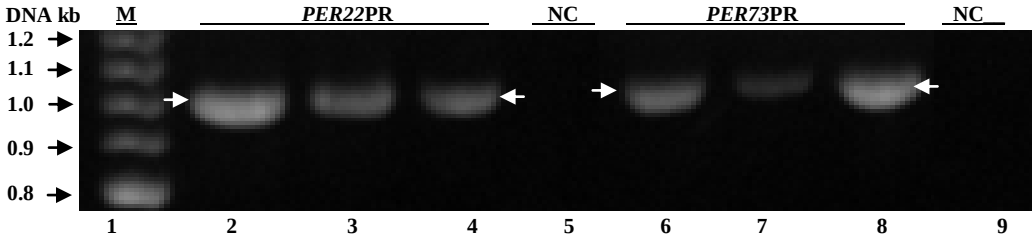

Figure 2.4. PfuUltra DNA polymerase amplification of *PER22* and *PER73* promoters. Lane 1, Amersham 100 bp DNA ladder. Lane 2-4, *PER22* promoter (1022 bp). Lane 5, Negative control for *PER22* promoter. Lane 6-8, *PER73* promoter (1055 bp). Lane 9, Negative control for *PER73*. PCR reactions using PfuUltra DNA polymerase amplified single products of the expected size (1022 bp for *PER22*PR, 1055 bp for *PER73*PR).

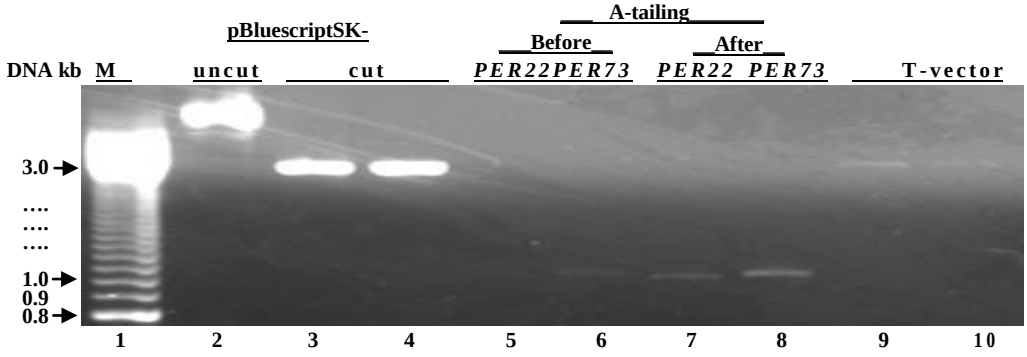

Figure 2.5. Components of TA cloning used to insert *PER22* and *PER73* promoters into pBluescriptSK- vector. Lane 1, Amersham 100 bp DNA ladder. Lane 2, pBluescriptSK- vector. Lane 3-4, linearized pBluescriptSK- vector generated by digestion with *Eco*RV. Lane 5, *PER22* promoter before A-tailing. Lane 6, *PE73* promoter before A-tailing. Lane 7, A-tailed *PER22* promoter. Lane 8, A-tailed *PER73* promoter. Lane 9-10, T-vector created by adding thymine overhang to linearized pBluescriptSK- vector. The pBluescriptSK-*PER22*PR and pBluescriptSK-*PER73*PR vectors were constructed by ligating A-tailed *PER22* promoter (1022 bp, lane 7) and A-tailed *PER73* promoter (1055 bp, lane 8) with T-vector (2958 bp, lane 9 and 10), respectively.

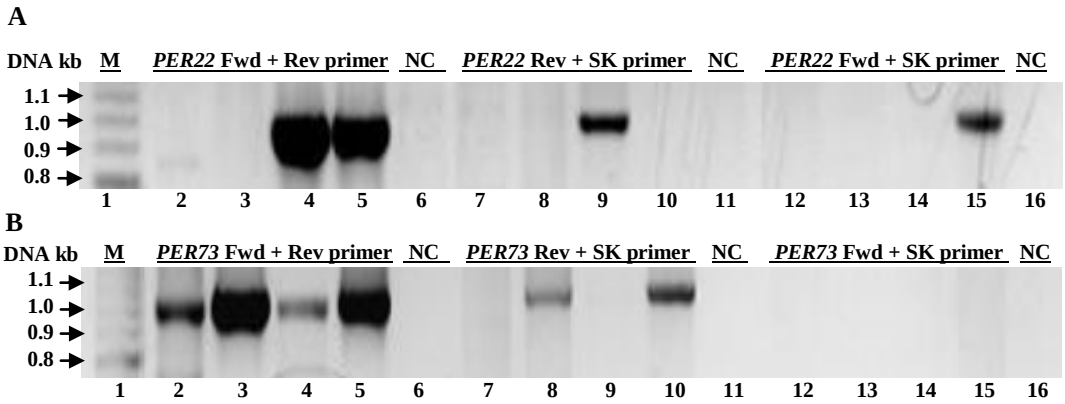

Figure 2.6. Results of colony PCRs using forward and reverse primers of *PER22* and *PER73* promoters in combination with SK primer. Colony PCR allowed the selection of positive *E. coli* transformants with promoters inserted in the desired orientation. Lane 1, Amersham 100 bp DNA ladder. Lane 2-5, colony PCR with forward and reverse primers amplified (A) *PER22* promoter (two positive transformants, lane 4 and 5) or (B) *PER73* promoter (four positive transformants, lane 2-5). Lane 6, negative control. Lane 7-10, colony PCR with reverse and SK primers to amplified (A) *PER22* promoter (lane 9) and (B) *PER73* promoter (lane 8 and 10) inserted in pBluescriptSK- in the desired orientation. Lane 11, negative control. Lane 12-15, colony PCR with forward and SK primers to amplified (A) *PER22* promoter (lane 15) inserted in pBluescriptSK- in the undesired orientation. For (B) *PER73* promoter, no products were amplified (lane 12-15). However, no troubleshooting experiments were conducted as promoter inserted in desired orientation was acquired. Lane 16, negative control. Amplicons produced by colony PCRs using reverse and SK primers indicate the *E. coli* transformants containing pBluescriptSK- vectors with the *PER22* promoter (A, lane 9) and *PER73* promoter (B, lane 8 and 10) inserted in the desired orientation.

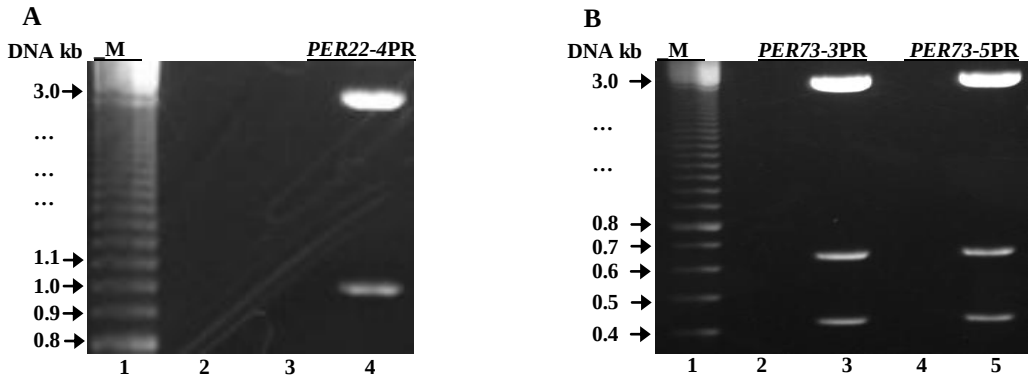

Figure 2.7. Verification of the pBluescriptSK-*PER22*PR and pBluescriptSK-*PER73*PR vectors by restriction digests analysis. (A) Lane 1, Amersham 100 bp DNA ladder. Lane 2 and 3, blank. Lane 4, pBluescriptSK-*PER22*PR (*PER22-4*PR) digested by *Bam*HI and *Nco*I. (B) Lane 1, Amersham 100 bp DNA ladder. Lane 2 and 4, blank. Lane 3 and 5, pBluescriptSK-*PER73*PR (*PER73-3*PR and *PER73-5*PR) vectors digested by digested by *Bam*HI and *Nco*I. (A) *Bam*HI and *Nco*I restriction enzyme digest of pBluescriptSK-*PER*22PR (*PER22*-3PR) vector produced two expected DNA fragments with different sizes (2929 bp and 1042 bp). (B) *Bam*HI and *Nco*I restriction enzyme digest of pBluescriptSK-*PER*73PR (*PER73*-2PR and *PER73*-4PR) vectors produced three expected DNA fragments of different sizes (2938 bp, 653 bp, and 423 bp).

A

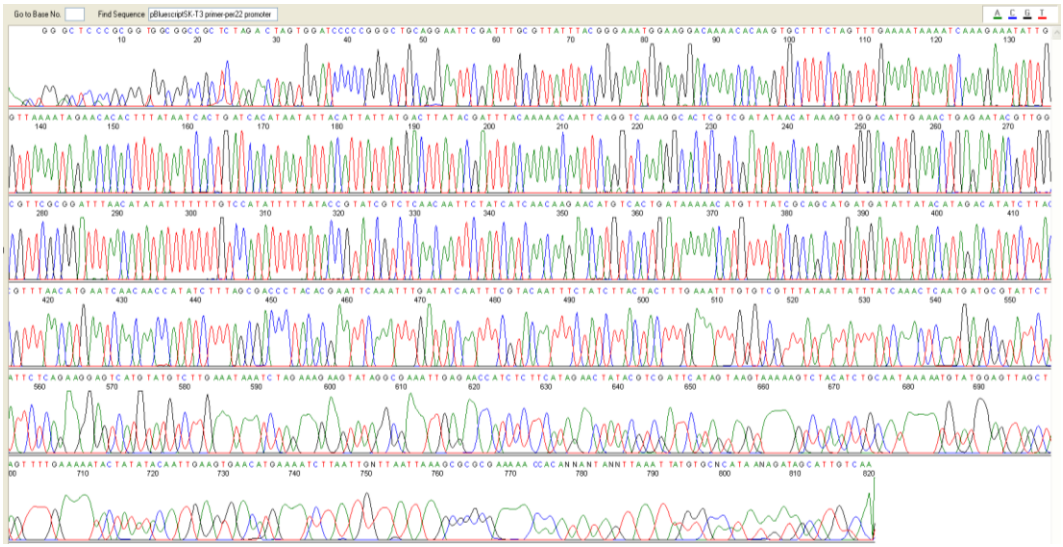

B

Figure 2.8. Chromatographic sequencing results of the *PER22* promoter in pBluescriptSK-*PER22*PR vector by T_3 and T_7 primers. (A) Sequence of the *PER22* promoter produced by T_3 primer. (B) Sequence of the *PER22* promoter produced by T_7 primer. In this region, the *PER22* promoter contains a cluster of 20 adenines (in red circle) approximately 150 bp upstream of the start codon.

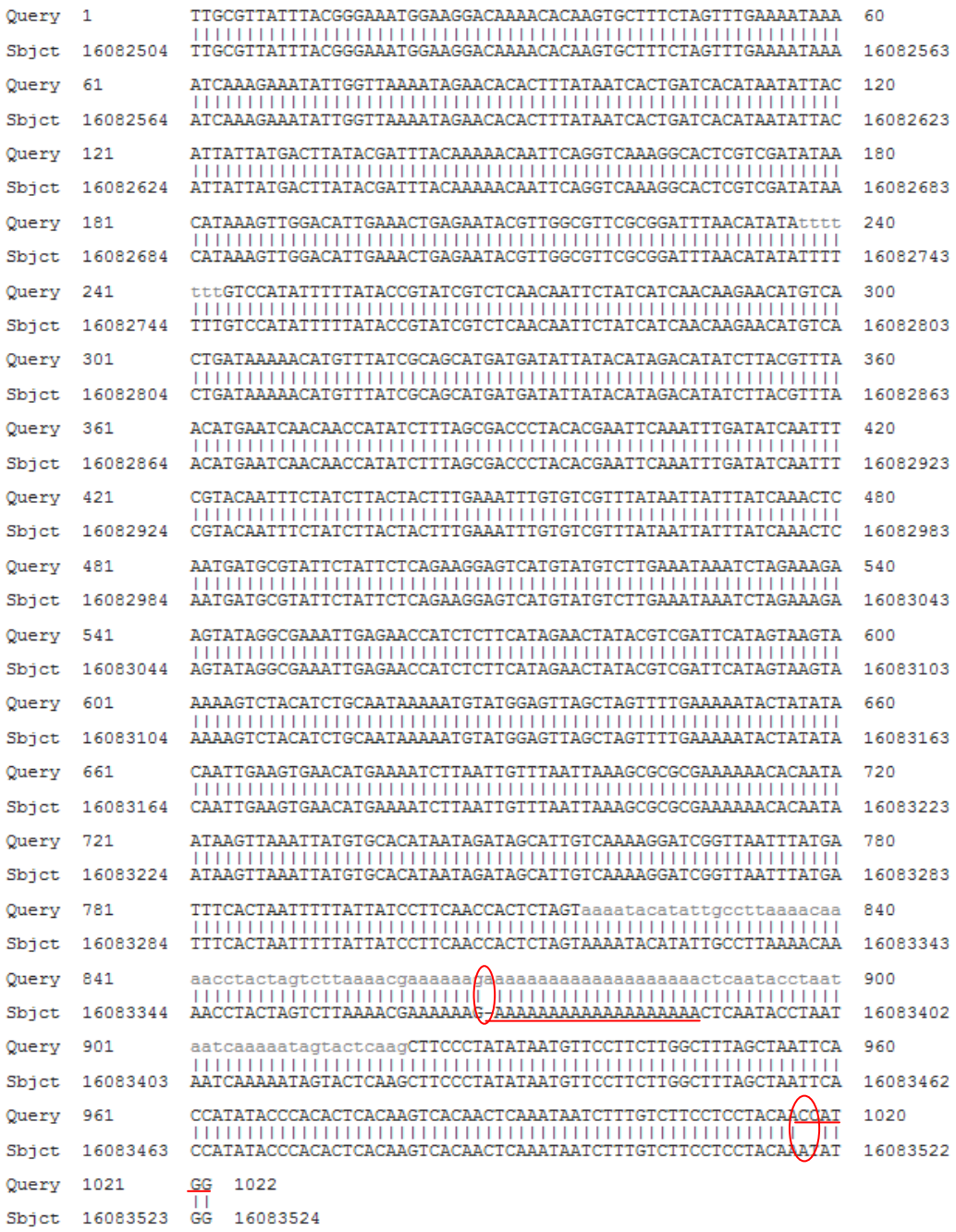

Figure 2.9. Sequence alignment of the *PER22* promoter obtained in this study and the *PER22* promoter (GeneID: 818419) in the NCBI database. *PER22* promoter sequence was BLASTed against *Arabidopsis* genomic DNA. Sequence discrepancies (in red circles and underlined) were caused by one additional adenine (-131) upstream of the start codon and *Nco*I restriction site (C ↓ CATGG) engineered for promoter::*GUS* fusion.

A

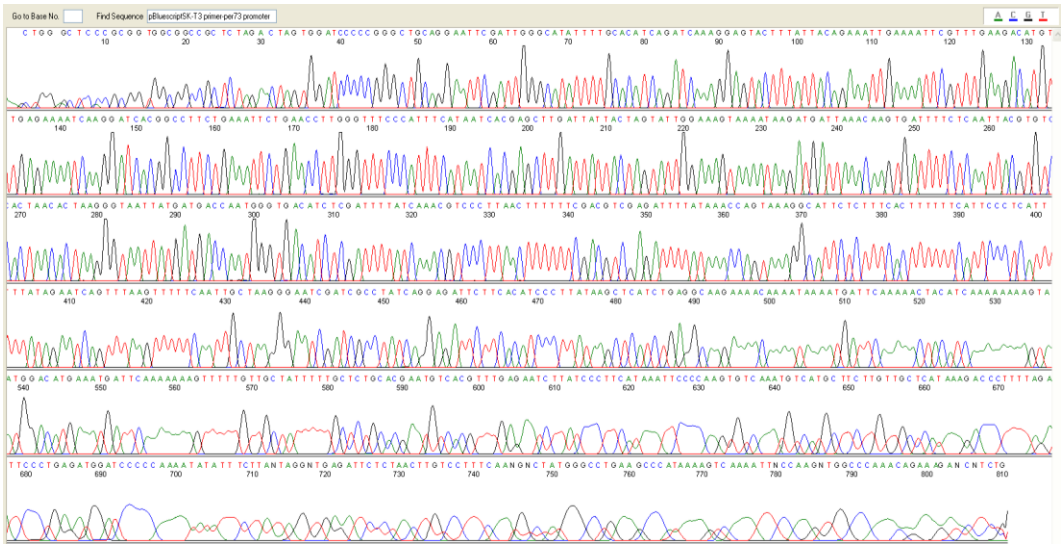

B

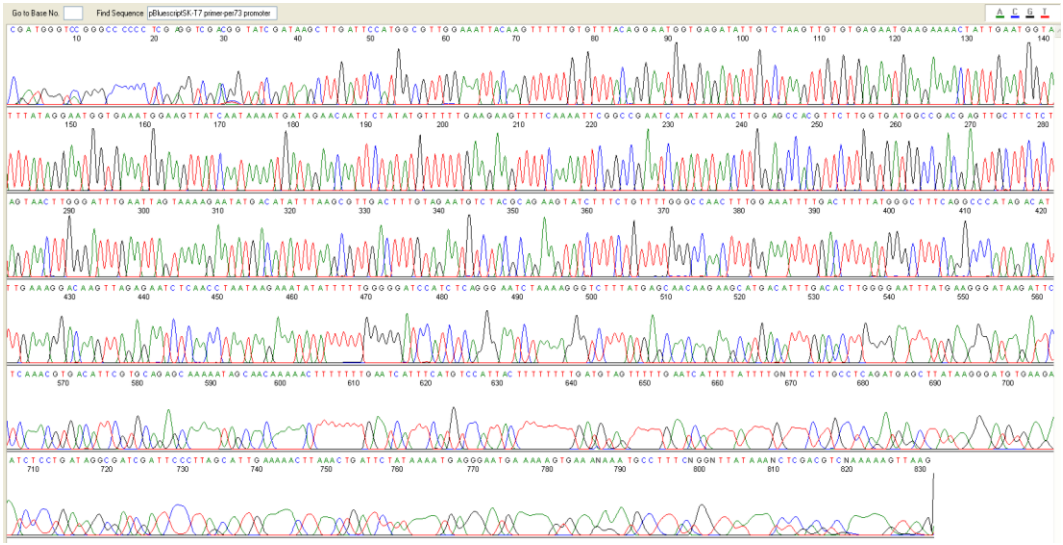

Figure 2.10. Chromatographic sequencing results of the *PER73* promoter in pBluescriptSK-*PER73*PR vector by T_3 and T_7 primers. (A) Sequence of the *PER73* promoter produced by T_3 primer. (B) Sequence of the *PER73* promoter produced by T_7 primer.

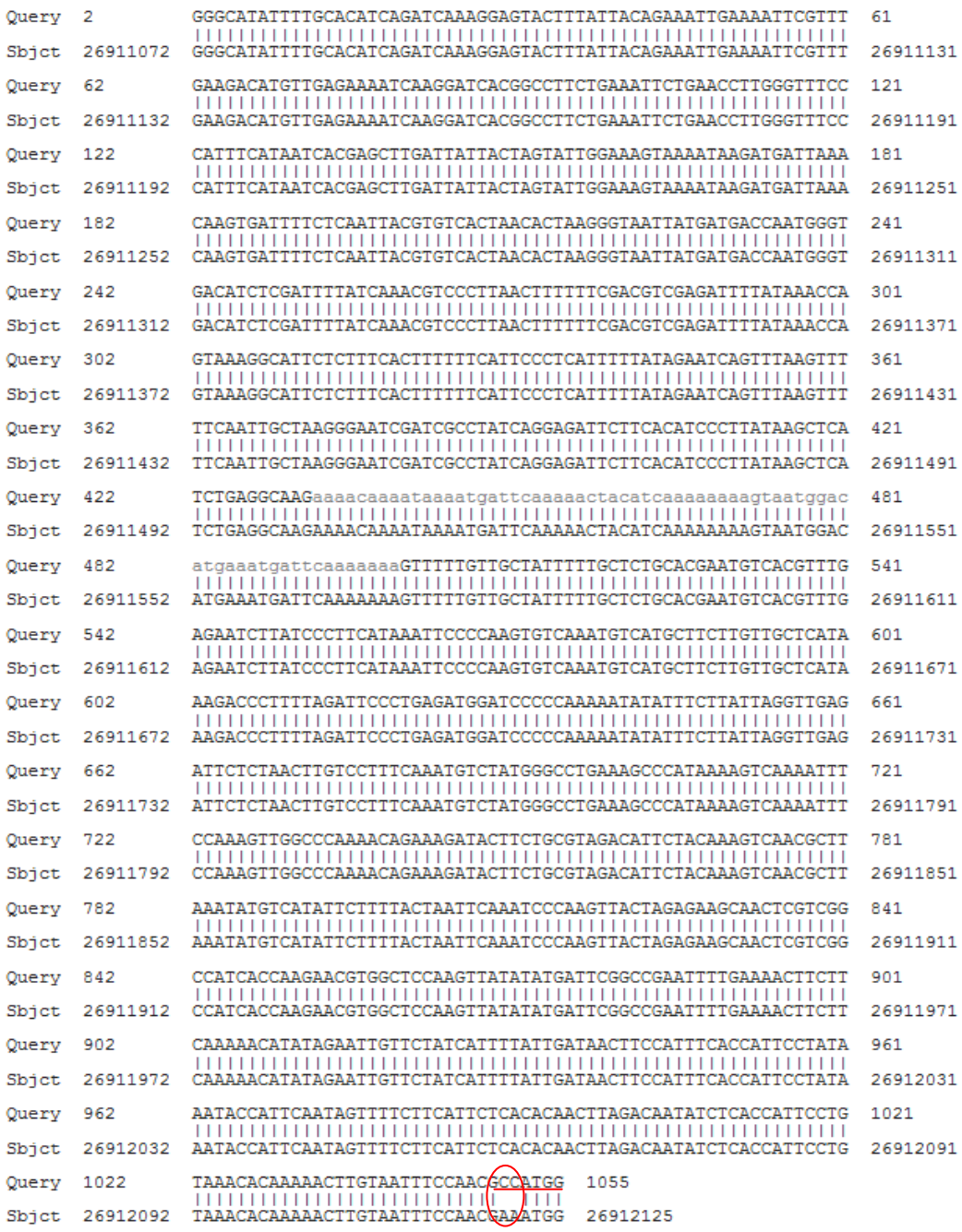

Figure 2.11. Sequence alignment of the *PER73* promoter obtained in this study and the *PER73* promoter (GeneID: 836876) in the NCBI database. *PER73* promoter sequence was BLASTed against *Arabidopsis* genomic DNA. Sequence discrepancies (in red circles and underlined) were caused by *Nco*I restriction site (C ↓ CATGG) engineered for promoter::*GUS* fusion.

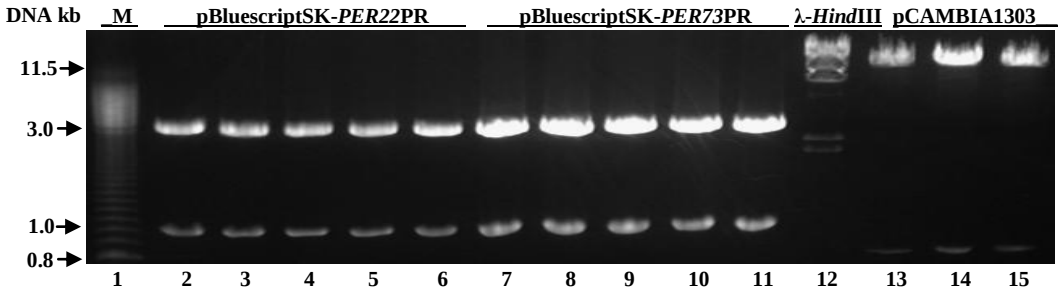

Figure 2.12. Restriction digests of the pBluescriptSK-*PER22*PR, pBluescriptSK-*PER73*PR, and pCAMBIA1303 vectors for 'short-gun' cloning. The promoters of *PER22* and *PER73* were separated from pBluescriptSK- vector with restriction enzymes *Bam*HI and *Nco*I and *Eco*RI and *Nco*I, respectively; pCAMBIA1303 vector was digested with the same combination of restriction enzymes to break CaMV35S promoter::*GUS* fusion. Lane 1, Amersham 100 bp DNA ladder. Lane 2-6, restriction digests of pBluescriptSK-*PER22*PR vector by *Bam*HI and *Nco*I. Lane 7-11, restriction digests of pBluescriptSK-*PER73*PR vector by *Eco*RI and *Nco*I. Lane 12, λ genomic DNA digested with *Hind*III. Lane 13, restriction digests of pCAMBIA1303 vector by *Bam*HI and *Nco*I. Lane 14 and 15, restriction digests of pCAMBIA1303 vector by *Eco*RI and *Nco*I. Instead of gel recovering DNA products from this restriction digest reaction, four DNA fragments of different sizes from lane 2-6 (1049 bp and 2932 bp) and lane 13 (793 bp and 11568 bp) were mixed in one ligation reaction and four DNA fragments of different sizes from lane 7-11 (1064 bp and 2950 bp) and lane 14-15 (814 bp and 11547 bp) were mixed in one ligation reaction. The ligation mixtures were used for 'shot-gun' cloning.

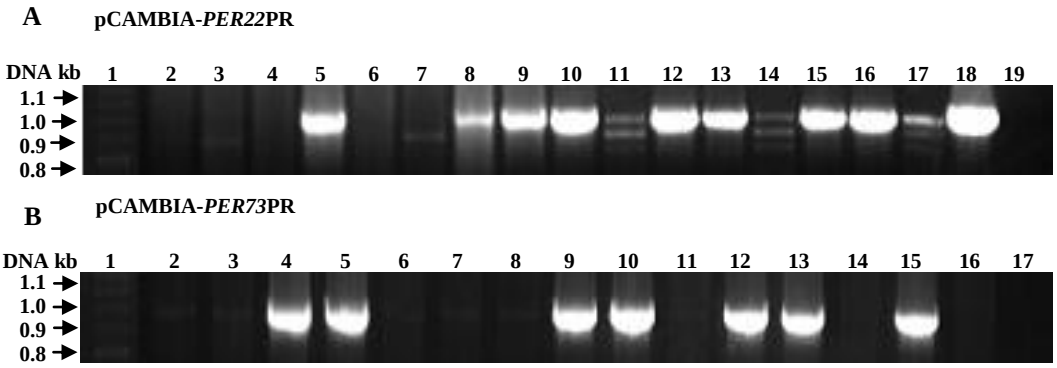

Figure 2.13. Colony PCR results of the positive *E. coli* transformants containing pCAMBIA-*PER22*PR and pCAMBIA-*PER73*PR vectors. (A) Lane 1, Amersham 100 bp DNA ladder. Lane 2-18, colony PCR confirmed 9 positive *E. coli* transformants containing pCAMBIA-*PER22*PR vectors (lane 5, 8, 9, 10, 12, 13, 15, 16, and 18). Lane 19, negative control. (B) Lane 1, Amersham 100 bp DNA ladder. Lane 2-16, colony PCR confirmed 7 positive *E. coli* transformants containing pCAMBIA-*PER73*PR vectors (lane 4, 5, 9, 10, 12, 13, and 15). Lane 17, negative control.

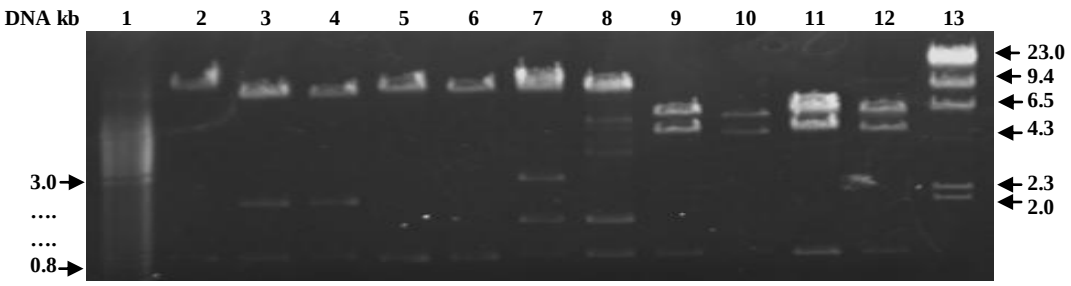

Figure 2.14. Restriction digests analysis of pCAMBIA-*PER22*PR, pCAMBIA-*PER73*PR, and pCAMBIA-*35S* vectors. Four independent plasmids of pCAMBIA-*PER22*PR (pCAM-*PER22-1*PR and pCAM-*PER22-2*PR) and pCAMBIA-*PER73*PR (pCAM-*PER73-1*PR and pCAM-*PER73-2*PR) extracted from positive *E. coli* transformants were analyzed by multiple restriction enzymes. Lane 1, Amersham 100 bp DNA ladder. Lane 2, pCAMBIA-*35S* digested by *Xho*I. Lane 3 and 4, pCAM-*PER22-1*PR and pCAM-*PER22-2*PR digested by *Xho*I and *Bgl*II. Lane 5 and 6, pCAM-*PER22-1*PR and pCAM-*PER22-2*PR digested by *Xho*I and *Pst*I. Lane 7 and 8, pCAM-*PER73-1*PR and pCAM-*PER73-2*PR digested by *Xho*I and *Bam*HI. Lane 9 and 10, pCAM-*PER22-1*PR and pCAM-*PER22-2*PR digested by *Xho*I and *Sph*I. Lane 11 and 12, pCAM-*PER22-1*PR and pCAM-*PER22-2*PR digested by *Xho*I and *Sph*I. Lane 13, λ genomic DNA digested with *Hind*III. In the end, all the restriction digests produced DNA fragments with expected sizes, except pCAM-*PER73-2*PR (lane 8) digested by *Xho*I and *Bam*HI. Therefore, pCAM-*PER73-2*PR was not carried forward for *Agrobacterium* transformation due to the possible mutations in the restriction sites of *Xho*I and/or *Bam*HI.

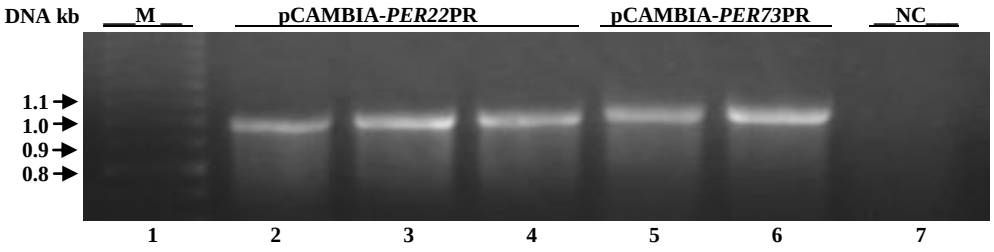

Figure 2.15. Colony PCR results of the positive *Agrobacterium* transformants containing pCAMBIA-*PER*22PR and pCAMBIA-*PER*73PR vectors. pCAMBIA-*PER22*PR (pCAM-*PER22-1*PR) and pCAMBIA-*PER73*PR (pCAM-*PER73-1*PR) vectors were used to transform *Agrobacterium* using free-thaw method. Lane1, Amersham 100 bp DNA ladder. Lane 2-5, 3 positive *Agrobacterium* transformants for pCAMBIA-*PER22*PR (1022 bp). Lane 5-6, 2 positive *Agrobacterium* transformants for pCAMBIA-*PER73*PR (1055 bp). Lane 7, negative control.

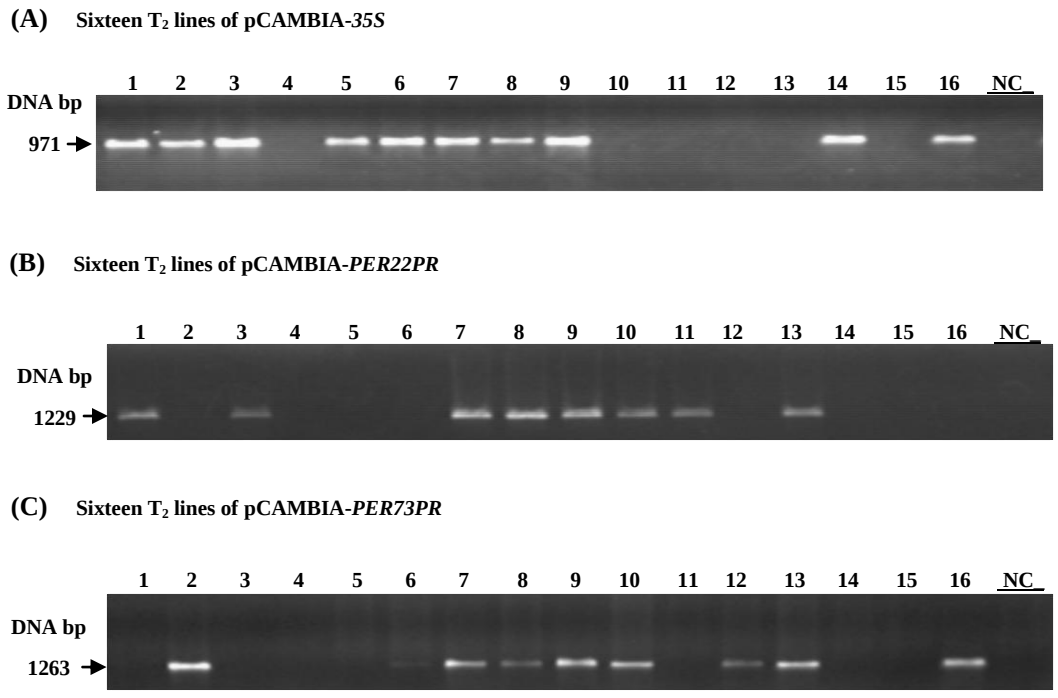

Figure 2.16. Genomic PCR results for 16 T_2 lines of pCAMBIA-*35S*, pCAMBIA-*PER22*PR, and pCAMBIA-*PER73*PR. The amplicon sizes for (A) pCAMBIA-*35S*, (B) pCAMBIA-P*ER22*PR, and (C) pCAMBIA-*PER73*PR are 971 bp, 1229 bp, and 1263 bp, respectively. For each T-DNA construct, sixteen T_2 lines were tested for each of the 15 T_1 lines. Genomic PCR amplified DNA products (positive bands on the gel) that represent insertion(s) of T-DNA construct(s) in the *Arabidopsis* genome. The genotype of these T_2 lines is either AA or Aa.

Putative homozygous lines of pCAMBIA-*PER*22PR and pCAMBIA-*PER*73PR

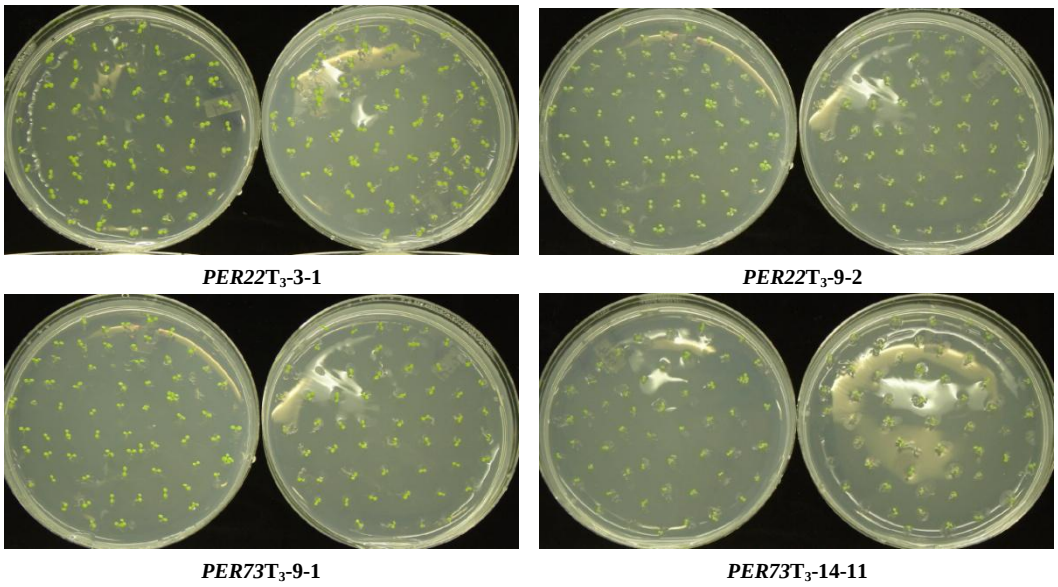

***PER22*T$_3$-3-1** ***PER22*T$_3$-9-2**

***PER73*T$_3$-9-1** ***PER73*T$_3$-14-11**

Heterozygous line of pCAMBIA-*PER*22PR (*PER22*T$_3$-2-11)

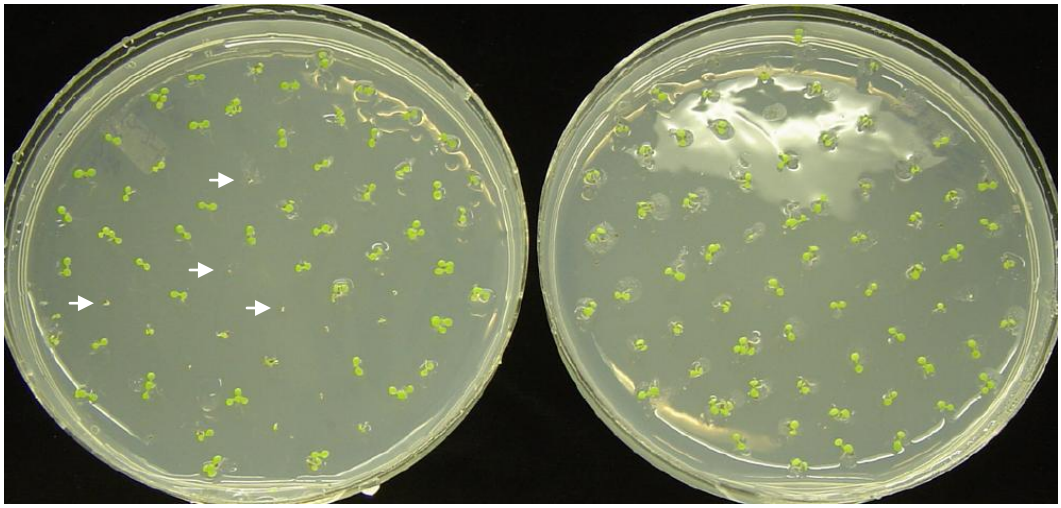

Figure 2.17. Hygromycin B screening results of transgenic lines containing T-DNA construct(s) of pCAMBIA-*35S*, pCAMBIA-*PER22*PR, and pCAMBIA-*PER73*PR. Four putative homozygous T_3 lines are shown as examples of 100% resistance to hygromycin B. The phenotypic contrast of resistant versus non-resistant seeds was reflected in the left plate of the heterozygous line (*PER22*T_3-2-11). In each pair, the left plate is a 1/2 MS basal medium plate with hygromycin B, and the right plate is a 1/2 MS basal medium plate.

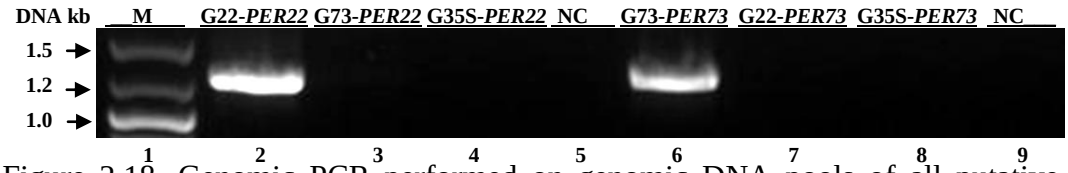

Figure 2.18. Genomic PCR performed on genomic DNA pools of all putative homozygous transgenic lines of pCAMBIA-*35S*, pCAMBIA-*PER22*PR, and pCAMBIA-*PER73*PR. Genomic PCR on DNA pools was used to test for cross contamination. Genomic DNA pools generated by all the putative single-copy, homozygous lines of pCAMBIA-*35S*, pCAMBIA-*PER22*PR, and pCAMBIA-*PER73*PR are named as G35S, G22, and G73, respectively. Amplicons produced only by genomic PCR with DNA pools of G22 and G73 indicated that no cross contamination occurred in these transgenic lines. Lane 1, GeneRuler DNA Ladder Mix. Lane 2, genomic PCR on G22 with *PER22* primers. Lane 3, genomic PCR on G73 with *PER22* primers. Lane 4, genomic PCR on G35S with *PER22* primers. Lane 5, negative control. Lane 6, genomic PCR on G73 with *PER73* primers. Lane 7, genomic PCR on G22 with *PER73* primers. Lane 8, genomic PCR on G35S with *PER73* primers. Lane 9, negative control.

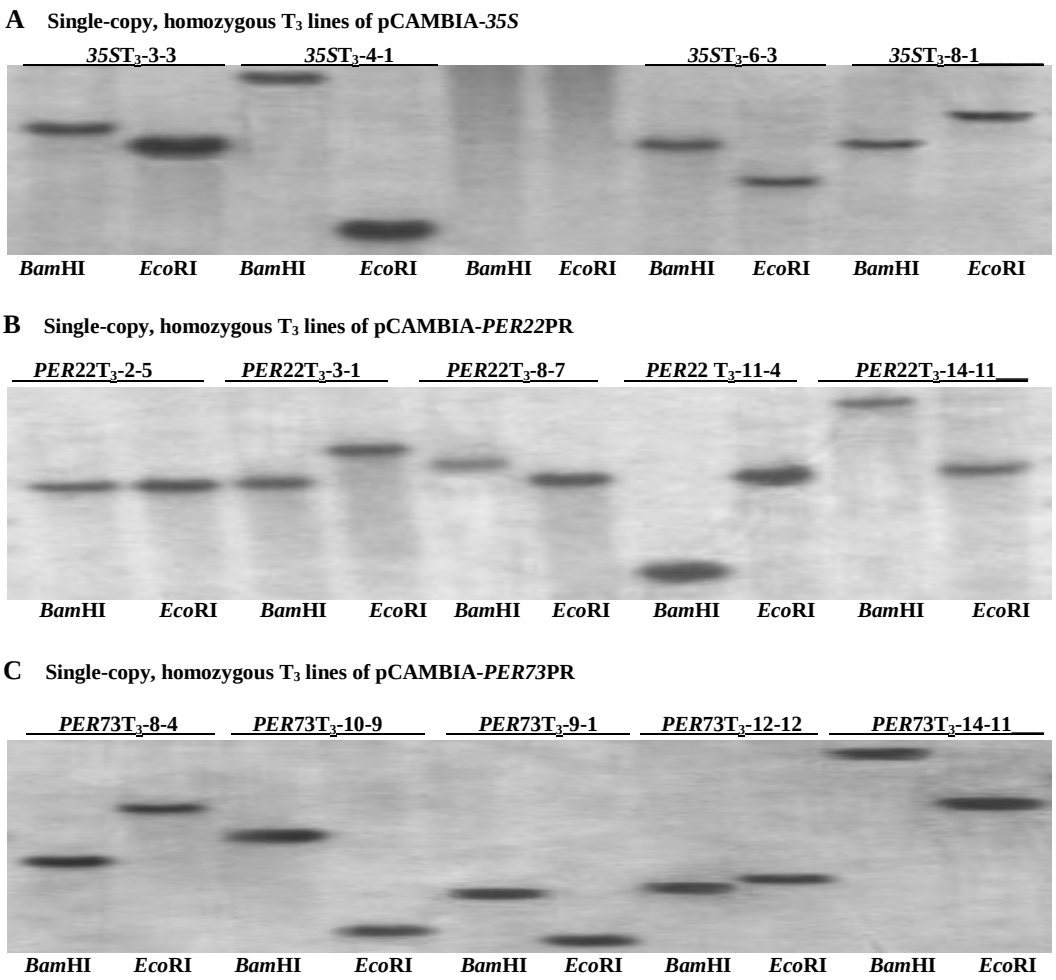

Figure 2.19. Southern blot analysis of T_3 homozygous, transgenic lines with a single-copy T-DNA insert. Genomic DNA for each of the homozygous, transgenic lines of pCAMBIA-*35S*, pCAMBIA-P*ER22*PR, and pCAMBIA-*PER73*PR were digested with *Bam*HI (left) and *Eco*RI (right) restriction enzymes. A total of 14 single-copy, homozygous transgenic lines were acquired, comprising (A) four lines for pCAMBIA-*35S*, (B) five lines for pCAMBIA-*PER22*PR, and (C) five lines for pCAMBIA-*PER73*PR. Single band of different size in each lane (present on the x-ray films) represent that single-copy T-DNA insert separated from the *Arabidopsis* genome by *Bam*HI and *Eco*RI independently and subsequently hybridized to the radioactive southern probe.

2.4. References

Bakalovic N, Passardi F, Ioannidis V, Cosio C, Penel C, Falquet L, Dunand C. 2006. PeroxiBase: a class III plant peroxidase database. Phytochemistry-US 67: 534-539.

Basu A, Basu U, Taylor GJ. 1994. Induction of microsomal membrane proteins in roots of an aluminum-resistant cultivar of *Triticum aestivum* L. under conditions of aluminum stress. Plant Physiol 104: 1007-1013.

Basu U, McDonald-Stephens JL, Archambault DJ, Good AG, Briggs KG, Taing-Aung, Taylor GJ. 1997. Genetic and physiological analysis of doubled-haploid, aluminum resistant lines of wheat provide evidence for the involvement of a 23 kD, root exudate polypeptide in mediating resistance. Plant Soil 196: 283-288.

Basu U, Good AG, Aung T, Slaski JJ, Basu A, Briggs KG, Taylor GJ. 1999. A 23 kD, aluminum-binding, root exudate polypeptide co-segregates with the aluminum-resistant phenotype in *Triticum aestivum*. Physiol Plant 106: 53-61.

Basu U, Francis JL, Whittal RM, Stephens JL, Wang Y, Zaiane OR, Goebel R, Muench DG, Good AG, Taylor GJ. 2006. Extracellular proteomes of *Arabidopsis thaliana* and *Brassica napus* roots: Analysis and comparison by MudPIT and LC-MS/MS. Plant Soil 286: 357-376.

Cai S, Lashbrook CC. 2008. Stamen abscission zone transcriptome profiling reveals new candidates for abscission control: enhanced retention of floral organs in transgenic plants overexpressing *Arabidopsis* ZINC FINGER PROTEIN2. Plant Physiol 146: 1305-1321.

Chen M, Presting G, Barbazuk WB, Goicoechea JL, Blackmon B, Fang G, Kim H, Frisch D, Yu Y, Sun S, Higingbottom S, Phimphilai J, Phimphilai D, Thurmond S, Gaudette B, Li P, Liu J, Hatfield J, Main D, Farrar K, Henderson C, Barnett L, Costa R, Williams B, Walser S, Atkins M, Hall C, Budiman MA, Tomkins JP, Luo M, Bancroft I, Salse J, Regad F, Mohapatra T, Singh NK, Tyagi AK, Soderlund C, Dean RA, Wing RA. 2002. An integrated physical and genetic map of the rice genome. Plant Cell 14: 537-545.

Clough SJ, Bent AF. 1998. Floral dip: a simplified method for *Agrobacterium* mediated transformation of *Arabidopsis thaliana*. Plant J 16:735-743.

Copenhaver GP, Browne WE, Preuss D. 1998. Assaying genome-wide recombination and centromere functions with *Arabidopsis* tetrads. Proc Natl Acad Sci USA 95: 247-252.

Cosio C, Zheng Y, Perry S, Dunand C. 2008. Peroxidases involved in pod shatter mechanisms. Physiol Plantarum 133: 10-19.

Cosio C, Dunand C. 2009. Specific functions of individual class III peroxidase genes. J Exp Bot 60: 391-408.

Costa R, Gotz M, Mrotzek N, Lottmann J, Berg G, Smalla K. 2006. Effects of site and plant species on rhizosphere community structure as revealed by molecular analysis of microbial guilds. FEMS Microbiol Ecol 56: 236-249.

Dale J, Schantz M. 2003. Chapter in: cutting and joining DNA, book "From Gene to Genomes". ISBN: 9780471497820. Wiley Interscience.

Ehlting J, Mattheus N, Aeschliman DS, Li E, Hamberger B, Cullis IF, Zhuang J, Kaneda M, Mansfied SD, Samuels L, Ritland K, Ellis BE, Bohlmann J, Douglas CJ. 2005. Global transcript profiling of primary stems from *Arabidopsis thaliana* identifies candidate genes for missing links in lignin biosynthesis and transcriptional regulators of fiber differentiation. Plant J 42: 618-640.

Höfgen R, Willmitzer L. 1988. Storage of competent cells for *Agrobacterium* transformation. Nucleic Acids Res 16: 9877

Jefferson RA, Kavanagh TA, Bevan MW. 1987. *GUS* fusions: beta-glucuronidase as a sensitive and versatile gene fusion marker in higher plants. EMBO J 6: 3901-3907.

Koncz C, Schell J. 1986. The promoter of the TL-DNA gene 5 controls the tissue-specifc expression of chimeric genes carried by a novel type of *Agrobacterium* binary vector. Mol Gen Genet 204: 383-396.

Kumari M, Taylor GJ, Deyholos MK. 2008. Transcriptomic responses to aluminum stress in roots of *Arabidopsis thaliana*. Mol Genet Genomics 279: 339-357.

Nunn CM, Djordjevic S, Hillas PJ, Nishida CR, Ortiz de Montellano PR. 2002. The crystal structure of *Mycobacterium tuberculosis* alkylhydroperoxidase AhpD, a potential target for antitubercular drug design. J Biol Chem 277: 20033-20040.

Lescot M, Dhais P, Thijs G, Marchal K, Moreau Y, Van de Peer Y, Rouz P, Rombauts S. 2002. PlantCARE, a database of plant *cis*-acting regulatory elements and a portal to tools for in silico analysis of promoter sequences. Nucleic Acids Res 30: 325-327.

Lin X, Kaul S, Rounsley S, Shea TP, Benito MI, Town CD, Fujii CY, Mason T, Bowman CL, Barnstead M, Feldblyum TV, Buell CR, Ketchum KA, Lee J, Ronning CM, Koo HL, Moffat KS, Cronin LA, Shen M, Pai G, Van Aken S, Umayam L, Tallon LJ, Gill JE, Adams MD, Carrera AJ, Creasy TH, Goodman HM, Somerville CR, Copenhaver GP, Preuss D, Nierman WC, White O, Eisen JA, Salzberg SL, Fraser CM, Venter JC. 1999. Sequence and analysis of chromosome 2 of the plant *Arabidopsis thaliana*. Nature 402: 761-768.

Emanuelsson O, Nielsen H, Brunak S, Von Heijne G. 2000. Predicting subcellular localization of proteins based on their N-terminal amino acid sequence. J Mol Biol 300: 1005-1016.

Emanuelsson O, Brunak S, Von Heijne G, Nielsen H. 2007. Locating proteins in the cell using TargetP, SignalP, and related tools. NatProtoc 2: 953-971.

Passardi F, Theiler G, Zamocky M, Cosio C, Rouhier N, Teixera F, Margis-Pinheiro M, Ioannidis V, Penel C, Falquet L, Dunand C. 2007. PeroxiBase: the peroxidase database. Phytochemistry-US 68: 1605-1611.

Shepherd T, Davies HV. 1994. Effect of exogenous amino acids, glucose and citric acid on the patterns of short-term accumulation and loss of amino acids in the root-zone of sand-cultured forage rape (*Brassica napus* L.). Plant Soil 158: 111-118.

Stanley T. 2001. DNA ligases. Chapter in: Current Protocols in Molecular Biology, Book 1. Wiley Interscience.

The *Arabidopsis* Genome Initiative. 2000. Analysis of the genome sequence of the flowering plant *Arabidopsis thaliana*. Nature 408: 796-815.

Tognolli M, Penel C, Greppin H, Simon P. 2002. Analysis and expression of the class III peroxidase large gene family in *Arabidopsis thaliana*. Gene 288: 129-138.

Valerio L, De Meyer M, Penel C, Dunand C. 2004. Expression analysis of the *Arabidopsis* peroxidase multigenic family. Phytochemistry-US 65: 1331-1342.

Wanapu C, Shinmyo A. 1996. cis-regulatory elements of the peroxidase gene in *Arabidopsis thaliana* involved in root-specific expression and responsiveness to high-salt stress. Ann N Y Acad Sci 782: 107-114.

Welinder KG. 1992. Plant peroxidases: structure fuction relationshops. In: Penel C, Gaspar T, Greppin H. Plant Peroxidases. University of Geneva, Geneva, Switzerland, pp 1-24.

Yamaguchi K, Yamaguchi M, Tomizawa J. 1982. Incompatibility of plasmids containing the replication origin of the *Escherichia coli* chromosome. Proc Natl Acad Sci USA 79: 5347-5351.

Zhang Z, Schwartz S, Wagner L, Miller W. 2000. A greedy algorithm for aligning DNA sequences. J Comput Biol 7: 203-214.

Chapter 3. Histochemical *GUS* staining of single-copy, homozygous, transgenic lines of *Arabidopsis* harbouring peroxidase promoter::*GUS* reporter fusions

3.1. Introduction

Because class III peroxidases function in such a broad range of physiological processes, their activities are detectable throughout the lifespan of various plants (Passardi *et al.*, 2005). Comparison of peroxidase activities at different situations indicates that the up-regulation of peroxidases is generally transient. Transient induction, however, does not always apply to all peroxidases. A basal level of peroxidase activity in plants probably serves to perform "housekeeping" functions such as their involvement in cell elongation and lignification (Passardi *et al.*, 2005). Gene expression of the class III peroxidase family of *Arabidopsis* has been studied by different research groups (Tognolli *et al.*, 2002; Valerio *et al.*, 2004). Nevertheless, expression patterns of some highly homologous peroxidases often vary from one study to another (Tognolli *et al.*, 2002; Valerio *et al.*, 2004).

Since the *Arabidopsis* genome has been sequenced and is available to the public, its global gene expression can be analyzed using microarray techniques. Microarray analysis provides a high-throughput platform to study expression of many genes simultaneously. Several types of microarray chips are commercially available, including cDNA macroarrays and oligomicroarrays. The advantage of using an oligomicroarray is the lower likelihood of cross-hybridization between homologous genes. A strategy used to avoid cross-hybridization in cDNA

macroarrays was to include the 5' and 3' untranslated regions in DIG-labeled probes. This enabled the detection of different expression patterns of peroxidases with high homology at the nucleotide level (such as *PER35* and *PER73*; 76.5% identity) (Tognolli *et al.*, 2002). An amplicon array approach employed several different web tools to design gene-specific primers for the 73 class III peroxidase genes in *Arabidopsis*. This included tools such as specific primers & amplicon design software (SPADS) (Thareau *et al.*, 2003), complete *Arabidopsis* transcriptome microarray (CATMA) (Crowe *et al.*, 2003), and manual BLAST. The amplicon hybridization results, however, differed from those of the cDNA macroarray study. The cDNA macroarray detected traces of *PER35* transcripts only in the roots, while *PER73* mRNA was ubiquitous in the plant (Tognolli *et al.*, 2002). However, the amplicon approach demonstrated the presence of *PER35* transcripts in every organ studied: roots, leaves, stems, and flowers, whereas *PER73* was expressed variably in roots, stems, and flowers, but there was no expression in leaves (Valerio *et al.*, 2004). The other pair, *PER22* and *PER23*, also displayed distinct patterns of expression (Valerio *et al.*, 2004).

My analysis of the homology between these two pairs of peroxidases suggests that cross-hybridization is inevitable in hybridization-based assays and neither the cDNA macroarray nor the amplicon array can differentiate the individual expression patterns of these genes accurately. At the mRNA level, *PER22* (At2g38380) and *PER23* (At2g38390) share 89.5% homology, while the homology between *PER35* and *PER73* is 76.5%. In our oligomicroarray studies, *PER73* (At5g67400) was up-regulated 7.39-fold higher than the control at 6 hours and showed no difference from the control at 48 hours of Al stress treatment, while *PER35* (At3g49960) remained unaffected at both time points (Kumari *et al.*, 2008). An analysis using 70-base-long oligonucleotides representing *PER22* and

PER73 genes demonstrates that the high homology between their corresponding homologous *PER23* and *PER35* results in cross-hybridization as well. The differential expression of *PER35* and *PER73* detected in our microarray studies could reflect positional artifacts on the gene chip introduced by spurious correlations between genes (Yu *et al.*, 2007)

Protein targeting predictions from Swiss-Prot show that both *PER35* and *PER73* proteins were predicted to be secreted (Gasteiger *et al.*, 2003). The *PER22* and *PER23* proteins were predicted to be secreted and/or vacuolar, as their carboxy-terminal extensions engender targeting to the vacuole (Gasteiger *et al.*, 2003). These predictions, however, are speculative until *in vivo* expression of individual peroxidases can be achieved.

Due to the high homology among many peroxidases, it is difficult to study gene expression of a single peroxidase via hybridization methods, such as *in situ* hybridization, northern blot analysis, or microarrays. However, a promising alternative is to make use of plants transformed with reporter gene constructs, where a reporter gene encoding β-glucuronidase (*GUS*) is fused to promoters of target genes such as *PER22* or *PER73*. This method is can provide information about spatial and developmental patterns of expression that is distinct from the background of other homologous peroxidases within this gene family.

One draw-back of analyzing gene expression by promoter::reporter gene fusion is that artifacts can be produced as a result of random insertion of T-DNA in the plant genome. Trans-acting enhancers, chromosomal regulation, and/or intragenic regions have been known to play a role in the regulation of gene expression (Seiburth and Meyerowitz, 1997; Taylor, 1997). Thus, promoter fusion analysis

cannot always accurately reflect *in vivo* regulation of the gene of interest (Taylor, 1997). It has also been reported that the promoters of interest and the CaMV35S promoter driving expression of plant selectable markers within the same T-DNA constructs can interfere with each other's activity in certain pCAMBIA vectors (Yoo *et al.*, 2005). The pCAMBIA research group acknowledges this problem with some of the vectors (e.g. pCAMBIA1281Z, 1291Z, 1381Z & 1391Z) on their website (http://www.cambia.org).

In order to accurately measure *GUS* expression spatially and quantitatively, several independent, single-copy, homozygous *Arabidopsis* transgenic lines are required as the position of the T-insertion is unknown and only consistent expression patterns among these lines would best represent the endogenous gene expression. However, *Agrobacterium* mediated transformation of *Arabidopsis* generates both single- and multiple-copy hemizygous T-DNA insertion lines (Ye *et al.*, 1999). Studying *GUS* staining patterns of single-copy, homozygous lines eliminates the complications of progeny segregation and promoter activation tagging introduced by the enhancer of CaMV35S promoter. Although single-copy transgenic lines still carry risk, multiple, independent, single-copy, transgenic lines showing the same gene expression patterns provide greater confidence in results.

GUS staining of multiple T_4 transgenic seedlings containing single-copy, homozygous T-DNA constructs of is an effective tool for determining where the promoters direct gene expression, which allows the identification of the biological processes in which they may be involved. So far only a handful of expression patterns for *Arabidopsis* class III peroxidases have been studied spatially and temporally at the tissue level (Tokunaga *et al.*, 2009). *GUS* staining analysis of

single-copy, homozygous T_4 lines will provide valuable insights on how *PER22* and *PER73* are regulated under Al stress.

3.2. Materials and methods

3.2.1. Plant seed material

Seeds of *Arabidopsis thaliana* (Columbia Col-0, Lehle Seeds, catalog number WT-2) and transgenic T_3 seeds containing single-copy, homozygous T-DNA constructs (2 independent lines for negative siblings; 4 independent lines for pCAMIBA-*35S*; 5 independent lines for pCAMBIA-*PER*22PR and pCAMBIA-*PER*73PR) were sterilized as described in section 2.2.1 to generate T_4 plant material.

3.2.2. A hydroponic system optimized for aluminum treatment

Aluminum (Al, 25 mM) stock solutions were prepared by adding $AlCl_3$ $6H_2O$ to 100 ml HCl solution with pH preadjusted to 3.0. Treatment solutions were prepared by adding 200 µl of $AlCl_3$ stock solution to 1 liter of 200 µM $CaCl_2$ (pH 4.3). The pH of the Al treatment solutions was maintained at ~4.3 over the treatment process in order to avoid precipitation of Al and prevent the formation of polymeric Al species (Kinraide and Parker, 1987). Aluminum (Al) stock solutions were made fresh at the beginning of each treatment.

Aluminum (Al) toxicity to *Arabidopsis* root growth was first tested on agar plates. Wild type seeds were surface sterilized and grown in 1/4 strength MS basal

medium (pH 5.6) on agar plates for two weeks after stratification at 4 ℃ for 3 days. Eight *Arabidopsis* seedlings with an average root length of 35 mm were transferred to 1/4 strength MS basal medium on agar plates with Al concentrations ranging from 0 to 125 μM for 120 hours. Root lengths were measured every 24 hours.

Dose response and time course experiments were performed to identify the optimum concentration and the length of exposure for Al treatments. These experiments were conducted in hydroponic culture. Circular, single-hole polypropylene rafts with a diameter of 30 mm (Kavanagh Plastics, Edmonton) were designed to grow single *Arabidopsis* seedlings in 50 ml polyethylene centrifuge tubes. Wild type *Arabidopsis* seedlings were grown in 1/6 strength MS basal salts (pH 5.6) for 14 days, then 80 plants were selected for uniformity and transferred to treatment solutions containing 0, 5, 10, 20, 30, 40, 50, 60, 80, and 100 μM $AlCl_3$ in 200 μM $CaCl_2$ (pH 4.3) for 48 hours. Each treatment was repeated by 8 plants in 8 unique centrifuge tubes (a total of 80 plants/tubes). Increases in root length were measured from day 14 to day 16 and a relative root growth increment (RRGI) was calculated as $(RL_{\text{day 16-treated}} - RL_{\text{day 14-treated}})/(RL_{\text{day 16-control}} - RL_{\text{day 14-control}}) \times 100$ (RL is the abbreviation for root length).

For the time course experiment, 14-day-old seedlings with an average root length of approximately 55 mm were exposed to 5 μM $AlCl_3$ in 200 μM $CaCl_2$ (pH 4.3) from 0 to 48 hours. Root length was recorded every 6 hours for 24 hours, and subsequently every 8 hours until 48 hours. Eight plants were measured and recorded at each time point (8 replicates). In both dose response and time course studies, experiments were repeated three times to ensure repeatability.

The growth solutions for dose response and time course experiments were changed every four days in order to avoid algal growth, depletion of oxygen, and to maintain ionic strength. Solution pH was maintained at pH 5.6 and monitored daily using a portable pH meter. Growth chamber conditions were the same as described in section 2.2.1.

Experiments designed to measure *GUS* expression required a different hydroponic system. Floatable polypropylene rafts 3 mm in thickness containing approximately 100 circular holes (3.5 mm in diameter) in a radial layout around one central hole (2 cm in diameter) were designed to grow multiple seedlings hydroponically. Nylon mesh with a pore size 1.5 μm was attached to the bottom of the rafts. Both nylon mesh and rafts were pre-soaked in 95% ethanol overnight before being glued together using Dow sealant-732 (Dow corning corporation, Midland, MI). Holes in the rafts were filled with 1/2 strength MS basal medium containing 0.7% phytagar for seed germination, support, and nutrient supply. Surface sterilized seeds mixed with 0.1% agar solution were plated on the top of the agar plug in each hole. Pots were planted with 25 seeds from four different genotypes. Therefore, a single replicate with 16 genotypes (WT plants, 14 different transgenic lines, and two negative siblings) required four pots, and a fully replicated design (n=3) required 12 pots. Rafts with multiple seeds in each hole were stratified at 4 ℃ for 72 hours before being transferred to 1 liter of 1/6 strength MS basal salts (Sigma-Aldrich, catalog number M5524) hydroponic solution (pH 5.6) in black polyethylene pots. Multiple seedlings growing in one hole were thinned out after 4 days to one healthy seedling for continuous growth. The hydroponic nutrient solutions were changed every 3 days and maintained at pH 5.6. Growth chamber conditions were the same as for Al dose response and time course treatments (section 3.2.2).

Fourteen-day-old, transgenic, *Arabidopsis* seedlings were exposed to Al treatment solutions (5 μM) and control solutions (0 μM) containing 200 μM $CaCl_2$ at pH 4.3. Ten transgenic seedlings representing each of the multiple independent lines of each T-DNA construct were harvested from different polyethylene pots and immediately placed in *GUS* staining solution every 8 hours until 48 hours. Ten transgenic seedlings growing in the same hydroponic condition were also harvested on days 8, 9, 14, and 21 after stratification. The above experiments were carried out in triplicate using randomized block design to avoid pseudoreplication (Hurlbert, 1984). The transgenic *Arabidopsis* seedlings were harvested in the growth chamber; harvesting times falling in the dark cycle were conducted in a dimmed light condition.

3.2.3. Histochemical *GUS* staining assay

The activity of β-glucuronidase (*GUS*) can be assayed qualitatively by staining with the chromogenic substrate X-Gluc (5-bromo-4-chloro-3-indolyl-β-D-glucuronide) or quantitatively with the fluorogenic substrate 4-MUG (4- methyl-lumbellyferyl-β-D-glucuronide) (Jefferson, 1987). *GUS* staining is a convenient way to examine the tissue- and development-specific distribution of reporter gene expression. After staining for *GUS* activity, tissue can be examined as a whole-mount preparation or processed further to observe activity patterns in sections. *GUS* activity can be accurately determined both in extracts and in intact plant tissue using 4-MUG as a substrate (Jefferson, 1987).

The *GUS* staining assay was conducted on independent lines of T_4 transgenic *Arabidopsis* seedlings and T_4 negative siblings. Whole seedlings were harvested

and incubated in 15 ml of staining solution {0.1 M sodium-phosphate buffer, pH 7.0, 2 mM $K_4Fe(CN)_6$, 2 mM $K_3Fe(CN)_6$, 0.2% Triton X-100, 10 mM EDTA, and 2 mM X-Gluc (5-Bromo-4-chloro-3-indoxyl-beta-D-glucuronide cyclohexyl-ammonium salt, Gold Biotechnology, St. Louis MO)} for 12 hours at 37 ℃ in the dark. The seedlings were subsequently washed two times with 70% (v/v) ethanol every 24 hours at room temperature to remove chlorophyll (Jefferson, 1987).

Whole seedling and/or specific tissues of each transgenic line were viewed and photographed with a wild M8 dissecting microscope mounted with a Nikon DXM1200 digital still camera, *GUS* staining pictures were processed with Act-1 application software (Advanced Microscopy Facility, Department of Biological Sciences, University of Alberta). Magnification was set to cover the whole seedling, the individual leaf, or specific stained tissues of each transgenic line within the viewing field.

3.2.4. Validation of *GUS* staining patterns by RT-PCR

Due to the specificity of the *GUS* staining patterns and the low amount of templates required for a one-step RT-PCR reactions, total RNA was extracted from leaf trichomes of transgenic seedlings of pCAMBIA-*PER*22PR, pCAMBIA-*PER*73PR, and negative siblings using QIAGEN RNeasy Micro Kit (QIAGEN, catalog number 74004). Trichomes were kept frozen by Histo-Freeze (Fisher Scientific, catalog number 15-232-23) during the harvesting process, individually removed from the leaf surface with ultrafine Dumostar #5 tweezers (Dumont forceps, part number 601750), and subsequently immersed in RNA*later* ™ solution (Ambion, catalog number 7020). Approximately 30 to 50 trichomes were harvested from each of the transgenic lines and negative siblings.

Primers were designed for RT-PCR using the online software WebPrimer (http://www.yeastgenome.org/cgi-bin/web-primer). The least homologous regions found in mRNA sequence alignments between the peroxidase genes (*PER22* and *PER23*, *PER35* and *PER73*) were used to design primers for RT-PCR. These primers contained the most differences in sequence identity in the 20-25 base pair primer annealing regions, with the highest difference designed at the 3' ends (Fig 3.6 A). Thus, each pair of primers should amplify one specific region of one peroxidase mRNA transcript. The peroxidase RT-PCR products were amplified using QIAGEN OneStep RT-PCR Kit (QIAGEN, catalog number 210210) and programmed according to the QIAGEN instruction manual with minor modifications (30 min reverse transcription at 50 ℃; 15 min initial PCR activation at 95 ℃; 35 cycles of 1 min denaturation at 94 ℃, 1 min annealing at Ta (48-60 ℃), 1 min extension at 72 ℃; and a 10 min final extension at 72 ℃). The final volume of the one step RT-PCRs was 25 µl. The specificity of the primers to amplify their corresponding gene was validated by restriction polymorphism analysis, in which allows restriction enzymes cut one of the homologous peroxidase RT-PCR products, but not the other. The peroxdiase RT-PCR products were subsequently cloned into the pBluescriptSK- vector via TA cloning as described in section 2.2.2. Table 3.1 provides a summary of all the primers used for RT-PCR in this chapter.

3.3. Results and discussion

3.3.1. Aluminum treatment conditions

In order to choose the Al stress treatment conditions, dose response and time course experiments were performed using WT *Arabidopsis* grown on 1/2 MS basal medium agar plates as well as hydroponically. Eight 14-day-old seedlings grown on agar plates were exposed to different concentrations of $AlCl_3$ (0-125 µM) for 120 h. Exposure to 75 µM $AlCl_3$ showed inhibition of root growth. Exposure to 100 and 125 µM $AlCl_3$ showed immediate inhibition of root growth (Fig 3.1 A). However, chlorosis appeared in seedlings treated with 50 to 125 µM of $AlCl_3$ (Fig 3.1 A). In hydroponic experiments, exposure to 5 µM $AlCl_3$ for 48h inhibited root growth by approximately 50% (Fig 3.2 A and B). Exposure to 80 µM $AlCl_3$ inhibited root growth immediately (Fig 3.2 A). Subsequent time course experiments indicated that control and treated seedlings started to differentiate after 24 h of Al exposure at 5 µM (Fig 3.2 B). Once again at the 48 h time point, seedlings treated with Al showed approximately 50% inhibition of root growth compared with the control (Fig 3.2 B). Plant roots exposed to low concentrations (e.g. 5 µM) of Al for a short time usually show accumulation of Al mainly in the cell walls (Matsumoto, 2000), which was also a possible target site for *PER22* and *PER73* (TargetP 1.1 server; Emanuelsson *et al.*, 2007). However, due to the other possible functions of class III peroxidases in ROS detoxification mechanism (Passardi *et al.*, 2004); Al exposure was extended up to 48 h.

3.3.2. Histochemical *GUS* staining of *PER22* and *PER73*

Transgenic T_4 seedlings of pCAMBIA-*PER22*PR, pCAMBIA-*PER73*PR, pCAMBIA-*35S*, and negative siblings aged 8, 9, and 14 days without Al exposure were examined to determine the developmental expression patterns of *PER22* and *PER73*. For each transgenic construct a number of different lines were analyzed. I analyzed four independent lines for *35S*, and five independent lines for *PER22* and *PER73*, respectively. The results reported in Figures 3.3 to 3.5 and Figures 3.8 to 3.10 represent the consensus expression pattern. The expression pattern from the independent multiple T-DNA insertion lines was not reported in this thesis. *GUS* staining assays of *PER22* showed strong expression in both shoot and root tissues (Fig 3.3). *GUS* staining assays of *PER73* showed more specific expression in the vascular tissue of leaves and roots (Fig 3.3). Transgenic seedlings of pCAMBIA-*35S* (positive control) showed strong constitutive expression in all tissues of all ages tested (Fig 3.3 and Fig 3.5 K-O). Negative siblings in the same generation as the T_4 transgenic lines were used as a negative controls in the *GUS* staining assay. No expression was observed in any seedlings (Fig 3.3 and Fig 3.4 L-O).

Expression patterns in various tissues of 8-, 9-, and 14-day-old transgenic seedlings of pCAMBIA-*PER22*PR and pCAMBIA-*PER73*PR indicated that *PER22* is highly expressed throughout seedlings, suggesting it might be involved in the regulation of growth; *PER73* was mainly expressed in the vascular tissues of the leaves and roots suggesting it might be involved in the lignification process of plant secondary cell walls. Further *GUS* staining assays using 21-day-old seedlings revealed an interesting specific expression pattern for *PER22*, with high levels of expression in leaf trichomes, root hairs, and strong expression in first

two true leaves (Fig 3.4 A-K). *GUS* staining assays of *PER73* showed that specific expression remained in the vascular tissues of leaves and roots (Fig 3.5 A-J).

3.3.3. RT-PCR confirms that *GUS* staining represents the endogenous expression of *PER22* and *PER73*

Reverse transcriptase PCR (RT-PCR) was used to determine if the *GUS* staining results indeed reflected the endogenous gene expression of *PER22* and *PER73*. RT-PCR primers were designed to anneal in the least homologous region after alignment of the two mRNA transcripts of *PER*22 and *PER*23 and *PER*35 and *PER*73, respectively (Fig 3.6 A). The specificity of these primers was tested by restriction digest analysis of the RT-PCR products. The restriction enzyme *Spe*I has no restriction site in *PER*22 RT-PCR products yielding one DNA fragment (266 bp) and one restriction site in *PER*23 RT-PCR products yielding two DNA fragments with different sizes (47 bp and 248 bp). Both *Hind*III and *Sal*I restriction enzymes have one restriction site in *PER*73 RT-PCR products yielding two DNA fragments with different sizes (366 bp and 511 bp and 430 bp and 447 bp, respectively). The restriction digestion results in Fig 3.6 B indicate that each pair of primers was specific enough for its designed peroxidase cDNA, and did not amplify most homologous peroxidase.

The RT-PCR results in Fig 3.7 confirmed the presence of endogenous *PER22* expression in the leaf trichomes of 21-day-old, WT, transgenic lines, and their negative siblings and corroborated the trichome-specific *GUS* staining results of pCAMBIA-*PER22*PR transgenic lines. The absence of *PER73* expression in leaf

trichomes in RT-PCR results were also consistent with the lack of *GUS* staining observed in trichomes for the pCAMBIA-*PER73*PR transgenic lines.

3.3.4. Expression of *PER22* and *PER73* under aluminum stress

GUS staining of 14-day-old, transgenic seedlings of pCAMBIA-*PER22*PR and pCAMBIA-*PER73*PR treated with $AlCl_3$ from 0 to 48 hours was compared with the staining patterns of the corresponding untreated seedlings. *GUS* expression under control of the *PER22* promoter was reduced at 8 h and 24 h, however with a more specific and enhanced expression in leaf trichomes (Fig 3.8). At 32 h, 40 h, and 48 h, *GUS* expression was enhanced in first two true leaves by $AlCl_3$ treatment compared to control seedlings. This enhanced expression was observed in all tissues of transgenic seedlings (Fig 3.8).

GUS expression under control of the *PER73* promoter was enhanced by $AlCl_3$ treatments compared to the control seedlings from 8 h to 48 h with the strongest expression at 40 h and 48 h (Fig 3.9). To further highlight the enhanced *GUS* expression in leaf vascular tissue of the Al treated pCAMBIA-*PER73*PR transgenic seedlings, leaves from the treated and control seedlings were lined up next to each other for a comparison view (Fig 3.10).

Even though spatial expression of *PER22* and *PER73* under Al stress was obtained, it is still difficult to pinpoint how these genes might be involved in Al detoxification. Transverse sectioning of roots of the *GUS*-stained pCAMBIA-*PER22*PR transgenic lines treated with and without Al could reveal if *PER22* does indeed respond to Al toxicity. Combining the available root hair and trichome-specific expression patterns of *PER22*, it is tempting to postulate that *PER22*

might participate in oxidative burst mechanism in response to pathogen attack and Al toxicity at the wounded areas. Measuring ROS levels and *PER22* expression in root border cells (RBC) would help determine if *PER22* participates in PCD mechanism, which as suggested by Tamas *et al.* (2005) might enable dead RBC, to trap Al and prevent the further penetration of Al into the root tissue. Vascular-specific and enhanced expression of *PER73* under Al stress suggest that *PER73* could increase lignification in the cell walls of Al induced lesion sites to limit entry of Al into the symplasm and reduce the effect of Al damage to root tissues. Staining of lignin, ROS, and Al accumulation sites in the root tissues of the *GUS*-stained pCAMBIA-*PER73*PR transgenic lines could help to understand the mechanism that interconnects Al toxicity and *PER73*. However, whether *GUS* expression levels were enhanced or reduced was based on subjective visual perception. The expression profiles of *PER22* and *PER73* under Al stress can be quantified through a fluorescent detection method to measure *GUS* enzyme activity with the substrate 4-MUG (Jefferson, 1987). Tissue-specific spatial expression conferred by *PER22* and *PER73* promoters under Al stress was the objective of the *GUS* staining assay.

3.3.5. Bioinformatic analysis of *PER22* and *PER73* promoters

The putative *cis*-elements in the promoter regions of *PER22* and *PER73* were analyzed using PlantCare (Lescot *et al.*, 2002). Putative *cis*-elements identified can be classified into four major groups according to their functions: light-responsive, plant hormone responsive, defense and stress responsive, and an endosperm-specific expression (Skn-1 motif) (Tables 3.2, 3.3). Given the multiple functions of class III peroxidases, it is not surprising that *PER22* and *PER73* may be regulated by different motifs at different stages of plant

development. Interestingly, the *PER22* promoter region contains two W-box elements (Table 3.2), suggesting that it might be involved with pathogen, fungal elicitor, and wound defense mechanisms and regulated by unknown WRKY transcription factors (TFs) (Laloi *et al.*, 2004). Aluminum toxicity in wheat and tobacco has been known to induce pathogenesis-related proteins such as β-1,3-glucanase and class III peroxidases (Ezaki *et al.*, 1996; Cruz-Ortega *et al.*, 1997; Richards *et al.*, 1998), which are also the enzymes that plants utilize to counter pathogen attacks and wounding (Antoniw *et al.*, 1980). The functions of *PER22* as a class III peroxidase present this gene as a good candidate in these defense mechanisms, either through generating hydroxyl radicals to kill pathogens or promoting the formation of lignin in wounded areas. The induction of pathogenesis-related enzymes by Al stress and pathogen attacks indicate there might be a common defense mechanism that plants utilize once a wound or lesion is exposed to the surrounding environment. Even though *PER22* did not show significant induction upon Al exposure through *GUS* staining of the transgenic lines, pathogen inoculation and wounding tests using the transgenic lines harbouring *PER22* promoter::*GUS* fusion generated in this research could provide more interesting results in characterizing *PER22* functions in pathogen defense. It would be interesting to test if *PER22* and *PER73* respond to specific plant hormones that correspond to the predicted hormone-responsive motifs present in the promoter regions. Subsequent promoter deletion analysis would help to determine if the predicted *cis*-element is indeed responsible for the corresponding shift in *GUS* staining patterns.

3.3.6. Putative functions of *PER22* and *PER73* deduced from tissue-specific gene expression patterns

To my knowledge, *PER22* is the first class III peroxidise in *Arabidopsis* to be found expressed in leaf trichomes through the histochemical *GUS* staining assay. However, transcriptional profiling of mature trichomes of *Arabidopsis*, using leaves without trichomes as control, has identified *PER33* to be one of the most up-regulated genes in trichomes (Jakoby *et al.*, 2008). *PER33* was suggested to be involved in cell wall biosynthesis (Jakoby *et al.*, 2008). Interestingly, *PER33* together with *PER34* have also been suggested to participate in an oxidative burst mechanism to counter pathogen attack in leaves (Bindschedler *et al.*, 2006) and to modify cell walls to regulate root length (Passardi *et al.*, 2006).

Independent studies focusing on plant pathogen defense (Mohr and Cahill, 2007; Bindschedler *et al.*, 2006), cell wall modification (Passardi *et al.*, 2006), Al stress (Richards *et al.*, 1998; Kumari *et al.*, 2008), oxidative stress (Ludwikow *et al.*, 2004), nutrient deficiency (Hammond *et al.*, 2003), and plant developmental regulation (Cai and Lashbrook, 2008) either identified or confirmed that *PER33* and/or *PER34* are involved. Could the proteins encoded by *PER33* and *PER34* possess so many functions of class III peroxidases and be able to perform them *in planta*? A review of the *PER33* and *PER34* coding sequences revealed that these genes share 90.3% homology in coding sequence and 95% homology at the protein level. It is not surprising that controversial results have been reported regarding the subcellular localization and organ-specific expression profiles of *PER33* and *PER34* in transgenic *Arabidopsis* (Cosio and Dunand, 2009). Given how strictly expression of class III peroxidase is developmentally regulated and how quickly expression profiles change under stress conditions, organ-specific

expression could be transient and discrepancies regarding up- or down-regulation of *PER33* and *PER34* expression could happen in response to the same Al stress treatment (Richards *et al.*, 1998; Kumari *et al.*, 2008). GENEVESTIGATOR expression data in anatomy, development, and stimulus support this hypothesis (http://www.genevestigator.com) (Zimmermann *et al.* 2004). However, these analyses were based on data that actually represented a combination of *PER33* and *PER34* expression as they were obtained from nucleotide hybridization-based northern and/or microarray techniques (Zimmermann *et al.* 2004).

Discrepancies among subcellular localizations in cell walls or vacuoles can be caused by the different molecular techniques and experimental designs employed. *PER33* and *PER34* proteins were identified in leaf vacuoles through proteome analysis, and a C-terminal propeptide (CTPP) was considered to be responsible for subcellular targeting (Carter *et al.*, 2004). Another subcellular localization study of *PER33* and *PER34* using a GFP fusion approach that included the N-terminal but not the C-terminal signal peptide might explain why they were found in apoplastic cell walls (Passardi *et al.*, 2006). These results also led to two interesting questions: (i) could *PER33* and *PER34* possess signal peptides to target their gene products to both cell walls and vacuoles? And (ii) could *PER33* and *PER34* regulate protein targeting mechanism to coordinate with function demand? It would be interesting to find out how *PER33* and *PER34* spatial expression patterns change in response to various stresses using a promoter::*GUS* fusion approach.

It has been reported that *PER22* responds to salt stress in roots of *Arabidopsis* (Jiang *et al.*, 2007) and to K^+ deficiency in *Arabidopsis* seedlings (Kang *et al.*, 2004) using a proteomic approach. *PER73* has been identified as the class III

peroxidase with the highest level of response during Al stress in roots of *Arabidopsis* through transcriptome analysis (Kumari *et al.*, 2008). Transcriptome analysis failed to detect any change in *PER22* transcript level, even when the same salt stress conditions for the proteomic assays mentioned above was used (Jiang *et al.*, 2006). This discrepancy might be due to the existence of post-transcriptional regulation mechanisms in class III peroxidases. The 5' UTR of the class III peroxidases are enriched in adenine, which were suspected to be involved in post-transcriptional regulation (Welinder *et al.*, 2002). Microarray and qRT-PCR techniques would not be able to detect such regulation, while my *GUS* staining assay can detect regulation by this mechanism as the 5' UTR was included in the promoter::*GUS* fusion construct. Further experiments using western blot analysis would be necessary to confirm if this discrepancy was indeed caused by regulation at the post-transcriptional level.

A more detailed characterization of the *PER22* promoter region was conducted by fusing its 5'-upstream region (580 bp, Ea-580) to the start codon of the *GUS* reporter gene; however no *GUS* staining assay was performed to analyze spatial expression patterns (Wanapu and Shinmyo, 1996). Tobacco plants transformed with a *cis*-regulatory element in an Ea-580::*GUS* fusion construct showed that *GUS* activity was higher in roots than in leaves and stems. Only *GUS* activity in leaves was measured under salt stress and found to be increased (Wanapu and Shinmyo, 1996). The root-specific expression of *PER22* conferred by the Ea-580 *cis*-regulatory element was determined by northern blot hybridization analysis (Intapruk *et al.*, 1994). These results could be misleading as cross-hybridization to the *PER23* transcript was unavoidable.

The temporal and tissue specificity of *PER22* expression obtained in this study indicates that *PER22* could be involved in plant defense mechanisms and lignification (as opposed to auxin metabolism). Trichomes are known to be a frontier of defense against pathogens. Combined with the pathogenesis-related function of class III peroxidases (through oxidative burst) (Bindschedler *et al.*, 2006), it is tempting to speculate that *PER22* plays a role in protecting against pathogens in *Arabidopsis* trichomes. However, as *Arabidopsis* unicellular trichomes are simple trichomes (ST) rather than glandular secreting trichomes (GST), it was doubted that the herbivore deterrence and pathogen defense mechanism of phytochemical secretion was utilized by *Arabidopsis* and mere physical protection against predator attacks was more likely to be the primary function of *Arabidopsis* trichomes (Maarit *et al.*, 2007). However, there is no direct experimental evidence to exclude the possibility of low level secretion by simple trichomes (Wagner *et al.*, 2004). Lignification occurs naturally in the development of specialized plant cells (e.g., in vascular tissues) and also in plant response to biotic and abiotic stresses (El Mansouri *et al.*, 1999). Lignification is an irreversible process in plant cell walls and *PER22* could play a role in reinforcing the cell walls of trichomes by promoting the formation of phenolic linkages upon pathogen attack (Pedreno *et al.*, 1995). Further experiments measuring ROS levels (e.g., H_2O_2), *GUS* activity, and lignin content in trichomes of pCAMBIA-*PER22*PR transgenic lines would help to determine if *PER22* is involved in defense mechanism via oxidative burst or in lignification process to reinforce cell walls. Transverse sectioning of the *GUS*-stained pCAMBIA-*PER*22PR transgenic lines and lignin staining at *GUS* expressed sites could reveal more detailed tissue-specific expression patterns. Subcellular localization studies of PER22 using a CaMV35S-*PER*22-GFP fusion approach would provide further information about the specific function of *PER22*.

The vascular tissue specificity of *PER73* expression suggests that it could be involved in a lignification process. Several class III peroxidases from *Arabidopsis* and other plant species have shown vascular-specific expression and function in lignification (Cosio and Dunand, 2009). Recently, spatial expression of *PER 47*, *PER64*, and *PER66* have been investigated using a promoter::*GUS* fusion approach (Tokunaga *et al.*, 2009). *PER66* was originally identified as a homolog of *ZPO-C* peroxidase, which was involved in vessel lignification and expressed specifically in differentiating tracheary elements (TE) (Sato *et al.*, 2006). *PER47* and *PER64* have the highest sequence similarity to *PER66* within the *Arabidopsis* class III peroxidase gene family. Subsequent *GUS* staining, lignin staining, and wound treatments revealed that *PER64* was stress-responsive and involved in lignification of sclerenchyma (Tokunaga *et al.*, 2009). In addition, *PER47* and *PER66* were involved in lignification of vessels (Tokunaga *et al.*, 2009). A tracheary-element-regulating *cis*-element (TERE; 11 bp-CTTNAAAGCNA) responsible for TE-specific expression was discovered in the *Zinnia* Cysteine Protease 4 gene (ZCP4), and a subsequent search for TERE-like elements among the genes involved in TE differentiation identified *PER64*, *PER66*, and *PER72* (Pyo *et al.*, 2007). Five tandem TEREs from *PER64* and *PER66* fused with a minimal 35S promoter and the *GUS* reporter gene were tested for TE-specific *GUS* expression pattern. Only the TERE from *PER66* was able to repeat the TE-specific expression pattern (Pyo *et al.*, 2007). Promoter sequence analysis of *PER73* revealed a TERE-like motif (CTTATAAGCTC, 9 out of 11 bp) within the 1 kb 5'-upstream region. It would be interesting to test if the TERE-like element can confer the TE-specific expression pattern to the *GUS* reporter gene. Again transverse sectioning of the *GUS*-stained pCAMBIA-*PER*73PR transgenic lines and lignin staining at *GUS* expressed sites and subcellular localization studies of

PER73 would generate more detailed information about the specific expression and function of *PER73* as well.

In summary, the promoter::*GUS* reporter gene fusion study of *PER22* and *PER73* revealed tissue-specific expression patterns for both peroxidases. *GUS* staining results of the independent transgenic T_4 lines suggest that *PER22* and *PER73* are involved in plant defense and/or lignification. This strengthens our understanding of the function(s) of individual class III peroxidase plays in response to Al stress.

Table 3.1. Sequences and functions of oligonucleotide primers used for RT-PCR.

Primer Name	Sequence (5'→ 3')	Function
*PER*_22 _RT_F	CAGAGTGACCAGGAACTCTTTT	Forward primer for RT-PCR amplification of *PER22*
*PER*_22 _RT_R	CCATATATATATCCCCAACATGG	Reverse primer for RT-PCR amplification of *PER22*
*PER*_35 _RT_F	AGAGTGACCAAGTGCTTTTCTCA	Forward primer for RT-PCR amplification of *PER23*
*PER*_35 _RT_R	AATGTTCCCACAATCCCACA	Reverse primer for RT-PCR amplification of *PER23*
*PER*_73 _RT_F	GTAGTCGTGACTCTTAGTCTTGCC	Forward primer for RT-PCR amplification of *PER73*
*PER*_73 _RT_R	CCTTGTTGAAAGCAACAGAATTC	Reverse primer for RT-PCR amplification of *PER73*

Table 3.2. Putative *cis*-regulatory elements identified in the promoter region of *PER22* gene.

Motif	Sequence	Position	Strand	Function of regulatory elements
AAGAA-motif	GAAAGAA	-482	+	unknown
ACE	CTAACGTATT	-811	-	*cis*-acting element involved in light responsiveness
Box I	TTTCAAA	-968/-374/-574	-/-/-	light responsive element
Box-W1	TTGACC	-860	-	fungal elicitor responsive element
ERE	ATTTCAAA	-574	-	ethylene-responsive element
GAG-motif	AGAGATG	-455	-	part of a light responsive element
GT1-motif	GTTAA	-942	+	light responsive element
GT1-motif	GGTTAAT	-249	+	light responsive element
I-box	GATATGG	-642	-	part of a light responsive element
P-box	CCTTTTG	-259	-	gibberellin-responsive element
Skn-1_motif	GTCAT	-890/-508	-/+	*cis*-acting regulatory element required for endosperm expression
TCA-element	CCATCTTTTT	-771	+	*cis*-acting element involved in salicylic acid responsiveness
TCT-motif	TCTTAC	-667/-583	+/+	part of a light responsive element
TGA-element	AACGAC	-562	-	auxin-responsive element
Unnamed_4	CTCC	-511/-10/-387	-/+/-	unknown
W box	TTGACC	-860	-	wounding and pathogen response
circadian	CAANNNNATC	-744/-270/ -645/-259	+/-/+/+	*cis*-acting regulatory element involved in circadian control
CAAT-box*	GGNCAATCT		+/-	common *cis*-acting element in promoter and enhancer regions
TATA-box*	TATAAA or variants		+/-	core promoter element around -30 of transcription start

*Positions of CAAT-box (25 loci) and TATA-box (46 loci) were not included in the table; start codon site was define as “0”.

PlantCare: http://bioinformatics.psb.ugent.be/webtools/plantcare/html/

Table 3.3. Putative *cis*-regulatory elements identified in the promoter region of *PER73* gene.

Motif	Sequence	Position	Strand	Function of regulatory elements
5'UTR Py-rich stretch	TTTCTTCTCT	-227	-	*cis*-acting element conferring high transcription levels
AAAC-motif	CAACAAAAACCT	-552	-	light responsive element
ABRE	TACGTG	-852	+	*cis*-acting element involved in the abscisic acid responsiveness
	ACGTGGC	-197	+	
	AGTACGTGGC	-200	+	
ARE	TGGTTT	-755	-	*cis*-acting regulatory element essential for the anaerobic induction
ATCT-motif	AATCTAATCC	-507	+	part of a conserved DNA module involved in light responsiveness
Box I	TTTCAAA	-373/-163	+/-	light responsive element
C-repeat/DRE	TGGCCGAC	-214	-	regulatory element involved in cold- and dehydration-responsiveness
CATT-motif	GCATTC	-743	+	part of a light responsive element
G-Box	CACGTA	-852	-	*cis*-acting regulatory element involved in light responsiveness
	CACGTT	-198/-517/ -517/-198	-/+/+/-	
	TACGTG	-852	+	
	GACACGTAGT	-854	-	
GARE-motif	AAACAGA	-315	+	gibberellin-responsive element
HSE	AGAAAATTCG	-1002	+	*cis*-acting element involved in heat stress responsiveness
I-box	GATAAGATT	-507	-	part of a light responsive element
MRE	AACCTAA	-399	-	MYB binding site involved in light responsiveness
Skn-1_motif	GTCAT	-822/-236/-471	-/+/+	*cis*-acting regulatory element required for endosperm expression
TC-rich repeats	ATTTTCTCCA	-980/-863	-/+	*cis*-acting element involved in defense and stress responsiveness
	ATTCTCTAAC	-389/-514	+/-	
	GTTTTCTTAC	-623	-	
	ATTTTCTTCA	-75	+	
Unnamed_1	CGTGG	-196	+	unknown
Unnamed_3	CGTGG	-196	+	unknown
Unnamed_4	CTCC	-1023/-191/-658	-/+/-	unknown
CAAT-box*	GGNCAATCT		+/-	common *cis*-acting element in promoter and enhancer regions
TATA-box*	TATAAA or variants		+/-	core promoter element around -30 of transcription start

*Positions of CAAT-box (17 loci) and TATA-box (33 loci) were not included in the table; start codon site was define as "0".

PlantCare: http://bioinformatics.psb.ugent.be/webtools/plantcare/html/

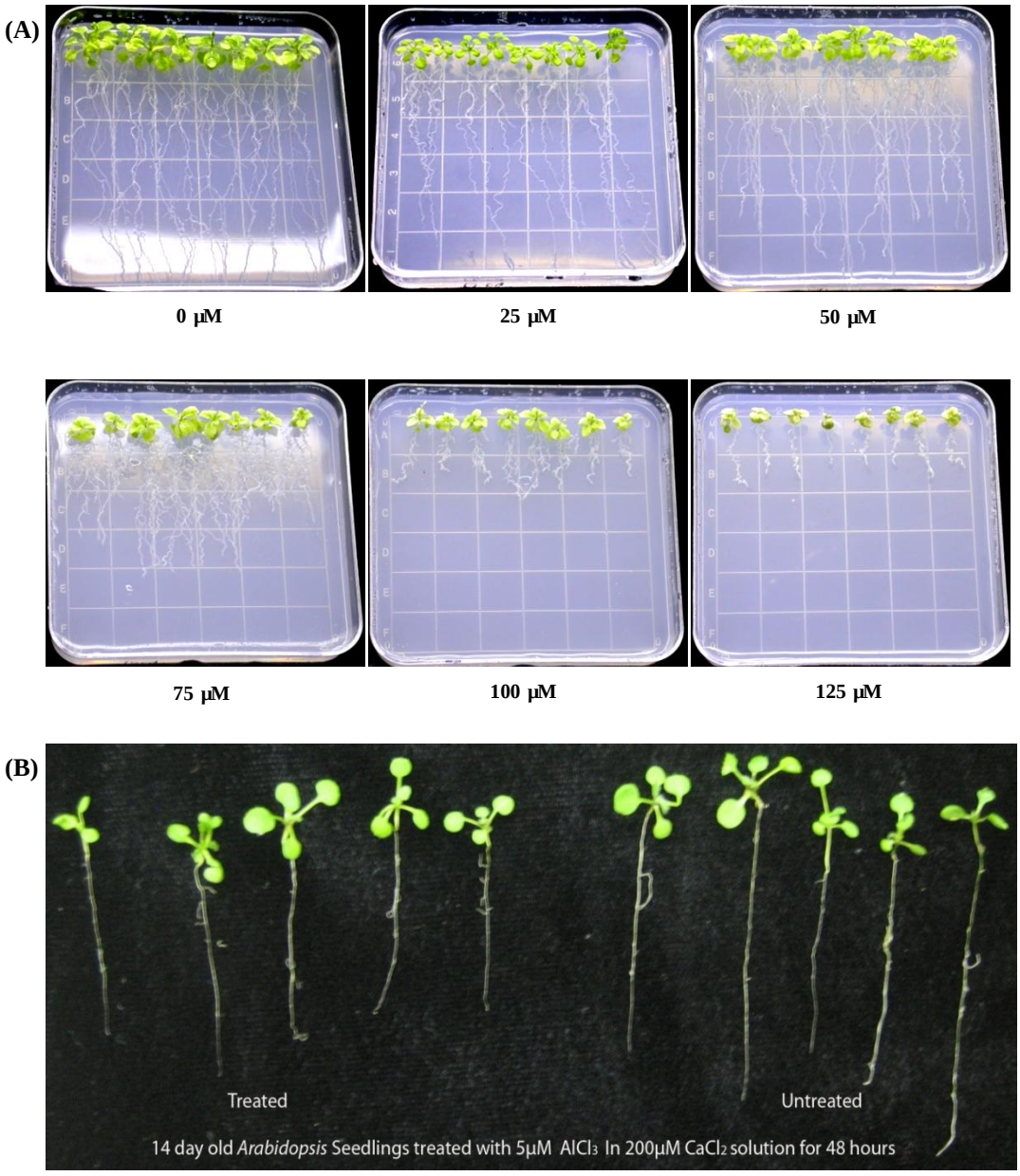

Figure 3.1. The phenotypes of wild type *Arabidopsis* seedlings treated with different concentration of $AlCl_3$ on agar plates and hydroponically. (A) Eight 14-day-old seedlings grown on agar plates were subject to different concentrations of $AlCl_3$ (0-125 µM) for 120 hours. (B) Five 14-day-old seedlings grown hydroponically were subjected to $AlCl_3$ (5 µM) for 48 hours.

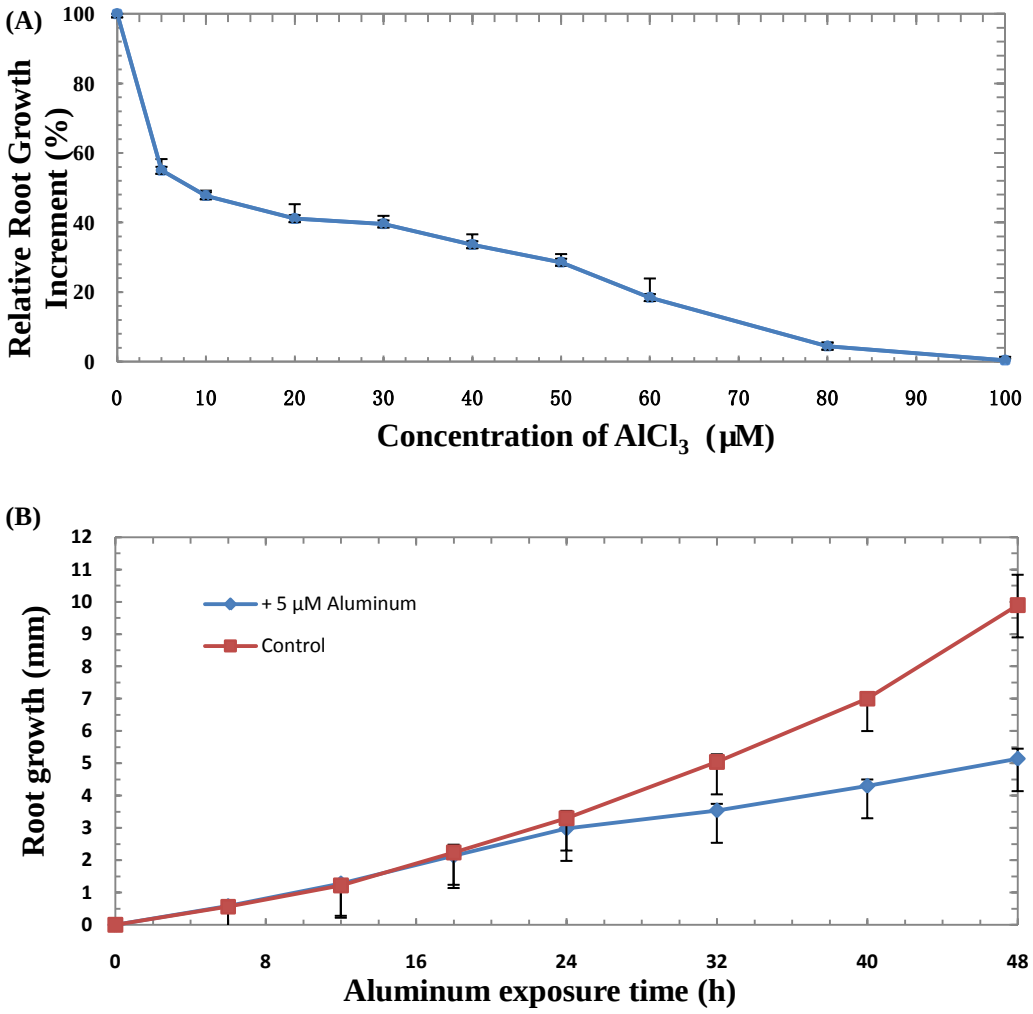

Figure 3.2. Root growth of 14-day-old *Arabidopsis* seedlings subjected to different concentrations and exposure times of $AlCl_3$. (A) Eight 14-day-old seedlings grown hydroponically were subject to different concentrations of $AlCl_3$ (0-100 µM) for 48 hours. Relative root growth increments (RRGI) were calculated for 10 different concentrations of $AlCl_3$. (B) Eight 14-day-old seedlings grown hydroponically were subjected to 5 µM $AlCl_3$ in 200 µM $CaCl_2$ for 48 hours. Root length was recorded every 6 hours for 24 hours, and subsequently every 8 hours until 48 hours. Values are mean $\pm$ SE of eight replicates. Both dose response and time course experiments were repeated three times to ensure repeatability and one set of representative data were shown for Al dose response and time course experiments.

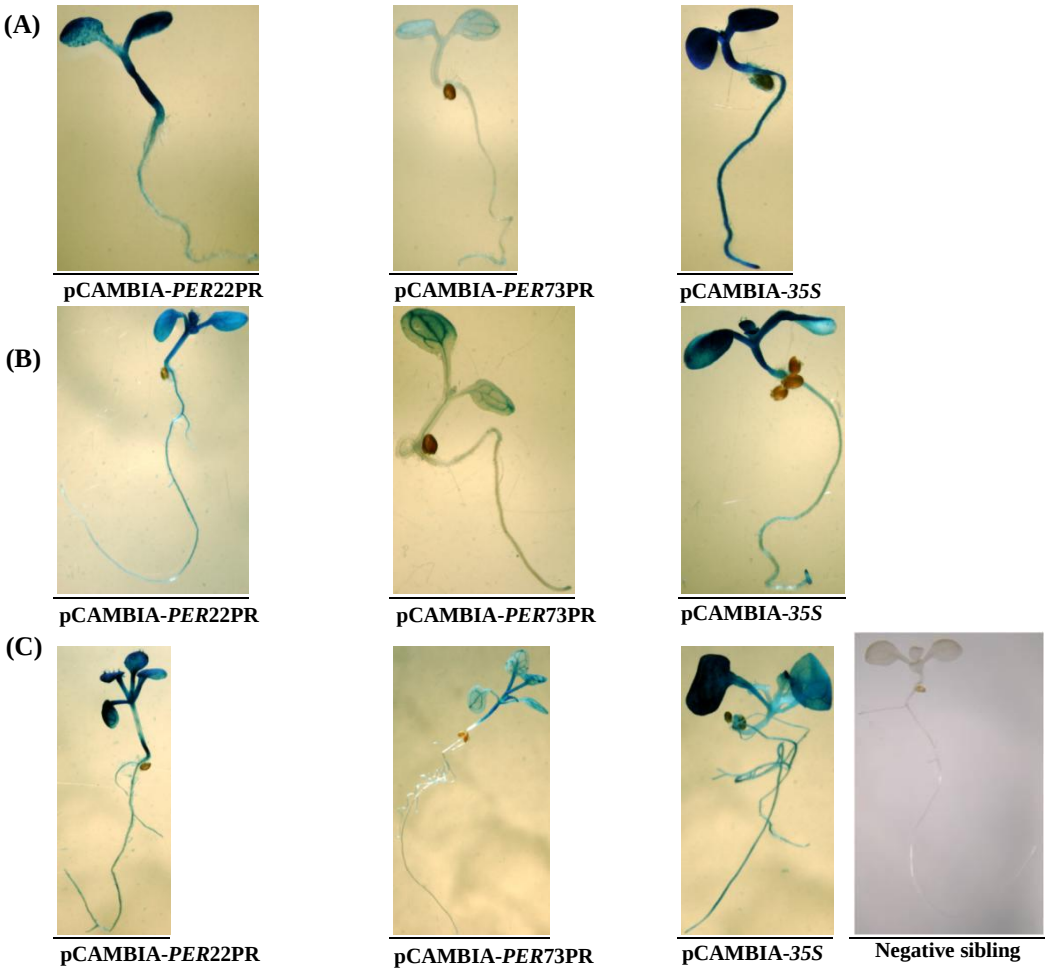

Figure 3.3. *GUS* staining assays of 8-day-old, 9-day-old, and 14-day-old, transgenic *Arabidopsis* seedlings grown under control conditions hydroponically. (A) The first two true leaves of *Arabidopsis* emerge in 8-day-old seedlings. (B) Enhanced *GUS* staining was observed for 9-day-old seedlings comparing to 8-day-old seedlings. (C) *GUS* staining of 14-day-old seedlings showed the same expression pattern as 8- and 9-day-old seedlings. *GUS* staining of these transgenic seedlings revealed that *PER22* and *PER73* promoters drive whole seedling and vascular tissue-specific expressions of *GUS* reporter gene, respectively. *GUS* staining of negative siblings showed no *GUS* expression. *GUS* staining of positive control (*35S*) showed constitutive expression throughout the transgenic seedlings at different ages. *GUS* staining results shown are consensus obtained from multiple independent lines (>3).

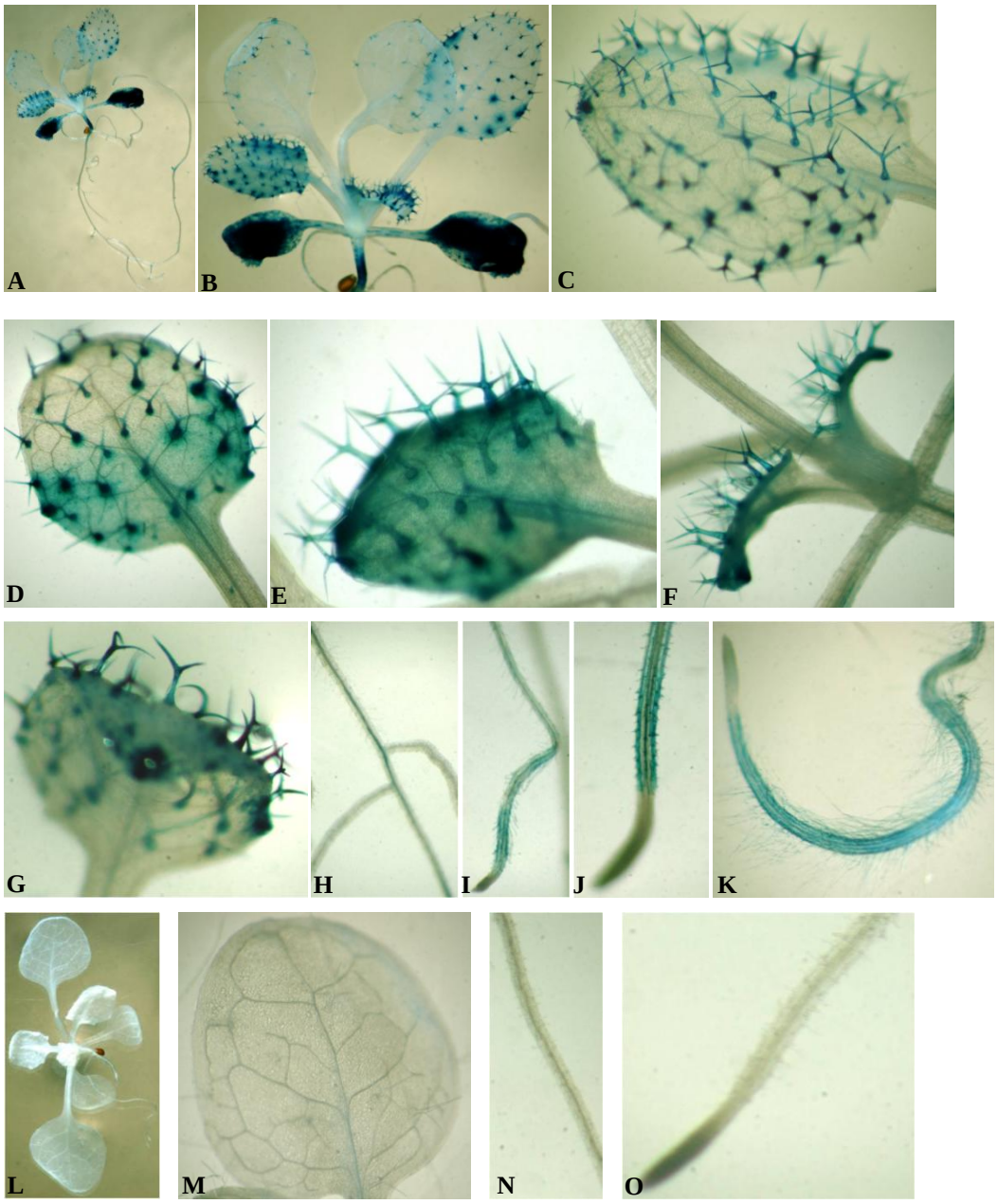

Figure 3.4. *GUS* staining assays of seedlings of 21-day-old, transgenic lines of pCAMBIA-*PER22*PR and negative siblings. The promoter of *PER22* conferred specific expression in leaf trichomes (A-G), root hairs (H-K), and with strong expression in first two true leaves (A-B). No *GUS* expression was observed in any tissues of the negative siblings (L-O). *GUS* staining results shown are consensus obtained from multiple independent lines (>3).

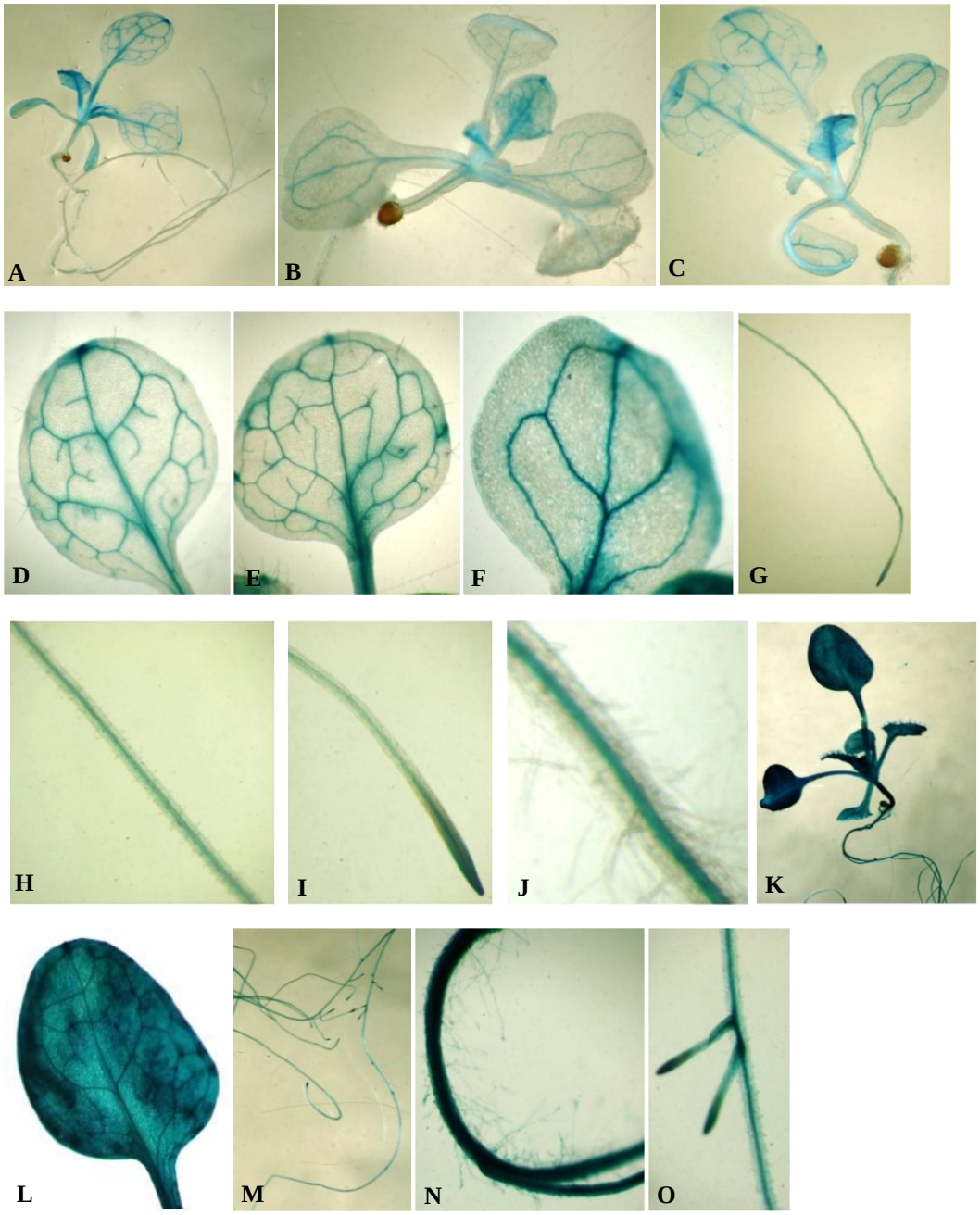

Figure 3.5. *GUS* staining assays of seedlings of 21-day-old, transgenic lines of pCAMBIA-*PER73*PR and pCAMBIA-*35S*. The promoter of *PER73* conferred specific expression in the vascular tissues of leaves (A-F) and roots (G-J). Transgenic seedlings of pCAMBIA-*35S* showed strong constitutive expression in all tissues (K-O). *GUS* staining results shown are consensus obtained from multiple independent lines (>3).

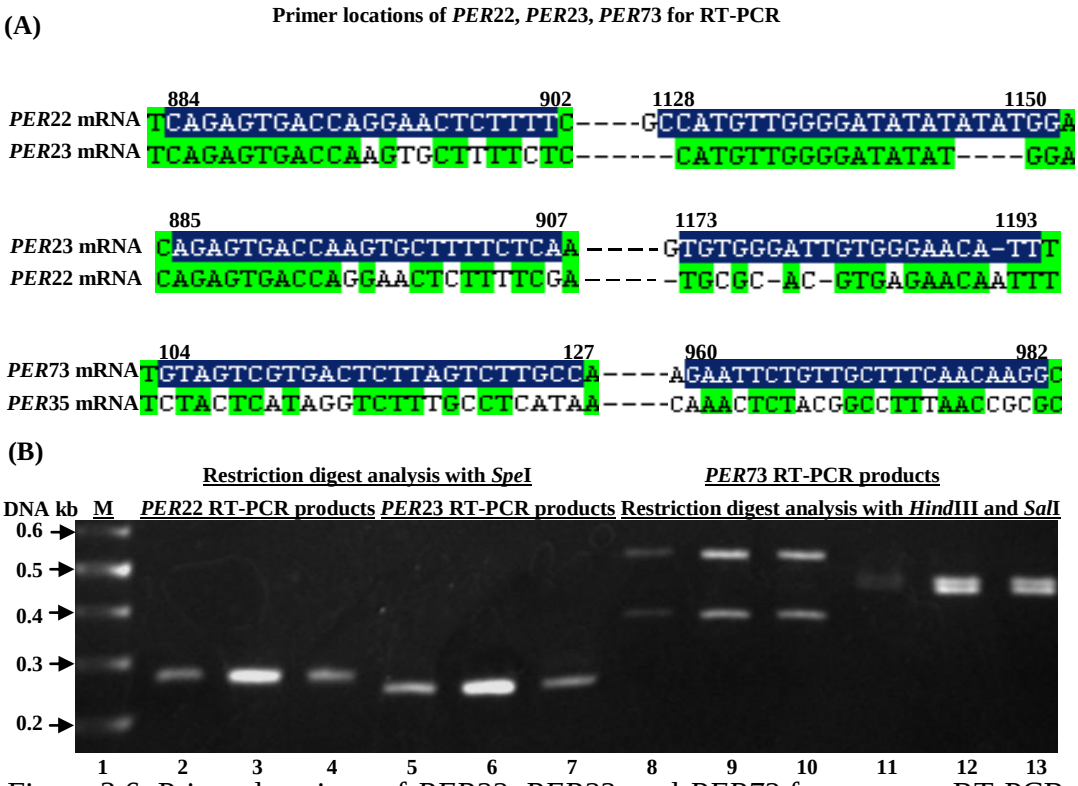

Figure 3.6. Primer locations of *PER22*, *PER23*, and *PER73* for one step RT-PCR and verification of the specificity of these primers using restriction digestion of RT-PCR products. (A) Primers for *PER22*, *PER23*, and *PER73* were designed to anneal to the least homologous regions in mRNA sequence alignments between the two homologous peroxidase genes (*PER22* and *PER23*, *PER35* and *PER73*). (B) Lane 1, Generuler DNA Ladder Mix. Lane 2-4, *Spe*I has no restriction site in *PER*22 RT-PCR products yielding a single DNA fragment (266 bp). Lane 5-7, *Spe*I has one restriction site in *PER*23 RT-PCR products yielding two DNA fragments with different sizes (47 bp and 248 bp). The smaller DNA fragment (47 bp) of *PER23* RT-PCR products did not show on the gel due to agarose gel resolution limit (>50 bp). Lane 8-10, *Hind*III has one restriction site in *PER*73 RT-PCR products, which yielded two DNA fragments of different sizes (366 bp and 511 bp). Lane 11-13, *Sal*I has one restriction site in *PER*73 RT-PCR products, which yielded two DNA fragments of different sizes (430 bp and 447 bp).

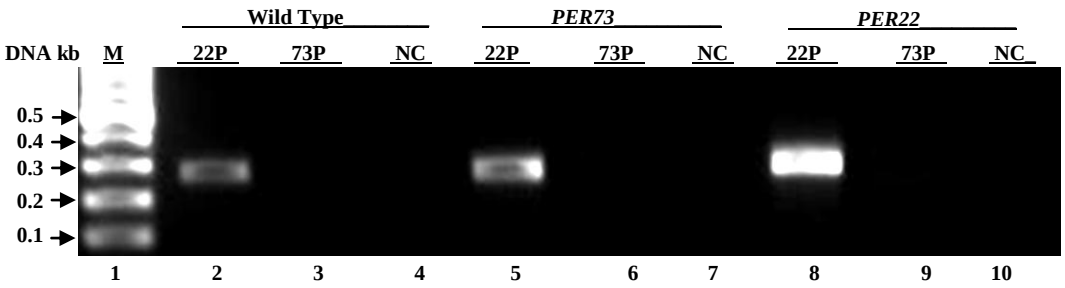

Figure 3.7. Results of RT-PCR amplification of *PER22* and *PER 73* from leaf trichomes. Total RNA extracted from trichomes of 21-day-old pCAMBIA-*PER22*PR and pCAMBIA-*PER73*PR transgenic lines and WT negative siblings were used as templates for RT-PCR. Lane 1, GeneRuler DNA Ladder Mix. Lane 2 and lane 3, RT-PCR performed using WT total RNA templates with *PER22* and *PER73* RT-PCR primers (22P and 73P). Lane 4, negative control. Lane 5 and lane 6, RT-PCR performed using transgenic lines of pCAMBIA-*PER73*PR total RNA templates with *PER22* and *PER73* RT-PCR primers. Lane 7, negative control. Lane 8 and lane 9, RT-PCR performed using transgenic lines of pCAMBIA-*PER22*PR total RNA templates with *PER*22 and *PER*73 RT-PCR primers. Lane 10, negative control.

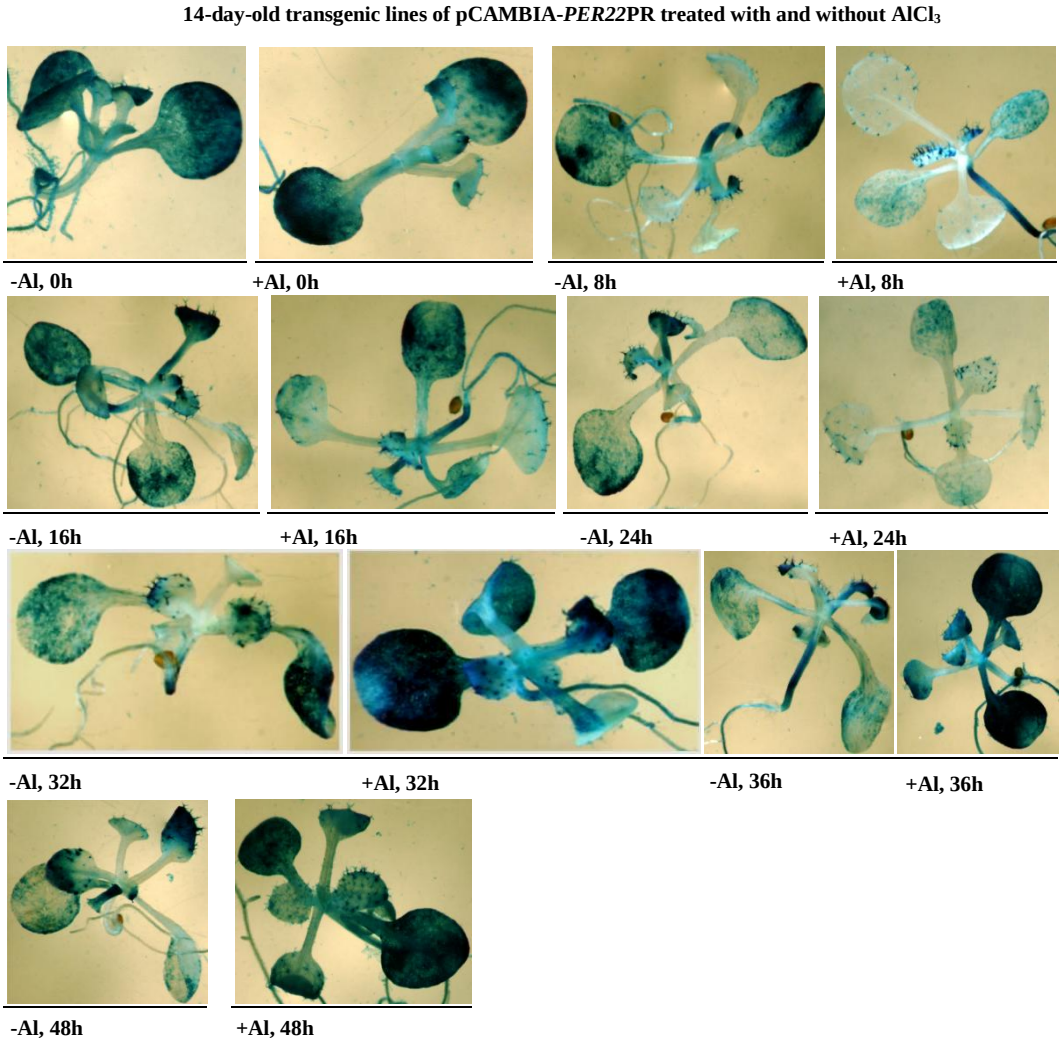

Figure 3.8. *GUS* staining patterns of 14-day-old, transgenic lines of pCAMBIA-*PER22*PR treated with and without $AlCl_3$ from 0 to 48 h. *GUS* expression of transgenic lines of pCAMBIA-*PER22*PR was reduced after 8 and 24 h exposure to Al compared to the corresponding untreated seedlings, however, a more specific and enhanced expression in leaf trichomes was observed. At other time points, *GUS* expression was enhanced in the first two true leaves by $AlCl_3$ treatment compared to control seedlings. *GUS* staining results shown are consensus obtained from multiple independent lines (>3).

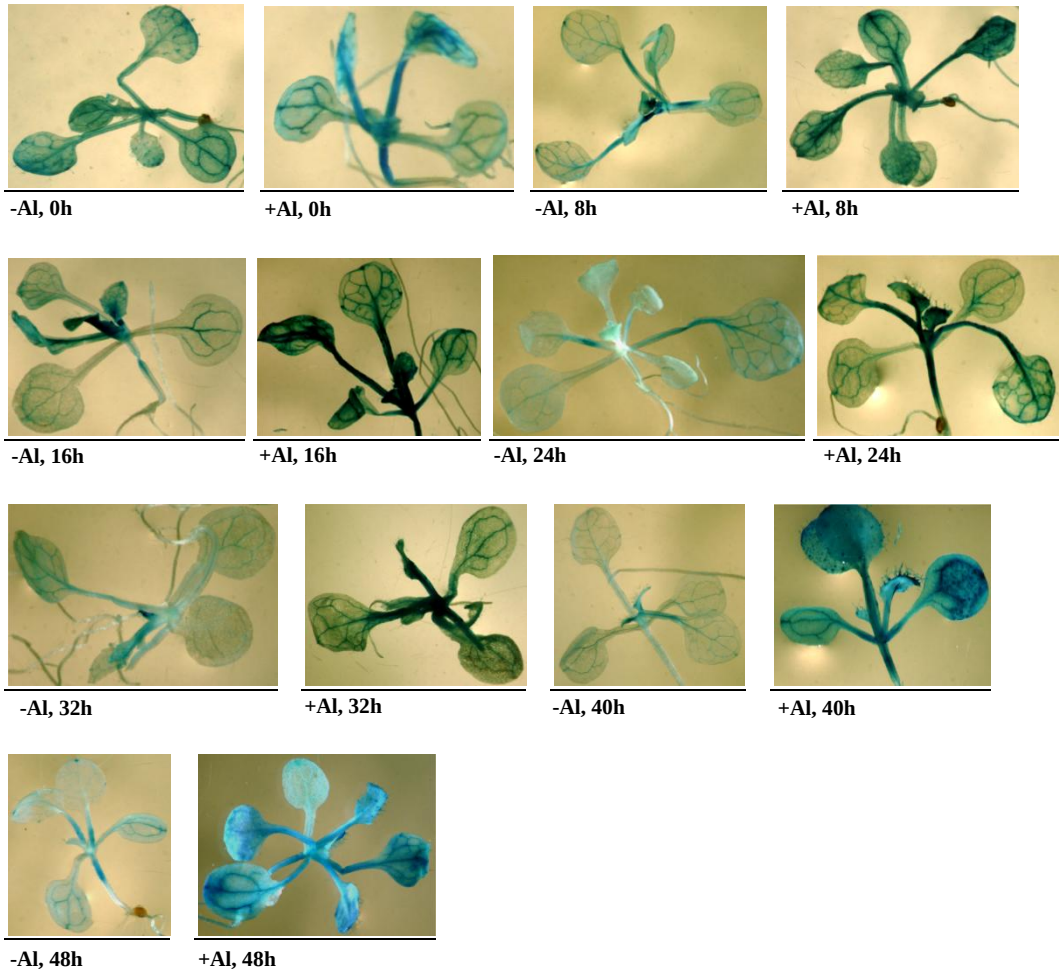

Figure 3.9. *GUS* staining patterns of 14-day-old, transgenic lines of pCAMBIA-*PER73*PR treated with and without $AlCl_3$ from 0 to 48 h. *GUS* expression of transgenic lines of pCAMBIA-*PER73*PR was enhanced from 8 to 48 h exposure to Al compared to the corresponding untreated seedlings, a more significant contrast was observed for 40 h and 48 h time points between treated and control seedlings. *GUS* staining results shown are consensus obtained from multiple independent lines (>3).

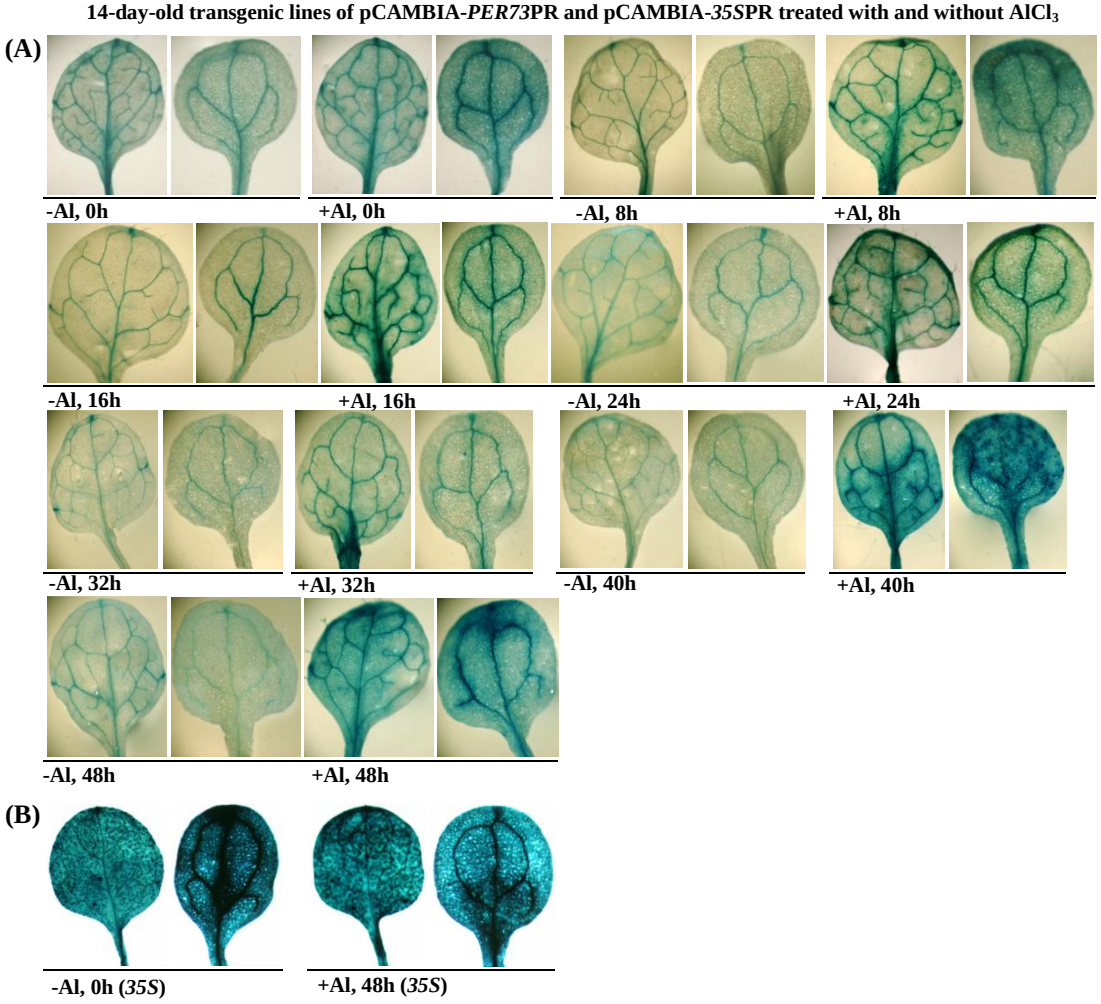

Figure 3.10. *GUS* staining patterns in leaves (two different developmental stages) of 14-day-old, transgenic lines of pCAMBIA-*PER73*PR treated with and without $AlCl_3$ from 0 to 48 h. (A) *GUS* staining of leaves between treated and control seedlings showed that from 8 to 48 h, *GUS* expression was enhanced, especially at 40 h and 48 h time points. (B) *GUS* staining of leaves of 14-day-old, transgenic lines of pCAMBIA-*35S* showed no difference between treated and control conditions. *GUS* staining results shown are consensus obtained from multiple independent lines (>3).

3.4. References

Antoniw JF, Ritter CE, Pierpoint WS, Van Loon LC. 1980. Comparison of three pathogenesis-related proteins from plants of two cultivars of tobacco infected with TMV. J Gen Virol 47: 79-87.

Arteca RN, Arteca JM. 2000. A novel method for growing *Arabidopsis thaliana* plants hydroponically. Physiol Plant 108: 188-193.

Branco-Price C, Kawaguchi R, Ferreira RB, Bailey-Serres J. 2005. Genome wide analysis of transcript abundance and translation in *Arabidopsis* seedlings subjected to oxygen deprivation. Ann Bot 96: 647-660.

Bindschedler LV, Dewdney J, Blee KA, Stone JM, Asai T, Plotnikov J, Denoux C, Hayes T, Gerrish C, Davies DR, Ausubel FM, Bolwell GP. 2006. Peroxidase dependent apoplastic oxidative burst in *Arabidopsis* required for pathogen resistance. Plant J 47: 851-863.

Cai S, Lashbrook CC. 2008. Stamen abscission zone transcriptome profiling reveals new candidates for abscission control: enhanced retention of floral organs in transgenic plants overexpressing *Arabidopsis* ZINC FINGER PROTEIN2. Plant Physiol 146: 1305-1321.

Carter C, Pan SQ, Jan ZH, Avila EL, Girke T, Raikhel NV. 2004. The vegetative vacuole proteome of *Arabidopsis thaliana* reveals predicted and unexpected proteins. Plant Cell 16: 3285-3303.

Cosio C, Dunand C. 2009. Specific functions of individual class III peroxidase genes. J Exp Bot 60: 391-408.

Crowe ML, Serizet C, Thareau V, Aubourg S, Rouze P, Hilson P, Beynon J, Weisbeek P, van Hummelen P, Reymond P, Paz-Ares J, Nietfeld W, Trick M. 2003. CATMA: a complete *Arabidopsis* GST database. Nucl Acids Res 31: 156-158.

Cruz-Ortega R, Cushman JC, Ownby JD. 1997. cDNA clones encoding 1,3-glucanase and a fimbrin-like cytoskeletal protein are induced by Al toxicity in wheat roots. Plant Physiol 114: 1453-1460.

Czechowski T, Stitt M, Altmann T, Udvardi MK, Scheible WR. 2005. Genome-wide identification and testing of superior reference genes for transcript normalization in *Arabidopsis*. Plant Physiol 139:5-17.

El Mansouri I, Mercado JA, Santiago-Domenech N, Pliego-Alfaro F, Valpuesta V, Quesada MA. 1999. Biochemical and phenotypical characterization of transgenic tomato plants overexpressing a basic peroxidase. Physiol Plant 106: 355-362.

Ezaki B, Tsugita S, Matsumoto H. 1996. Expression of a moderately anionic peroxidase is induced by aluminum treatment in tobacco cells: possible involvement of peroxidase isozymes in aluminum ion stress. Physiol Plant 96: 21-28.

Gasteiger E, Gattiker A, Hoogland C, Ivanyi I, Appel RD, Bairoch A. 2003. ExPASy: the proteomics server for in-depth protein knowledge and analysis. Nucleic Acids Res 31: 3784-3788.

Gibeaut DM, Hulett J, Cramer GR, Seemann JR. 1997. Maximal biomass of *Arabidopsis thaliana* using a simple, low-maintenance hydroponic method and favorable environmental conditions. Plant Physiol 115: 317-319.

Hammond JP, Bennett MJ, Bowen HC, Broadley MR, Eastwood DC, May ST, Rahn C, Swarup R, Woolaway KE, White PJ. 2003. Changes in gene expression in *Arabidopsis* shoots during phosphate starvation and the potential for developing smart plants. Plant Physiol 132: 578-596.

Hurlbert SH. 1984. Pseudoreplication and the design of ecological field experiments. Ecol Monogr 54: 187-211.

Huttner D, Bar-Zvi D. 2003. An improved, simple, hydroponic method for growing *Arabidopsis thaliana*. Plant Mol Biol Rep 21: 59-63.

Intapruk CK, Yamamotmo M, Sekine A, Takano SM. 1994. Regulatory sequences involved in the peroxidase gene expression inhubidopsis *thaliana*. Plant Cell Rep 13: 123-129.

Jakoby MJ, Falkenhan D, Mader MT, Brininstool G, Wischnitzki E, Platz N, Hudson A, Hülskamp M, Larkin J, Schnittger A. 2008. Transcriptional profiling of mature *Arabidopsis* trichomes reveals that NOECK encodes

the MIXTA-like transcriptional regulator MYB106. Plant Physiol 148: 1583-1602.

Jefferson RA. 1987. Assaying chimeric genes in plants: the *GUS* gene fusion system. Plant Mol Biol Rep 5: 387-405.

Jiang YQ, Deyholos M. 2006. Comprehensive transcriptional profiling of NaCl-stressed *Arabidopsis* roots reveals novel classes of responsive genes. BMC Plant Bio 6: 25-45.

Jiang YQ, Yang B, Harris NS, Deyholos M. 2007. Comparative proteomic analysis of NaCl stress-responsive proteins in *Arabidopsis* roots. J Exp Bot 58: 3591-3607.

Kang JG, Pyo YJ, Cho JW, Cho MH. 2004. Comparative proteome analysis of differentially expressed proteins induced by K+ deficiency in *Arabidopsis thaliana*. Proteomics 4: 3549-3559.

Kinraide TB, Parker DR. 1987. Cation amelioration of aluminum toxicity in wheat. Plant Physiol 83: 546-551.

Klok EJ, Wilson IW, Wilson D, Chapman SC, Ewing RM, Somerville SC, Peacock WJ, Dolferus R, Dennis ES. 2002. Expression profile analysis of the low-oxygen response in *Arabidopsis* root cultures. Plant Cell 14: 2481-2494.

Kochian LV, Hoekenga OA, Pineros MA. 2004. How do crop plants tolerate acid soils? Mechanisms of aluminum tolerance and phosphorous efficiency. Annu Rev Plant Biol 55: 459-493.

Kumari M, Taylor GJ, Deyholos MK. 2008. Transcriptomic responses to aluminum stress in roots of *Arabidopsis thaliana*. Mol Genet Genomics 279: 339-357.

Laloi C, Mestres-Ortega D, Marco Y, Meyer Y, Reichheld JP. 2004. The *Arabidopsis* cytosolic thioredoxin h5 gene induction by oxidative stress and its W-box-mediated response to pathogen elicitor. Plant Physiol 134: 1006-1016.

Lescort M, Dehais P, Thijs G, Marchal K, Moreau Y, Van de Peer Y, Rouze P, Rombauts S. 2002. PlantCARE, a database of plant *cis*-acting regulatory

elements and a portal to tools for in silico analysis of promoter sequences. Nucleic Acids Res 30: 325-327.

Ludwikow A, Gallois P, Sadowski J. 2004. Ozone-induced oxidative stress response in *Arabidopsis*: transcription profiling by microarray approach. Cell and Mol Biol Lett 9: 829-842.

Maarit K, Katri K, Myriam G, Geir L, Jon A. 2007. Gene, phenotype and function: GLABROUS1 and resistance to herbivory in natural populations of *Arabidopsis* lyrata. Mol Ecol 16: 453-462.

Manfield IW, Jen CH, Pinney JW, Michalopoulos I, Bradford JR, Gilmartin PM, Westhead DR. 2006. *Arabidopsis* Co-expression Tool (ACT): web server tools for microarray-based gene expression analysis. Nucleic Acids Res 34: 504-509.

Matsumoto H. 2000. Cell biology of aluminum toxicity and tolerance in higher plants. Int Rev Cytol 200: 1-46.

Meinke DW, Cherry JM, Dean C, Rounsley SD, Koornneef M. 1998. *Arabidopsis thaliana*: A Model Plant for Genome Analysis. Science 282: 662-682.

Mohr PG, Cahill DM. 2007. Suppression by ABA of salicylic acid and lignin accumulation and the expression of multiple genes, in *Arabidopsis* infected with *Pseudomonas syringae* pv tomato. Funct and Integr Genomics 7: 181-191.

Noren H, Svensson P, Andersson B. 2004. A convenient and versatile hydroponic cultivation system for *Arabidopsis thaliana*. Physiol Plant 121: 343-348.

Passardi F, Penel C, Dunand C. 2004. Performing the paradoxical: how plant peroxidases modify the cell wall. Trends Plant Sci 9: 534-540.

Passardi F, Cosio C, Penel C, Dunand C. 2005. Peroxidases have more functions than a Swiss army knife. Plant Cell Rep 24: 255-65.

Passardi F, Tognolli M, De Meyer M, Penel C, Dunand C. 2006. Two cell wall associated peroxidases from *Arabidopsis* influence root elongation. Planta 223: 965-974.

Pedreno MA, Ferrer MA, Gaspar T, Munoz R, Ros Barcelo A. 1995. The polyfunctionality of cell wall peroxidases avoids the necessity of an independent H_2O_2-generating system for phenolic coupling in the cell walls. Plant Peroxidases Newsl 5: 3-8.

Pyo, H., Demura, T. and Fukuda, H. 2007. TERE; a novel *cis*-element responsible for a coordinated expression of genes related to programmed cell death and secondary wall formation during differentiation of tracheary elements. Plant J 51: 955-965.

Richards KD, Schott EJ, Sharma YK, Davis KR, Gardner RC. 1998. Aluminum induces oxidative stress genes in Arabidopsis thaliana. Plant Physiol 116: 409-418.

Robison MM, Smid MPL, Wolyn DJ. 2006. High-quality and homogeneous *Arabidopsis thaliana* plants from a simple and inexpensive method of hydroponic cultivation. Can J Bot 84: 1009-1012.

Sato Y, Demura T, Yamawaki K, Inoue Y, Sato S, Sugiyama M, Fukuda H. 2006. Isolation and characterization of a novel peroxidase gene *ZPO-C* whose expression and function are closely associated with lignification during tracheary element differentiation. Plant Cell Physiol 47: 493-503.

Schenk PM, Kazan K, Wilson I, Anderson JP, Richmond T, Somerville SC, Manners JM. 2000. Coordinated plant defense responses in *Arabidopsis* revealed by microarray analysis. Proc Natl Acad Sci USA 97: 11655-11660.

Schlesier B, Breton F, Mock HP. 2003. A hydroponic culture system for growing *Arabidopsis thaliana* plantlets under sterile conditions. Plant Mol Biol Rep 21: 449-456.

Sieburth LE, Meyerowitz EM. 1997. Molecular dissection of the AGAMOUS control region shows that *cis* elements for spatial regulation are located intragenically. Plant Cell 9: 355-365.

Tamas L, Budíkov á S, Huttov á J, Mistr ík I, Simonovicov á M, Sirok á B. 2005. Aluminum-induced cell death of barley-root border cells is correlated with peroxidase- and oxalate oxidase-mediated hydrogen peroxide production. Plant Cell Rep 24: 189-194.

Taylor CB. 1997. Promoter Fusion Analysis: An Insufficient Measure of Gene Expression. Plant Cell 9: 273-275.

Tokunaga N, Kaneta T, Sato S, Sato Y. 2009. Analysis of expression profiles of three peroxidase genes associated with lignification in *Arabidopsis thaliana*. Physiol Plant 136: 237-249.

Thareau V, Dehais P, Serizet C, Hilson P, Rouze P, Aubourg S. 2003. Automatic design of gene-specific sequence tags for genome-wide functional studies. Bioinformatics 19: 2191-2198.

Tocquin P, Corbesier L, Havelange A, Pieltain A, Kurtem E, Bernier G, Perilleux C. 2003.A novel high efficiency, low maintenance, hydroponic system for synchronous and flowering *Arabidopsis thaliana*. BMC Plant Biol 3: 2-12.

Tognolli M, Penel C, Greppin H, Simon P. 2002. Analysis and expression of the class III peroxidase large gene family in *Arabidopsis thaliana*. Gene 288: 129-138.

Valerio L, De Meyer M, Penel C, Dunand C. 2004. Expression analysis of the *Arabidopsis* peroxidase multigenic family. Phytochemistry-US 65: 1331-1342.

Wagner GJ, Wang E, Shepherd RW. 2004. New Approaches for Studying and Exploiting an Old Protuberance, the Plant Trichome. Ann Bot-London 93: 3-11.

Wanapu C, Shinmyo A. 1996. *cis*-regulatory elements of the peroxidase gene in *Arabidopsis thaliana* involved in root-specific expression and responsiveness to high-salt stress. Ann N Y Acad Sci 782: 107-114.

Welinder KG, Justesen AF, Kjaersgård IV, Jensen RB, Rasmussen SK, Jespersen HM, Duroux L. 2002. Structural diversity and transcription of class III peroxidases from *Arabidopsis thaliana*. Eur J Biochem 269: 6063-6081.

Ye GN, Stone D, Pang SZ, Creely W, Gonzalez K, Hinchee M. 1999. *Arabidopsis* ovule is the target for *Agrobacterium* in planta vacuum infiltration transformation. Plant J 19: 249-57.

Yoo SY, Bomblies K, Yoo SK, Yang JW, Choi MS, Lee JS, Weigel D, Ahn JH. 2005. The 35S prmoter used in a selectable marker gene of a plant transformation vector affects the expression of the transgene. Planta 221: 523-530.

Yu H, Nguyen K, Royce T, Qian J, Nelson K, Snyder M, Gerstein M. 2007. Positional artifacts in microarrays: experimental verification and construction of COP, an automated detection tool. Nucleic Acids Res 35: e8.

Zimmermann P, Hirsch-Hoffmann M, Hennig L, Gruissem W. 2004. GENEVESTIGATOR. *Arabidopsis* microarray database and analysis toolbox. Plant Physiol 136: 2621-2632.

Chapter 4. General discussion and conclusions

Aluminum toxicity is a major factor limiting crop-yield on acidic soils (Von Uexkull and Mutert, 1995). Although Al is a non-redox-active metal, and thus is not able to catalyze redox reactions, a pro-oxidant activity of Al has been hypothesized through formation of an Al-superoxide, semi-reduced radical ion (Exley, 2004). This hypothesis could explain why Al can induce oxidative stress without a redox metal (e.g., Fe) in the treatment condition (Richards *et al.*, 1998; Yamamoto *et al.*, 2001).

Given this relationship between Al toxicity and oxidative stress, it is perhaps not surprising that class III peroxidases have been implicated in plant response to Al. Previously, *PER34* (one of the class III peroxidase) has been found to be induced (up to 50-fold) as early as 15 minutes after exposure to Al and reached the highest expression level at 48 h (Richards *et al.*, 1998). However, overexpression of *PER34* in *Arabidopsis* conferred resistance to oxidative stress induced by diamide, but failed to show resistance to Al stress (Ezaki *et al.*, 2000). A review of the *PER34* cDNA clone sequence revealed that the observed up-regulation of *PER34* transcripts by Al stress (Richards *et al.*, 1998) and in transgenic *Arabidopsis* overexpressing *PER34* (Ezaki *et al.*, 2000) actually reflected combined transcript abundance of *PER33* and *PER34* due to high levels of sequence similarity (90.3% homology in coding sequence and 95% homology at the protein level).

Recently, microarray analysis of roots of *Arabidopsis* exposed to Al stress for 6 h has identified *PER73* to be the most up-regulated class III peroxdiase. In clear contrast to the results of Richards *et al.* (1998), *PER34* was down-regulated (Kumari *et al.*, 2008). A review of the 70-mer oligo sequences representing

PER35 and *PER73* on the *Arabidopsis* array (Qiagen Operon Array-Ready OligoSet™) revealed that the 70-mer oligo of *PER35* share 100% sequence similarity with the cDNA of *PER73* and the 70-mer oligo of *PER73* share 76% sequence similarity with the cDNA of *PER35*. Therefore, cross-hybridization of the 70-mer oligos to transcripts of these peroxidases could mean that the detected up- (*PER73*) and down-regulation (*PER34*) of peroxidases under Al stress actually reflected combined transcript abundance of *PER33* and *PER34* and *PER35* and *PER73*. Cross-hybridization in microarray experiments lead to 'false positives' and spurious correlations have been reported (Wu *et al.*, 2005; Okoniewski and Miller, 2006). Thus, a promoter::*GUS* reporter gene fusion approach was utilized to study the expression pattern of *PER73* under Al stress.

In another study, proteomic analysis of extracytosolic proteins secreted by roots of canola identified *PER22* as a homologue of one of the most abundant root proteins (Basu *et al.*, 2006). Proteomic analysis of vacuolar proteins in *Arabidopsis* identified a highly conserved C-terminal propeptide (CTPP) responsible for targeting to the vacuole (Carter *et al.*, 2004). Both *PER22* and *PER23* and *PER33* and *PER34* were found to contain this vacuolar targeting signal peptide (Carter *et al.*, 2004). Considering *PER22* is secreted to the rhizosphere by roots of canola and the major binding sites of Al in apoplasm (Basu *et al.*, 2006), it would be interesting to find out the spatial expression pattern of *PER22* and how it responds to Al stress.

To investigate expression patterns of *PER22* and *PER73* under Al stress, single-copy, homozygous, transgenic *Arabidopsis* harbouring the individual promoter::*GUS* reporter gene constructs were generated. Histochemical *GUS* staining of 21-day-old transgenic seedlings revealed trichome-specific and vascular-specific expression patterns for *PER22* and *PER73*, respectively.

Furthermore, *GUS* staining assays of transgenic seedlings under Al stress demonstrated that both *PER22* and *PER73* responded to Al stress at certain time points. Further experiments measuring *GUS* activities under Al stress could provide quantitative results in illustrating of up- or down-regulation of expression profiles of *PER22* and *PER73*. The temporal and spatial expressions of *PER22* and *PER73* suggest that they might be involved in pathogen defense and/or lignification. In order to further characterize the roles of *PER22* and *PER73* in the context of Al stress, transverse sectioning of root tissues from *GUS*-stained pCAMBIA-*PER*22PR and pCAMBIA-*PER*73PR transgenic lines treated with and without Al stress will help determine which specific tissues and cell types these peroxidases are expressed in and how they respond to Al stress spatially.

Combining the previous reported induction of *PER22* expression under the conditions of potassium deficiency (Kang *et al.*, 2004) and salt stress (Jiang *et al.*, 2007), I hypothesized that *PER22* is involved in ROS scavenging to alleviate oxidative stress induced by abiotic stress. However, the trichome-specific expression of *PER22*, the extracytosolic localization of the *PER22* protein (Basu *et al.*, 2006), and putative pathogen-responsive motif (W-box element, Table 3.2) present in the promoter region of *PER22* suggest that *PER22* might participate in the oxidative burst mechanism in response to pathogen attack. Further experiments measuring ROS levels with 2', 7'-dichlorofluorescein diacetate (H_2DCF-DA) (Zhu *et al.*, 1994) in root tissues could determine how *PER22* regulates the ROS levels, either removing ROS to alleviate oxidative stress or increasing ROS through an oxidative burst. Measuring *PER22* expression, ROS levels, and activities of intracellular antioxidant defense enzymes in root tissues under Al stress could reveal if *PER22* participates in a PCD mechanism. Tamas *et al.* (2005) suggested that plant roots might utilize PCD to sacrifice root border

cells (RBC) as a means to trap Al and prevent the further penetration of Al into the root tissue.

Due to the enhanced expression of *PER73* in lignifying tissue (vascular) under Al stress and the predicted apoplastic localization of the *PER73* protein, I hypothesized that *PER73* increases lignin deposition in the cell walls in root tissues to prevent Al enter the symplasm. Therefore, phloroglucinol staining of lignin (Nakano and Meshitsuka, 1992) and quantification of the lignin content (Hatfield and Fukushima, 2005) in root tissues that show *GUS* staining of *PER73* under Al stress conditions could help determine if *PER73* indeed participate in the lignification process.

Prior to my work, no reports of the spatial expression patterns of *PER22* and *PER73* had been published, probably due to the presence of highly homologous genes within the class III peroxidase family. Generation and analysis of promoter::*GUS* reporter gene fusions proved to be a feasible and effective approach to distinguish expression patterns among the highly homologous genes. The experimental design used in this project provides a framework for characterizing the expression patterns of other highly homologous peroxidases within the class III peroxidase gene family, such as *PER33* and *PER34*. The histochemical *GUS* staining assay revealed tissue-specfic expression patterns for *PER22* and *PER73* and provided preliminary evidence relating to their potential involvement in plant defense, lignifications, and Al detoxification mechanisms. Trichome- and vascular-specific expression directed by promoters of *PER22* and *PER73* bear potential biotechnology application in plant biopharming.

4.1. References

Basu U, Francis JL, Whittal RM, Stephens JL, Wang Y, Zaiane OR, Goebel R, Muench DG, Good AG, Taylor GJ. 2006. Extracellular proteomes of *Arabidopsis thaliana* and *Brassica napus* roots: Analysis and comparison by MudPIT and LC-MS/MS. Plant Soil 286: 357-376.

Bindschedler LV, Dewdney J, Blee KA, Stone JM, Asai T, Plotnikov J, Denoux C, Hayes T, Gerrish C, Davies DR, Ausubel FM, Bolwell GP. 2006. Peroxidase dependent apoplastic oxidative burst in *Arabidopsis* required for pathogen resistance. Plant J 47: 851-863.

Carter C, Pan SQ, Jan ZH, Avila EL, Girke T, Raikhel NV. 2004. The vegetative vacuole proteome of *Arabidopsis thaliana* reveals predicted and unexpected proteins. Plant Cell 16: 3285-3303.

Cosio C, Dunand C. 2009. Specific functions of individual class III peroxidase genes. J Exp Bot 60: 391-408.

Exley C. 2004. The pro-oxidant activity of aluminum. Free Radic Biol Med 36: 380-387.

Ezaki B, Gardner RC, Ezaki Y, Matsumoto H. 2000. Expression of aluminum-induced genes in transgenic *Arabidopsis* plants can ameliorate aluminum stress and/or oxidative stress. Plant Physiol 122: 657-665.

Hatfield, H., Fukushima, R. (2005). Can lignin be accurately measured? Crop Sci 45: 832-839.

Jefferson RA. 1987. Assaying chimeric genes in plants: the *GUS* gene fusion system. Plant Mol Biol Rep 5: 387-405.

Jiang YQ, Yang B, Harris NS, Deyholos M. 2007. Comparative proteomic analysis of NaCl stress-responsive proteins in *Arabidopsis* roots. J Exp Bot 58: 3591-3607.

Kang JG, Pyo YJ, Cho JW, Cho MH. 2004. Comparative proteome analysis of differentially expressed proteins induced by K^+ deficiency in *Arabidopsis thaliana*. Proteomics 4: 3549-3559.

Kumari M, Taylor GJ, Deyholos MK. 2008. Transcriptomic responses to aluminum stress in roots of *Arabidopsis thaliana*. Mol Genet Genomics 279: 339-357.

Nakano J, Meshitsuka G. 1992. The detection of lignin. In: Lin SY, Dence CW (eds) Methods in Lignin Chemistry. Springer-Verlag, New York, pp 23-32.

Okoniewski MJ, Miller CJ. 2006. Hybridization interactions between probesets in short oligo microarrays lead to spurious correlations. BMC Bioinformatics 7: 276-289.

Passardi F, Tognolli M, De Meyer M, Penel C, Dunand C. 2006. Two cell wall associated peroxidases from *Arabidopsis* influence root elongation. Planta 223: 965-974.

Richards KD, Schott EJ, Sharma YK, Davis KR, Gardner RC. 1998. Aluminum induces oxidative stress genes in *Arabidopsis thaliana*. Plant Physiol 116: 409-418.

Tamas L, Budíkov á S, Huttov á J, Mistrík I, Simonovicov á M, Sirok á B. 2005. Aluminum-induced cell death of barley-root border cells is correlated with peroxidase- and oxalate oxidase-mediated hydrogen peroxide production. Plant Cell Rep 24: 189-194.

Von Uexkull HR, Mutert, E. 1995. Global extent, development and economic impact of acid soils. Plant Soil 171: 1-15.

Wu C, Carta R, Zhang L. 2005. Sequence dependence of cross-hybridization on short oligo microarrays. Nucleic Acids Res 33: 84-90.

Yamamoto Y, Kobayashi Y, Matsumoto H. 2001. Lipid peroxidation is an early symptom triggered by aluminum, but not the primary cause of elongation inhibition in pea roots. Plant Physiol 125:199-208.

Zhu H, Bannenberg GH, Moldeus P, Shertzer HG. 1994. Oxidation pathways for the intracellular probe 2', 7'-dichlorofluorescin. Arch Toxicol 68: 582-587.